INFORMATION TO USERS

This manuscript has been reproduced from the microfilm master. UMI films the text directly from the original or copy submitted. Thus, some thesis and dissertation copies are in typewriter face, while others may be from any type of computer printer.

The quality of this reproduction is dependent upon the quality of the copy submitted. Broken or indistinct print, colored or poor quality illustrations and photographs, print bleedthrough, substandard margins, and improper alignment can adversely affect reproduction.

In the unlikely event that the author did not send UMI a complete manuscript and there are missing pages, these will be noted. Also, if unauthorized copyright material had to be removed, a note will indicate the deletion.

Oversize materials (e.g., maps, drawings, charts) are reproduced by sectioning the original, beginning at the upper left-hand corner and continuing from left to right in equal sections with small overlaps. Each original is also photographed in one exposure and is included in reduced form at the back of the book.

Photographs included in the original manuscript have been reproduced xerographically in this copy. Higher quality 6" x 9" black and white photographic prints are available for any photographs or illustrations appearing in this copy for an additional charge. Contact UMI directly to order.

UMI

A Bell & Howell Information Company
300 North Zeeb Road, Ann Arbor MI 48106-1346 USA
313/761-4700 800/521-0600

SUMMATION OF AMPA-MEDIATED EPSPS IN RAT NEOCORTICAL PYRAMIDAL NEURONS

by

Jilda Suzanne Nettleton

A dissertation submitted in partial fulfillment of the requirements for the degree of

Doctor of Philosophy

University of Washington

1998

Approved by 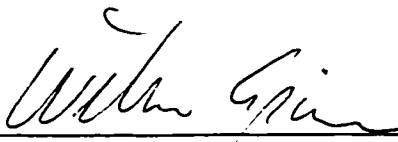

Chairperson of Supervisory Committee

Program Authorized to Offer Degree Physiology and Biophysics

Date November 19, 1998

Doctoral Dissertation

In presenting this dissertation in partial fulfillment of the requirements for the Doctoral degree at the University of Washington, I agree that the Library shall make its copies freely available for inspection. I further agree that extensive copying of this dissertation is allowable only for scholarly purposes, consistent with "fair use" as prescribed in the U.S. Copyright Law. Requests for copying or reproduction of this dissertation may be referred to University Microfilms, 1490 Eisenhower Place, P.O. Box 975, Ann Arbor, MI 48106, to whom the author has granted "the right to reproduce and sell (a) copies of the manuscript in microform and/or (b) printed copies of the manuscript made from microform."

Signature 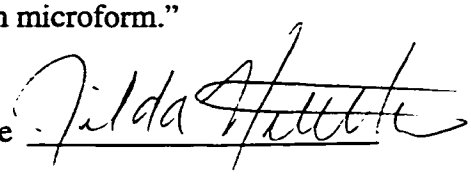

Date November 19, 1998

University of Washington

Abstract

SUMMATION OF AMPA-MEDIATED EPSPS IN RAT NEOCORTICAL PYRAMIDAL NEURONS

by Jilda Suzanne Nettleton

Chairperson of the Supervisory Committee: Associate Professor William J. Spain, M. D.
Department of Physiology and Biophysics

It has been hypothesized that voltage-sensitive conductances present on the dendrites of neurons can influence the summation of EPSPs and hence affect how neurons compile information. Greater than linear summation of EPSPs has been postulated to facilitate coincidence detection by cortical neurons. This study examined whether the summation of subthreshold AMPA-mediated EPSPs generated on layer V neocortical pyramidal neurons in vitro was linear or nonlinear, and if any nonlinearities could be attributed to dendritic conductances. Evoked EPSPs (1-12 mV) were recorded somatically by means of intracellular sharp electrodes in the presence of 100 μM AP-5 and 3 μM bicuculline. Two independent EPSPs were evoked by two stimulating electrodes, one in layer I and another in layers III-V. The areas of stimulation were isolated from each other by a horizontal cut below layer I. To block post-synaptic conductances (i.e. Na^+, Ca^{2+}) in a subset of neurons, 50 mM QX-314 was included in the recording electrode. The presence of QX-314 in the electrodes significantly decreased the

amount of superlinear summation compared to control conditions. With KCl electrodes, but not QX-314 electrodes, EPSP summation was affected by changes in postsynaptic membrane potential. Superlinear summation of EPSPs decreased as the time between stimuli decreased only when using KCl electrodes. To determine the role of dendrites play in non-linear summation, a current pulse (simulated EPSP) delivered at the soma was substituted for either or both of the proximally and distally evoked EPSPs. Simulated EPSPs combined with either an evoked EPSP or another simulated EPSP showed significantly less superlinear summation then two evoked EPSPs, indicating that the dendritic conductances are largely responsible for the observed superlinear summation.

TABLE OF CONTENTS

LIST OF FIGURES

ACKNOWLEDGMENTS

Although this thesis has only one name on the outside, there are many others whose contributions were needed for completing this dissertation. To begin with I would like to thank everyone on my thesis committee, Dr. William Spain, Dr. Wayne Crill, Dr. Marc Binder, Dr. Phillip Schwartzkroin, and Dr. Dennis Baskin for all their scientific advise and discussions. I also owe a debt of gratitude to everyone in the Spain laboratory, especially my advisor, Dr. Bill Spain. Bill along with Dr. Hans van Brederode advised me on experimental design and techniques as well as provided feedback on writing and presentations. My experiments would never have been completed without Dick Lee's help in making solutions and performing surgery. I'd also like to thank Dr. Anita Hendrickson for use of her lab to do histology, along with Andra Erickson for providing technical assistance. I owe extra thanks to Dr. Keely Bumsted who taught me the histological techniques. Additonally, Lorraine Gibbs did some of the histology for my thesis work.

I also owe a big thanks to all my friends and family members who have provided endless encouragement and support.

DEDICATION

I dedicate this dissertation to my former boss, Dr. Ging Kuo Wang for inspiring me to go to graduate school, and to my spouse and closest friend, Dr. Anthony B. Russell, for helping me get through it.

INTRODUCTION

The question of how a neuron processes information from other neurons has been continually asked since the time of Ramón y Cajal (Yuste and Tank, 1996). Early theories about signal processing treated neuronal dendrites as electrically passive structures. Assuming the dendrites were passive created the groundwork for understanding how a neuron's morphology and electrical characteristics shape and integrate synaptic inputs. This assumption ignored the potential role of voltage-sensitive conductances in synaptic integration. In recent years, with the improvement of histological and electrical recording techniques, the support for the idea that dendritic voltage-sensitive conductances are involved in synaptic integration has expanded tremendously (for excellent recent reviews see Johnston, et al., 1996; Yuste and Tank, 1996). Voltage-sensitive conductances have been postulated to play a role in synaptic integration, but the nature of this role is just starting to be explored. In my thesis, I address the following aspects of synaptic integration in layer V pyramidal neurons: 1) how excitatory postsynaptic potentials (EPSPs) sum, and 2) the effect of voltage-sensitive ionic conductances in the soma and dendrites on EPSP summation.

The earliest theory about neuronal integration was the theory of dynamic polarization formulated by Santiago Ramon y Cajal in the 1800's. According to his theory of dynamic polarization, neurons receive signals through synaptic contacts located in the

dendrites and soma (Ramón y Cajal, 1937). The signals combine to create an output signal that leaves the neuron through the axonal arborization. One important question that arose from this theory is how do these inputs combine? In this introductory chapter, I will discuss how studies on the passive and voltage-sensitive (or active) dendritic properties have contributed to knowledge about the summation of synaptic inputs.

PASSIVE DENDRITIC PROPERTIES

CABLE THEORY: BRIEF OVERVIEW

Cable theory was originally used by Lord Kelvin to explain how electrical signals would travel in leaky electrical cables (Kelvin, 1855). In the neuroscience field, modeling the axon as a leaky cable helped explain how electrical signals could propagate in axons (Hodgkin and Rushton, 1946). The following is a brief summary from Jack, et al., 1975 (pg. 25-28), and Spruston, et al., (1994) outlining conduction of electrical signals in cables. According to linear cable theory, in cables and cable-like structures such as nerve fibers, conduction of an electrical signal is determined not by the physical length of the cable, but by its electrotonic length. The electrotonic length is defined as the physical length of a cable divided by the cable's space constant. The space constant is defined as:

$$\lambda = \sqrt{aR_m/2R_i} \qquad (1)$$

with λ (in cm) being the space constant of the cable, a (in cm), the radius of the cable, R_m, the specific membrane resistivity (in $\Omega \bullet cm^2$), and R_i, the internal resistivity (in $\Omega \bullet cm$). In linear cable theory, the membrane and axial resistances are assumed to be voltage-independent and constant over the length of the cable. The space constant, λ, gives the distance over which a voltage response decays to 1/e of its original value or:

$$V(x) = V_O e^{-x/\lambda} \qquad (2)$$

In equation 2, V(x) is the amplitude of the voltage response at a distance x from the original site of the voltage response. V_O is the size of the original signal and λ is the space constant (equation 1). Equation 2 predicts that a signal arriving in a dendrite with a long space constant will be less attenuated than a signal arriving in a dendrite of the same physical length but with a short space constant. The electrotonic length of dendrites is measured in units of space constants.

In the earlier half of this century, most researchers believed that the dendrites were electrotonically long (i.e. dendrites were believed to be many space constants long) and thus, distal synaptic inputs would be heavily attenuated. This led to two different ideas about distal synaptic inputs. Eccles (1957) proposed that distal inputs would be completely attenuated and consequently had no contribution to synaptic integration. A competing theory by Lorente de Nó (1959) proposed that the dendrites were capable of decremental conduction. According to Nó, decremental conduction

would allow electrical signals to propagate through dendrites in a fashion similar to action potentials, except that the amplitude of the electrical signal would decrease as the signal traveled in the dendrites. Via decremental conduction, synaptic signals could propagate to the soma without being completely attentuated by the passive cable properties of the dendrites. An improved understanding of the electrophysiological characteristics of neurons was needed to resolve this conflict.

RALL'S MODEL OF PASSIVE DENDRITES

In practice, applying linear cable theory to the complicated branching structure typical of dendrites was difficult given the techniques available during the 1950's and 1960's (Rall, 1964). To overcome the problem of determining the electrotonic length of a multitude of dendritic branches, Rall developed the "equivalent cylinder model", also referred to as the "Rall model" (Rall, 1977; Rall, 1964). Although the Rall model was based on an idealized model of neuron structure, it provided a general theoretical framework for predicting how synaptic inputs would propagate passively and interact with each other (Rall, 1964; Rall, et al., 1967).

The Rall model dealt with the problem of electrical signal flow in the extensively branched dendritic structure by collapsing the entire dendritic tree into one equivalent cable (Rall, 1962). A graphic representation of a dendritic tree being collapsed is shown in Figure 1. Rall (1962) demonstrated mathematically that it was possible to model the entire dendritic tree as one linear cable, if at each branch point the dendrite

split into smaller branches according to the 3/2 power rule. According to the 3/2 power rule, the sum of the smaller branches' diameters raised to the 3/2 power must be equal to the original dendrite's diameter raised to the 3/2 power (Rall, 1962). The validity of this restriction on dendritic morphology and its effect on the conclusions of this model will be discussed later. The Rall model, as well as other models based on linear cable theory, assumed that the dendrites were passive and thus the membrane resistance remained constant throughout the dendritic tree and was independent of the membrane potential.

Based on the his studies using the equivalent cylinder model, Rall predicted how current and voltage signals could passively spread through the dendritic branches and to the soma. Figure 2 (from Rall (1977)) shows how the same synaptic input originating at different areas of the dendrites would appear in the soma. The EPSP's size and shape should vary with its distance from the soma. Namely, EPSPs from regions of the dendritic tree farthest from the soma were the slowest and smallest EPSPs that reach the soma. (Rall, 1967). The Rall model led to the conclusion that the amount of attenuation and the time course of the signal depended upon its electronic distance from the soma (Rall, 1967).

Applying Rall's model to a biological neuron allowed an estimation of the electrotonic length of the dendrites (Lux, et al., 1970). By using ^{3}H-glycine filled intracellular electrodes, Lux et al. (1970) determined the morphology as well as the input resistance and membrane time constant of 7 spinal motoneurons. Since the morphology of

the dendrites did follow Rall's 3/2 power rule, Lux et al. (1970) were able to use the Rall model with their measurements of input resistance and membrane time constant. They found that the dendrites extended about 1.5λ from the soma. One reason their conclusion differed from Eccles (1957) was that Lux et al. (1970) found a much higher specific membrane resistivity, 2750 ± 1010 (STD) $\Omega \bullet cm^2$, than previously found by Coombs et al. (1959, 600 $\Omega \bullet cm^2$). Lux et al. (1970) concluded that the neurons were electrotonically compact enough to allow synaptic inputs arriving anywhere on the dendritic tree of motoneurons to reach the soma.

The Rall model also determined the expected shapes of EPSPs reaching the soma from different locations (Rall, 1967). In a linear cable, both the rise time and decay time of the EPSP increase as its electrotonic distance from the soma increases (Rall, 1967). Therefore, measurable EPSP shape indices (i.e. rise time, half width, and time to peak) should be related to each other in a predictable manner (Rall, et al., 1967). This prediction was supported by measurements of shape indices from EPSPs recorded in motoneurons. In these measurements, the EPSPs with the faster times to peak also had the shorter half-widths compared to EPSPs with the longer times to peak (Rall, et al., 1967).

Redman and Walmsley (1983) provided the most direct evidence for the shape of EPSPs being dependent upon the electronic distance. Redman and Walmsley (1983) measured EPSPs in motoneurons created by single Ia afferent fiber stimulation, and then histologically reconstructed the connection between the Ia fiber and the

motoneuron. They determined that the shape and size of the EPSPs was dependent on the inputs' electrotonic distance from the soma as predicted by linear cable theory.

Based on the how EPSP shape and size were affected by the cable properties of the dendrites, Rall also made predictions about how synaptic potentials coming into various regions of the dendritic tree would sum with each other. One prediction was that two synaptic potentials would sum sublinearly if the signal from one affected the synaptic driving force of the other (Rall, et al., 1967). This did not necessarily mean the two inputs had to be on the same dendritic branch. Based on the theoretical predictions from the equivalent cylinder model, Rall predicted that a large EPSP in one branch would passively spread to other branches as well as to the soma (Rall, et al., 1967). The change in membrane potential at these other branches created by this EPSP would temporarily decrease the synaptic driving force for any other EPSPs coming into those branches (Rall, et al., 1967). Alternatively, synaptic potentials would sum linearly if they were electrically isolated from each other (Rall, et al., 1967). Support for this theory came from measurements of evoked EPSP summation in motoneurons. In these experiments, Burke (1967) evoked two different EPSPs by stimulating Ia afferent fibers coming from different muscles. The response created by stimulating both fibers simultaneously was equal to or smaller than the algebraic sum of the individual EPSPs from each fiber (Burke, 1967). Presumably, the sublinear summation resulted in cases

where the EPSPs were able to interact while the linearly summing EPSPs were electrically isolated from each other (Burke, 1967; Rall, et al., 1967).

The idea that sublinear summation of EPSPs would occur if the inputs were close to each other was also supported by Kuno's and Miyahara's study (1969) on EPSP size fluctuations in spinal motoneurons. In this study, Kuno and Miyahara generated unitary EPSPs by stimulating single afferent fibers and measured both the fluctuation in EPSP amplitude and the transmission failure rate (the number of times a stimulus failed to generate a response per number of stimuli given). The fluctuation in EPSP size was smaller than what was expected from the transmission failure rate for that fiber according to the quantal hypothesis of synaptic transmission (del Castillo and Katz, 1954). This discrepancy could be accounted for by assuming that the unit potentials underlying the measured EPSPs were arriving at the same area of the dendrite and then the unit potentials were summing sublinearly in accordance with the Rall model. (Kuno and Miyahara, 1969).

Although the experimental evidence from summed EPSPs correlated well with the theoretical predictions of the Rall model, it did not actually prove the model. For instance, neither the inputs that summed sublinearly could not be shown to be electrotonically nearer to each other than inputs that summed linearly, nor was there a correlation between sublinear summation and EPSP shape in the few cases of sublinear summation that occurred. (Burke, 1967).

OTHER MODELS BASED ON LINEAR CABLE THEORY

One problem with Rall's model was that not all dendritic branching patterns followed the 3/2 power rule necessary for collapsing the dendritic tree (Ramon-Moliner, 1962). Although Lux et al. (1970) found that motoneuron dendrites followed the 3/2 power rule, in a later study by Barrett and Crill (1974), motoneuron dendrites did not follow the 3/2 power rule. Similar to the method used by Lux et al. (1970), Barrett and Crill (1974) measured the morphology and electrical properties of cat spinal motoneurons using Procion dye filled microelectrodes. Using the reconstructed morphologies from 10 spinal motoneurons, they modeled each neuron as a series of connecting cable segments. With this model as well as the measured input resistance and time constants, they found that on average the most distal dendrites were 1.4λ away from the soma. The similarity of this value to that found by Lux et al. (Lux, et al., 1970) suggests that, although not morphologically accurate, the Rall model could still give useful information about passive dendritic properties.

Cable theory continues to be used to measure the passive electrical properties of neurons. The estimated electrotonic length of dendrites has decreased with the use of whole-cell patch-pipettes instead of microelectrodes for intracellular recording (Spruston, et al., 1994). Based on current measurements using whole-cell patch-pipettes, motoneurons dendrites have been found to be electrotonically compact with a mean electrotonic length of $0.85 \pm 0.14\ \lambda$ (Thurbon, et al., 1998) compared to the value of 1.5

to 2λ found previously using microelectrodes (Barrett and Crill, 1974; Lux, et al., 1970, Rall, et al., 1967). Intracellular recording with whole-cell patch-pipettes has revealed that neurons' specific membrane resistivity is higher than the previous values for specific membrane resistivity obtained using microelectrodes (Major, et al., 1994; Spruston and Johnston, 1992). The underestimation of membrane resistivity in earlier works appears to be due to the somatic shunt created by microelectrode impalement (Clements and Redman, 1987; Spruston and Johnston, 1992).

The new higher estimation of membrane resistivity led Bernander et al. (1991), to propose that the synaptic conductance change could create a significant decrease in membrane resistance. Using the reconstructed morphology and electrical properties of a layer V pyramidal cell, Bernander et al. (1991) modeled the dendrites as a series of connecting cable segments. With this model, Bernander et al. (1991) demonstrated that the input resistance decreased during continual "background" synaptic activity. During a continual barrage of synaptic inputs, the synaptic channels (i.e. the AMPA recepters) open and thus the total dendritic conductance increases while the membrane resistance decreases (Bernander, et al., 1991). This decrease in membrane resistance will also cause the dendrites to be electrotonically longer, thus the size of EPSPs will be reduced (Bernander, et al., 1991). This effect was observed even at low levels of background firing activity implying that even when only a few inputs are active, the synaptic conductance change may lead to sublinear summation.

In summary, treating the dendrites as passive structures yields an important framework for understanding how synaptic inputs travel in dendritic trees. Two important conclusions about EPSP summation are reached from studies on the passive properties of dendrites. First, while the cable like properties of dendrites attenuates the synaptic inputs, the inputs are not prevented from reaching the soma. Second, in a completely passive dendritic tree, EPSPs would be expected to sum linearly if electrically isolated or sublinearly if one affects the synaptic driving force or creates a synaptic conductance change large enough to decrease membrane resistance.

VOLTAGE-DEPENDENT CONDUCTANCES IN DENDRITES

One of the assumptions of passive dentrite models was that dendrites did not possess voltage-sensitive conductances. Even during the time when the Rall model was being developed, it was not universally assumed that the dendrites were passive. Lorente de Nó and Condouris (1959) implied that voltage-sensitive conductances in the dendrites could allow synaptic inputs to propagate through the dendritic tree. Currently, there is mounting evidence that voltage- and time-sensitive conductances may play a large role in how synaptic inputs are shaped and integrated (for reviews see Johnston, et al., 1996; Yuste and Tank, 1996). Voltage-sensitive ionic conductances are now known to be present in the dendrites in addition to being in the soma (Hoffman, et al., 1997; Kim and Connors, 1993; Llinas and Sugimori, 1980; Magee and Johnston, 1995b; Markram and Sakmann, 1994; Spruston, et al., 1994; Stuart and Sakmann, 1994). One possible

consequence of dendritic voltage-sensitive conductance is that one synaptic potential in the dendrites will affect these voltage-sensitive conductances thereby changing the size and shape of subsequent synaptic potentials. One hypothesis is that two or more synaptic inputs may sum nonlinearly if one affects the voltage-sensitive conductances controlling the size and shape of the others. In this section, I will review the evidence that supports this hypothesis.

VOLTAGE-DEPENDENT CONDUCTANCES AFFECT SHAPE OF EPSPS.

In motoneurons, the size, shape, and summation of EPSPs could be explained by application of linear cable theory as discussed previously. For other types of neurons, especially hippocampal and neocortical pyramidal cells, the shape and time course of dendritic EPSPs were not always consistent with the predictions based on linear cable theory. Turner (1988) stimulated distal and proximal afferent fibers contacting CA1 hippocampal neurons and measured the resulting EPSP shape indices. For minimally evoked EPSPs (< 1 mV amplitudes), distal EPSPs did have slower rise times and longer half-widths than proximal EPSPs, consistent with predictions of a passive cable model (Turner, 1988). However, for larger EPSPs (> 1mV in amplitude), the difference in rise time and half width between distally and proximally generated EPSPs was no longer observed. A similar effect was observed for layer V pyramidal cells (Nicoll, et al., 1993). Nicoll et al. (1993), observed that EPSPs generated by stimulation in distal (i.e. layer I-II) layers had the same rise time and half-width as EPSPs from proximal layer (i.e. layer V-

VI) stimulation. One possible explanation for the discrepancy between experimental data and the predictions based on linear cable theory is that voltage- and time-dependent conductances are affecting EPSPs.

Other studies demonstrated that there were many voltage- and time-sensitive conductances that affect EPSP size and shape. In one of the earliest studies, Stafstorm et al. (1985), showed that for layer V cat neocortical pyramidal cells, EPSPs increase in size and have longer delay times when the holding potential is depolarized. The amplification of EPSPs was presumably due to activation of a persistent sodium conductance (Stafstorm, et al., 1985). Deisz et al. (1991) demonstrated that both Na^+ and Ca^{2+} conductances increased the size and duration of EPSPs. Deisz et al. (1991) found that intracellular QX-314, a compound that inhibits Na^+ conductances (Stafstorm, et al., 1985; Strichartz, 1973), blocked the amplification of EPSPs during depolarization. Deisz et al. (1991) also showed that the amplification of EPSP size was not due to activation of NMDA receptors during depolarization. During membrane depolarization that was large enough to amplify EPSPs, the size of voltage-clamped EPSCs was either not changed or decreased (Deisz, et al., 1991). If NMDA channels were being activated during the depolarization there should have been an increase in EPSC size during depolarization (Deisz, et al., 1991). These studies demonstrated that Na^+ or Ca^{2+} conductances could amplify EPSPs.

With the use of pharmacological agents, K^+ and I_h conductances were found to decrease EPSPs size and shorten the time course of EPSPs (Hoffman, et al., 1997; Stuart and Spruston, 1998). Recording intracellularly from CA1 pyramidal neurons, Hoffman et al. (1997) demonstrated that EPSPs increased in amplitude after I_A conductances were blocked by 4-AP. Additionally, Stuart and Spruston (1998) showed that the presence of external CsCl, a known I_h conductance blocker (Spain, et al., 1987), increased EPSP in size caused a slower decay rate. In layer V pyramidal neurons, external CsCl increased the size of IPSPs (van Brederode and Spain, 1995). These studies supported the idea that voltage-sensitive conductances could affect the size and shape of synaptic potentials.

VOLTAGE DEPENDENT IONIC CONDUCTANCES PRESENT ON THE DENDRITES

Since the 1980's, there have been many reports of clearly non-passive, excitable dendrites that can fire action potentials (Amitai, et al., 1993; Benardo, et al., 1982; Huguenard, et al., 1989; Kim and Connors, 1993; Llinas and Sugimori, 1980; Pockberger, 1991; Stuart and Sakmann, 1994). Using microelectrodes to record intradendritically, Llinas and Sugimori (1980), observed Ca^{2+} spikes in cerebellar Purkinje cells *in vitro*. Benardo et al. (1982) demonstrated that dendrites alone could generate action potentials by intracellularly recording action potentials in surgically isolated hippocampal pyramidal dendrites. Neocortical dendrites have also been found to generate both Na^+ and Ca^{2+} based action potentials (Amitai, et al., 1993; Kim and

Connors, 1993, Stuart and Sakmann, 1994). These studies and many others imply that there must be voltage-sensitive Na^+ and Ca^{2+} conductances on the dendrites generating these events (for review see Johnston, et al., 1996; Yuste and Tank, 1996).

The most direct evidence for dendritically localized Na^+, and Ca^{2+} channels has come from using dendrite-attached patch-clamp pipettes to record dendritic single channel activity (Magee, et al., 1995; Magee and Johnston, 1995a; Magee and Johnston, 1995b). Recording from the apical dendrite of CA1 pyramidal neurons (up to 350μm from soma), Magee and Johnston (1995b) observed TTX-sensitive Na^+ channels all along the recorded dendrite with an estimated density similar to that found for the soma. Using barium to enhance Ca^{2+} channel conductance in dendrite membrane patches, Magee and Johnston (1995b) demonstrated the presence of different types of Ca^{2+} channels located in the dendrites. Low-voltage activated (T-type) and high-voltage activated, medium conductance (R or N-type) Ca^{2+} channel activity were distributed all across the soma and dendrites, while large conductance (L-type) Ca^{2+} channel activity was primarily found in the soma. Since Na^+ and Ca^{2+} conductances, particularly low-voltage activated Ca^{2+} conductances enhance EPSP size, their presence in the dendrites suggests their importance in dendritic amplification of EPSPs.

Previous studies had shown that dendrites initiated spikes at a higher membrane potential compared to somatically initiated spikes (Spruston, et al., 1995; Stuart and Sakmann, 1994). This result was considered surprising given that the density

of Na^+ and Ca^{2+} channels on the dendrites was the same as the density measured on the soma (Magee and Johnston, 1995b). Hoffman et al. (1997) resolved this issue by showing that there was a higher density of A-type potassium channel on the dendrites compared to the somatic density. Using the dendrite attached patch-clamp technique, Hoffman et al. (1997) found that the current density in the distal dendrites was 6-fold that of the soma. Additionally, the voltage threshold of activation for A-type channels decreased for more distal patches (Hoffman, et al., 1997). Using a computer model based on measurements from theirs and Magee and Johnston's (1995b) studies, Hoffman et al. (1997) found that the high density of I_A channels could counteract the Na^+ and Ca^{2+} conductances. Such a reduction would result in a decrease in dendritic excitability and EPSP amplitude (Hoffman, et al., 1997).

Dendrites also appear to have another conductance that can oppose excitation, the hyperpolarization-activated conductance, I_h (Magee, 1998; Stuart and Spruston, 1998). Stuart and Spruston (1998) used a dual recording technique to measure the amount of attenuation of voltage pulses (both in control solutions and with I_h blocked with CsCl) as they traveled from soma to dendrite. For these experiments, one whole-cell patch-pipette recorded from the soma while another whole-cell patch-pipette recorded from the apical dendrite 508 to 563 μm from the soma. Using a morphologically realistic compartmental model of the same cells, Stuart and Spruston (1998) demonstrated that the

best fit to their experimental data occurred when they assumed a higher density of I_h in the distal apical dendrites.

Magee (1998) provided direct evidence that dendrites contain I_h conductances by recording in the cell-attached patch configuration from hippocampal CA1 pyramidal dendrites. In these membrane patches, Magee (1998) measured hyperpolarization-activated I_h currents all along the apical dendrite at distances up to 350μm from the soma. Similar to I_A currents, I_h current density increased 7-fold along the somatodendritic axis (Magee, 1998). In the presence of CsCl, somatically and dendritically recorded current simulated EPSPs (delivered in the dendrites) were larger and had longer durations compared to controls (Magee, 1998). Magee (1998) concluded that dendritic I_h can reduce the amplitude and time course of EPSPs.

From the evidence provided above as well as many other studies (reviewed in Yuste and Tank, 1996 and Johnston et al., 1996), there is a wealth of data to support the idea of voltage-sensitive conductances being located in the dendrites. Some of the dendritic conductances, such as Na^+ and Ca^{2+}, may amplify EPSPs (Deisz, et al., 1991; Stafstorm, et al., 1985). Other conductances, such as K^+ and I_h, decrease and shorten EPSPs (Hoffman, et al., 1997; Magee, 1998; Stuart and Spruston, 1998). Whether or not these conductances can affect synaptic input summation will depend upon whether or not the conductances' activation state is affected by synaptic inputs.

DENDRITIC VOLTAGE-DEPENDENT CONDUCTANCES ARE AFFECTED BY SYNAPTIC STIMULATION

The presence of Na^+, Ca^{2+}, K^+ and I_h channels on the dendrites raises the possibility that their activity may be altered by synaptic inputs traveling through the dendrites. Schwindt and Crill (1995, 1997) showed that activation of dendritic Na^+, Ca^{2+}, I_h, and K^+ conductances in the dendrites altered the synaptic current. In these experiments, Schwindt and Crill voltage-clamped the soma with microelectrodes and measured the current caused by steady iontophoresis of glutamate onto the apical dendrite. The apical dendrite itself would not have been voltage-clamped due to the poor space clamp typical of dendrites (Spruston, et al., 1993). Using this technique they observed that persistent Na^+ and high-voltage activated Ca^{2+} conductances amplified the synaptic current, while I_h and K^+ conductances reduced the synaptic current (Schwindt and Crill, 1995, 1997). This is consistent with the steady synaptic input activating voltage-sensitive channels, thereby affecting the total measured inward current (Schwindt and Crill, 1995, 1997).

Magee and Johnston (1995a) demonstrated that transient synaptic stimulation could also activate dendritic Na^+ and Ca^{2+} channels in hippocampal pyramidal CA1 neurons. In their experiments, they recorded simultaneously from the soma with a whole-cell patch pipette and from the dendrite with a cell-attached patch-pipette, up to 300μm from the soma. From the dendrite membrane patches, they observed that EPSPs

could activate Na^+, and low-voltage activated Ca^{2+} channels. Magee and Johnston (1995a) proposed that the activation of these channels would enhance the size and duration of synaptic inputs.

Three lines of evidence indicate that dendritic conductances affect summation of EPSPs. First, subthreshold EPSPs are shaped by voltage-sensitive ion conductances such as the Na^+, Ca^{2+}, K^+, and I_h conductances. Second, these conductances are found in the dendrites. Third, synaptic stimulation affects these conductances. One possibility is that one synaptic input may activate voltage-sensitive conductances, thereby affecting the size and shape of another synaptic input, which could lead to nonlinear summation of inputs. For instance, superlinear summation of inputs could occur if one synaptic input activates Na^+ or Ca^{2+} conductances causing the other input to be amplified. Conversely, sublinear summation could occur if K^+ conductances are activated. The expected effect of I_h on EPSP summation is less obvious. One argument is that I_h would lead to sublinear summation of inputs since it decreases and shortens EPSPs (Magee, 1998; Stuart and Spruston, 1998). Another possibility arises because I_h is turned off by depolarization (Spain, et al., 1987). If one EPSP can turn off I_h, then the subsequent increase in membrane resistance (Spain, et al., 1987) would allow another EPSPs to be amplified. Without direct measurements of EPSP summation, it is difficult to predict what the net effect of voltage-sensitive conductances will be on EPSP summation.

VOLTAGE DEPENDENT IONIC CONDUCTANCES AND SUMMATION OF INPUTS.

Cash and Yuste (1998) demonstrated that voltage-sensitive conductances can affect synaptic potential summation in cultured hippocampal pyramidal neurons. To examine synaptic input summation Cash and Yuste (1998) used iontophoretically applied glutamate to create potentials similar in size and time course to spontaneous EPSPs. Using this approach, they were able to apply pharmacological agents to measure the effects of different conductances on synaptic input summation. They observed sublinear summation (91±1%) for larger (summed EPSP amplitude > 10mV) AMPA-mediated glutamate induced inputs. Such a result could be consistent with the passive dendrite theory since these inputs may have affected the driving force (Rall, 1977) or synaptic conductance (Bernander, et al., 1991) of each other. Instead this sublinear summation of AMPA-mediated glutamate-induced potentials was eliminated by 4-AP, which is presumed to block I_A conductances. In contrast to I_A, neither Na^+ nor Ca^{2+} conductances appeared to be contributing to summation of inputs (Cash and Yuste, 1998). When Cash and Yuste (1998) blocked Na^+ conductances with TTX or Ca^{2+} conductances with NiCl, the amount of sublinear summation of AMPA-mediated inputs did not change. In these cells, glutamate induced inputs primarily activated I_A conductance, which led to a reduction in input size (Cash and Yuste, 1998). One implication of Cash and Yuste's (1998) study is that voltage-sensitive conductances do affect EPSP summation contrary to the assumptions of linear cable theory.

It is not known if all neurons will sum their EPSPs in a fashion similar to hippocampal pyramidal cells. One possibility is the relative density of depolarizing and hyperpolarizing currents predicts how EPSPs sum. For example, Hoffman et al. (1997) determined that the ratio of I_A to Na^+ currents in distal dendrite membrane patches is 3:1. One expectation from the relatively higher density of I_A is that EPSPs will turn on more I_A than Na^+, thus causing sublinear summation as observed by Cash and Yuste (1998). One implication of EPSP summation being related to the relative current density of different conductances is that a dendrite's voltage-sensitive conductances have a greater influence on EPSP summation than the dendrite's passive properties.

TEMPORAL INTEGRATION OF INPUTS

Most voltage-dependent ionic conductances are also time-dependent (Hille, 1992). This implies that the relative timing of inputs as well as the time dependence of the conductances activated by synaptic inputs will have an effect on synaptic summation. Some studies using computer simulated neurons indicate that layer V neurons could act as coincidence detectors such that only inputs within a millisecond of each other are able to inteact with each other (Konig, et al., 1996; Softky and Koch, 1993). Most integrate and fire neuron models assume that synaptic inputs will integrate over longer time courses (Shadlen and Newsome, 1994). Proponents of the coincidence detection model propose that the dendrite's electrophsyiological characteristics only allow integration on a short time scale (< 1 ms). For instance, computer simulated

neurons indicate that background synaptic activity can decrease membrane time constants thereby reducing the time course over which synaptic inputs can interact (Agmon-Snir and Segev, 1993; Barrett, 1975; Bernander, et al., 1991). Delayed rectifier and I_h conductances have been proposed to reduce somatic EPSP amplitude and duration thus shortening the time course over which these EPSPs may summate (Softky, 1994; Stuart and Spruston, 1998). Alternatively, coincidence detection may be caused by the dendrites having enough Na^+ and Ca^{2+} conductances such that every synaptic input causes a local spike. In this fashion, only inputs that occur within a millisecond of each other can summate (Softky, 1994, Softky and Koch, 1993). Other computer models of neurons suggest that Na^+ and Ca^{2+} conductances in the dendrite may not be strong enough to cause the fast signal needed for coincidence detection (Cook and Johnston, 1997). The time-dependence of synaptic summation in pyramidal neurons has not yet been measured experimentally.

SPECIFIC AIMS

Neurons posses different types of ionic conductances throughout their structures that may increase or decrease the effectiveness of synaptic inputs. Our current knowledge about both the passive and active dendritic properties of neurons permits us to make predictions about how EPSPs may sum, but these predictions have not been fully tested in neocortical pyramidal neurons. The goal of this thesis was to test some of these predictions by addressing the following specific aims in layer V pyramidal neurons:

1) Determine if EPSPs sum linearly or nonlinearly and if this effect can be blocked by intracellular QX-314, which is known to block several voltage-sensitive ionic conductances, i.e. Na^+, Ca^{2+} and I_h.

2) Measure the effect of somatic holding potential and EPSP size on summation of EPSPs. Changes in membrane potential would be expected to affect EPSP summation by changing the activation of voltage-sensitive conductances

3) Measure the effect of time between EPSPs on summation of EPSPs. Since the activation of most voltage-sensitive conductances changes with time, there may also be a time-dependant component to EPSP summation.

4) Use somatically injected current pulses to simulate EPSPs and determine if contributions to non-linear summation in these experiments are primarily due to somatic or dendritic conductances.

The data chapters in this dissertation cover these four specific aims. To summarize the results, EPSPs summed superlinearly in layer V pyramidal neurons due to postsynaptic, QX-314 sensitive conductances. The degree of non-linear summation was voltage and time dependent. Finally, dendritic conductances contributed to the superlinear summation.

Figure 1. Collapsing of a branched dendritic structure into an equivalent cylinder. Figure from Rall (1977). The dendritic tree in A follows the 3/2 power rule and can be represented in the Rall model as the equivalent cylinder shown below. The dashed lines shows where which areas of the dendrites in would be represented in the equivalent cylinder. In B, the equivalent cylinder is divided into 5 compartments (top). Those 5 compartments correspond to the first 5 compartments in the 10 linked compartment diagram below. The 10 linked compartments in this figure correspond to the 10 linked compartments in figure 2.

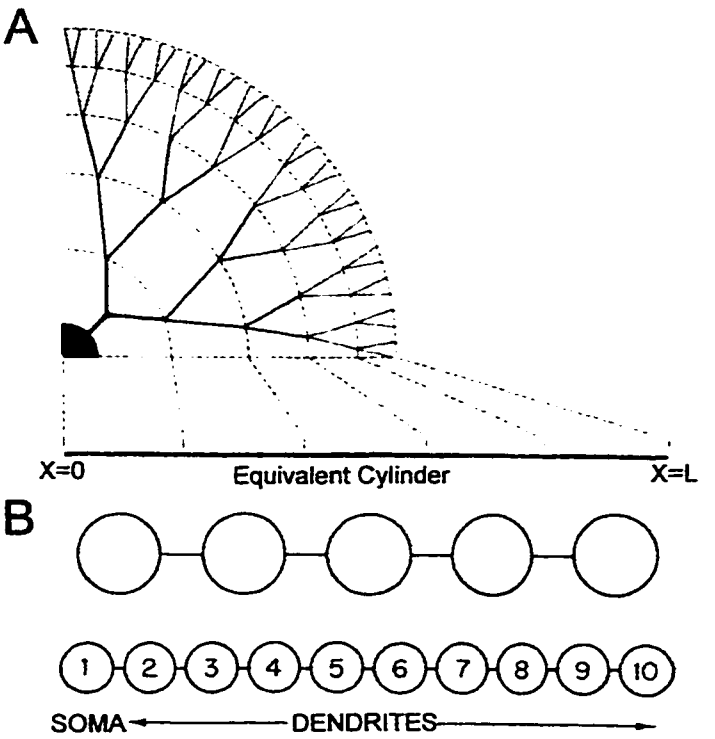
A
X=0
Equivalent Cylinder
X=L
B
1
2
3
4
5
6
7
8
9
10
SOMA
DENDRITES

Figure 2. The size and shape of EPSPs at the soma depends upon location

From Rall (1977). Shown in dimensionless units are the EPSPs that would reach the soma if they originated at different points (labeled as E's in the corresponding 10 compartment diagram) along the equivalent cable, shown in this figure as 10 linked compartments. Compartment 1 represents the soma and each compartment after that represents a 0.2λ increase in electrotonic length with the total electrotonic length of the compartments equal to 2λ.

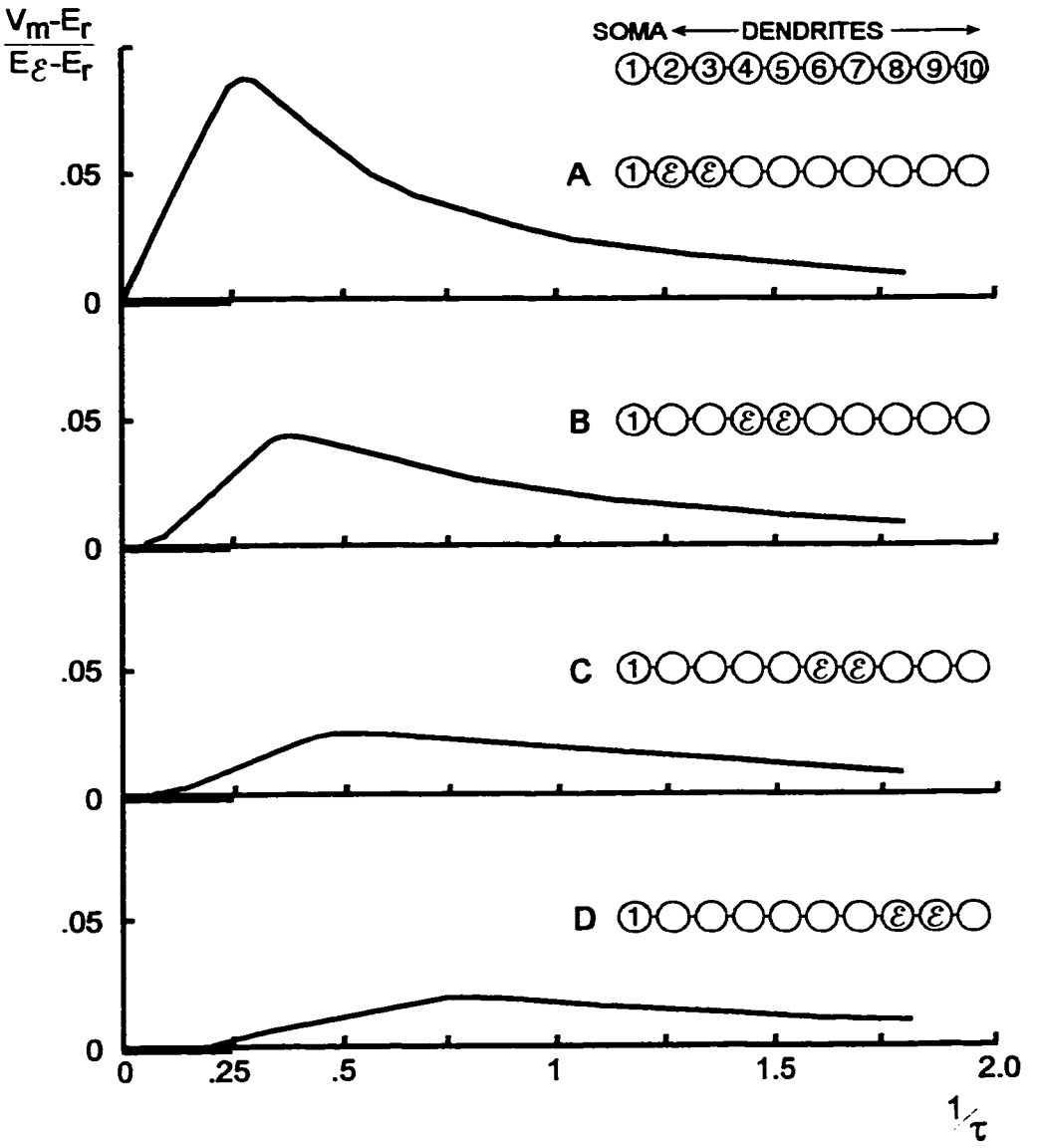
$\frac{V_m-E_r}{E_\mathcal{E}-E_r}$
SOMA ← DENDRITES →
1 2 3 4 5 6 7 8 9 10
A
B
C
D
.05
0
0
.25
.5
1
1.5
2.0
1/τ

CHAPTER 1: METHODS AND MATERIALS

TISSUE PREPARATION

Slices of sensorimotor cortex were obtained from 24 - 90 day old Srague-Dawley rats of either sex as described previously (Cerne and Spain, 1997). Rats were anesthetized with intraperitoneal injections of a 3:1 mixture of ketamine (100 mg/ml) and xylazine (20 mg/ml). Once the animal was areflexive to strong foot pinch, the carotid arteries were cut and sensorimotor cortex was excised. To excise the sensorimotor cortex, two cuts were made perpendicular to the midline of the brain. The first cut was 1 mm rostral to the bregma and the second cut was 2 mm caudal from the bregma. A third cut was made along the midline between the two cuts. Finally, the block of tissue was removed from the brain by a horizontal cut underneath the cortex. (Zilles, 1985). Either 350 μM or 400 μM thick coronal slices were cut on a Vibratome and maintained at 33° C in a carbogenated (95% O_2-5% CO_2) ringer solution containing (in mM) 130 NaCl, 3 KCl, 2 $CaCl_2$, 2 $MgCl_2$, 1.2 NaH_2PO_4, 26 $NaHCO_3$, and 10 dextrose (pH 7.4). For recording, slices were transferred to a submerged-type chamber (volume = 0.5 ml) and perfused at 2.5 ml per minute with the carbogenated Ringer Solution (34±1° C).

INTRACELLULAR RECORDING

Recordings were performed intracellularly on the presumed somata of layer V pyramidal neurons. Recording electrodes were made from borosilicate glass (O.D/I.D= 1.0 mm/0.58 mm, Sutter Instruments, Novato, CA), pulled on a Flaming/Brown Micropipette Puller P-87 (Sutter Instruments, Novato, CA), and filled with 2.7 mM KCl and 1% biocytin. Electrode resistance was 25 - 60 MΩ. For cells recorded with KCl electrodes, all action potentials peaked above 0 mV. The average resting potential was -74±1 mV (SEM, n=34) and the average input resistance was 21±1 MΩ (SEM, n=34). Input resistance was measured from the end of 5-10 mV hyperpolarizing responses evoked by 1 s negative current pulses. For some experiments, electrodes also contained 50 mM QX-314 (Alomone Labs or Sigma). Cells recorded with QX-314 had an average resting membrane potential of -69 ±1 mV (SEM, n=22) and an average input resistance of 67±11 MΩ (SEM, n=22), measured as noted above. For cells recorded with QX-314 electrodes, the baseline holding potential remained steady (±2 mV) after 40 minutes. If the baseline holding potential for neurons recorded with QX-314 electrode began to steadily depolarize (increase by > 5mV in 15 sec), the neuron was considered to be unhealthy and recording was stopped. The reasons for differences between KCl and QX-314 recordings are discussed in next chapter.

Recording was done in current-clamp using the bridge mode of an AxoClamp amplifier (Axon Instruments, Foster City, CA). Current and membrane potential were low-pass filtered (5 kHz) and recorded on videocassettes using pulse-code

modulation (44 kHz) (Neuro-Corder DR-890, Neurodata, NY, NY). All stimulating protocols, data collection, and analysis were computerized using Igor Pro (WaveMetrics, Inc. Lake Oswego, Oregon) on a Quadra 800 (Apple Computers, Cupertino, CA) and an ITC16 computer interface (Instrutech, Great Neck, NY) using customized programs (See Appendix). During the experiment, both evoked and simulated EPSPs were digitized at 0.1 ms. Measured values are reported as mean ± SEM. Unless otherwise stated, all statistical comparisons were performed using a two-tailed Student's t-test with the significance criterion set at $P<0.05$ and done using SPSS 7.5 (SPSS, Inc). Gaussian curves were fit to histograms using a non-linear, least-squares fitting routine (Levenberg-Marquardt algorithm).

HISTOLOGY

During the course of these experiments, two techniques were used to recover morphological information about the recorded cell. The histology was necessary to ensure that the apical dendrite reached past the cut since horizontal pathways in layer 1 were being stimulated to create the distal EPSP. After recording all tissue was fixed for 4-24 hours at 4°C using 4% paraformaldehyde in a phosphate buffer solution (PBS) containing (in mM) 19 NaH_2PO_4, 83 Na_2HPO_4, 150 NaCl, 3 KCl. Once fixed, tissue was either sliced further or left in whole-mount sections. The tissue was then processed using either a diaminobenzidine reaction or an avidin conjugated fluorescent probe that would react with the biocytin that had diffused into the cell during recording. Most tissue in this

study was in whole-mount sections and most cells were visualized using Neutra-avidin conjugated Oregon Green (Molecular Probes, Eugene, OR).

In order to section the tissue further, the fixed tissue was cured in 30% sucrose PBS for at least 8 hours at 4°C. The tissue was then sectioned from an approximately 400 µm slice into 4-7 80 µm slices using a sliding knife microtome. All sectioned tissue was processed using a diaminobenzidine reaction to biocytin using a VectaStain ABC kit (Vector Laboratories, Burlingame, CA) based on methods from previous studies (Horikawa and Armstrong, 1988). The tissue was mounted on microscope slides, washed, dehydrated, and defatted following standard protocol. In addition, the slices were counterstained with Cresyl Violet, coverslipped in permount and then viewed with bright-field microscope.

This method was inadequate for two reasons. Sectioning the tissue caused it in some cases to tear at the cut. Additionally, small sections of tissue could be lost during sectioning. In some cases, I was unable to confirm that the dendrites remained intact past the cut and thus had to exclude the cell from analysis. For this reason, the tissue was left in whole mount sections and the DAB reaction performed as before. This allowed visualization of the entire cell with its dendrites. The thicker tissue in whole mounts did not dry well and thus were only coverslipped in glycerol and were not defatted and stained as before.

To circumvent the high DAB background staining, a florescent probe that cross-reacts with biocytin was used to visualize the recorded neuron in whole-mount tissue. This alternative procedure had the advantages of allowing the use of the confocal microscope to visualize the fine dendritic processes in three dimensions. Three florescent dyes were used: Texas-Red, Texas-RedX or Oregon Green (Molecular Probes, Eugene OR) for 4-6 days. Oregon Green was used predominately because it produced much lower levels of background than the Texas Red dyes (see Figure 3A for example). The slices were incubated for 4-7 days in a solution of PBS with a 1:100 dilution of florescent probe at 8°C. Triton X (0.5%) was also added to enhance dye penetration into the tissue. With the florescent dye visualization of the fine dendritic and some of the axonal processes was possible. Twenty-one of the 62 cells used in analysis were processed using DAB reaction including 2 cells as whole mounts. Of the remaining 41 cells imaged using florescent probes , 39 were visualized using Oregon Green, while 2 were imaged using Texas Red-X.

ISOLATION OF EPSPS

Figure 3 shows the method used to isolate two sites of stimulation, so that stimulation at one site did not affect fibers stimulated by the other site. A small piece of razor blade was guided by a micromanipulator to make a cut in the slice just below layer I. The cut extended from near the apical dendrite of the recorded neuron to the lateral edge of the slice. The distal stimulating electrode (Ds) was placed in layers 1-2 (above the

cut) and the more proximal stimulating electrode (Px) was placed below the cut in lower layer 3 to upper layer 5. While using a dissecting scope to observe the tissue, both electrodes were placed the same horizontal distance from the soma and 150 to 350 μm lateral from the end of the cut nearest to the apical dendrite. After recording, a diagram was made of the slice with the cut and the location of the two stimulating electrodes. This diagram was used with the histologically processed tissue to determine the distance of the proximal and distal stimulating electrodes from the apical dendrite. The distal stimulating electrode was approximately 200 to 500 μm from the middle of the distal tuft, while the proximal stimulus was approximately 200 to 500 μm from the main trunk of the apical dendrite and 150 to 300 μm toward the pia from the soma.

To isolate AMPA-receptor mediated EPSPs, slices were perfused continuously with 3 μM bicuculline (to block $GABA_A$-receptor mediated responses) and 100 μM AP-5 (to block NMDA-receptor mediated responses). The slices were perfused for at least 20 minutes before summation experiments were performed. These neurons had little or no $GABA_B$-mediated responses at the low stimulus strengths used in this study (Benardo, 1994; van Brederode and Spain, 1995). Furthermore, as shown in Figure 4, the EPSPs elicited in these experiments were completely blocked by 20 - 60 μM DNQX (Tocris Cookson, St. Louis, MO). Residual EPSPs or IPSPs were not seen at holding potentials of -69 to -97 mV.

In most experiments, fine point monopolar stainless steel electrodes were used. In the remaining experiments, concentric bipolar electrodes were used (FHC Inc., Bowdoinham, ME). Each stimulating electrode was separately driven by a constant-current Stimulus Isolator A365 (WPI, Sarasota, FL) using either a 1 ms or 0.2 ms TTL pulse. The current amplitude (range, 1.7 to 70 μA) was adjusted so that the isolated EPSPs were at least 1 mV, but below the amplitude that evoked large regenerative depolarizations. When recording with KCl electrodes, these regenerative depolarizations were characterized as action potentials on a slower depolarizing envelope. When recording with QX-314 electrodes, these regenerative depolarizations were large slow depolarizations with a peak amplitude frequently greater than 50 mV from the baseline potential. With either type of electrodes, these regenerative events typically had a delayed latency of at least 30 - 40 ms and were a consequence of having inhibition partially blocked (Chagnac-Amital and Connors, 1989). They did not occur before the addition of bicuculline to the bath.

I looked for possible interactions between the two stimulus sites by comparing responses from paired Px and Ds stimuli with responses from paired-pulses at one of the stimulus sites. Paired-pulse facilitation and paired-pulse depression result from stimulating the same fibers twice within 10 to 1000 ms (Gil, et al., 1997). If the two stimuli in these experiments are stimulating some of the same fibers, then paired-pulse depression or paired-pulse facilitation should be observed when the Px and Ds stimuli are given 50-70 ms apart (Gil, et al., 1997). In some cases, I observed paired-pulse

facilitation or depression when the Px-Px or Ds-Ds paired stimuli were separated by 50 - 70 ms between stimuli. In contrast, I did not observe any paired-pulse facilitation or paired-pulse depression for Px-Ds or Ds-Px paired stimuli when the proximal and distal stimuli were 50 - 70 ms apart (Figure 5).

The distal and proximal EPSPs appeared to be arriving at the soma from different distances. The latency of the Ds evoked EPSP was significantly longer, 4.9±0.2 ms, than the latency, 2.9±0.1 ms, of the Px EPSPs. These results are consistent with previous studies in which EPSPs from layer 1 stimulation had longer delays compared to EPSPs generated from stimulation closer to the soma (Cauller and Connors, 1994). They are also consistent with predictions from the Rall model (See Figure 1-Introduction) in which the rising phase of the most distal inputs is later than the rising phase of the more proximal inputs. Linear cable theory also predicts that the rates of rise for distal inputs will be slower than the rate of rise for more proximal inputs (Rall, 1977). In my experiments, the distal EPSPs took a significantly longer time to reach their peak amplitude (7.3 ± 0.4 ms) compared to the proximal EPSPs (5.0 ± 0.2 ms). Inconsistent with a purely passive dendritic tree, the 20 to 80% rate of rise for both Px and Ds EPSPs were not significantly different (1.3±0.2 mV/ms for Px EPSPs compared to 1.1±0.2 mV/ms for Ds EPSPs, Figure 6). This result indicates that some of the rising shape of the EPSPs may be due to voltage-sensitive conductances. Previous studies have shown that postsynaptic dendritic conductances can also affect relative rates of rise of EPSPs evoked by proximal and distal stimuli (Nicoll, et al., 1993; Stuart and Spruston, 1996). Based on

the longer latency and the slower time to peak for EPSPs evoked by distal stimulation, it is likely that they are being generated farther away from the soma than the EPSPs evoked by proximal stimulation.

STIMULATION PROTOCOL

Experimental protocols for stimulation were given as shown in Figure 7A. First, the Ds and Px stimuli were given individually 10 - 15 times each at a rate of 0.33 Hz. The two stimuli were then given together 15 - 20 times (with interstimulus delay ranging from 0 to 30 ms). Finally, the individual Px and Ds stimuli were again delivered 10 - 15 times each. Analysis was performed on the averaged responses to individual Px, Ds, and simultaneous Px plus Ds evoked EPSPs. For each cell-summed EPSP (response from both stimuli), I checked for nonstationarity of EPSPs by comparing the first 15 ms integral of the algebraic sum of the individual Px and Ds EPSPs evoked before the cell-summed EPSP to the same integral from the individual Px and Ds EPSPs evoked after the cell-summed EPSP. Figure 5B shows the stability of evoked EPSPs during the course of the stimulation protocol. Data was only used from the EPSPs whose algebraically summed integral changed by less than 15%, which was chosen based on the amount of random EPSP size fluctuations observed in these experiments.

Figure 3. Experimental setup

Experimental setup used to measure EPSP summation. *A*, Photomicrograph of florescently labeled biocytin-filled layer V pyramidal neuron in a 400μM thick slice taken from rat neocortex. Solid line indicates where a cut was made in the tissue to isolate two stimulation sites (•) which are labeled Ds and Px. Scale bar, 125 μM *B*, Superimposed individual responses from 1 ms stimulating pulses delivered at the two stimulating sites. Stimulation intensity was 8.5 μA for Ds and 2.8 μA for Px. The lower traces, labeled "Ds and Px", are the responses resulting when these two stimuli are given simultaneously. Holding potential in all traces is -76 mV.

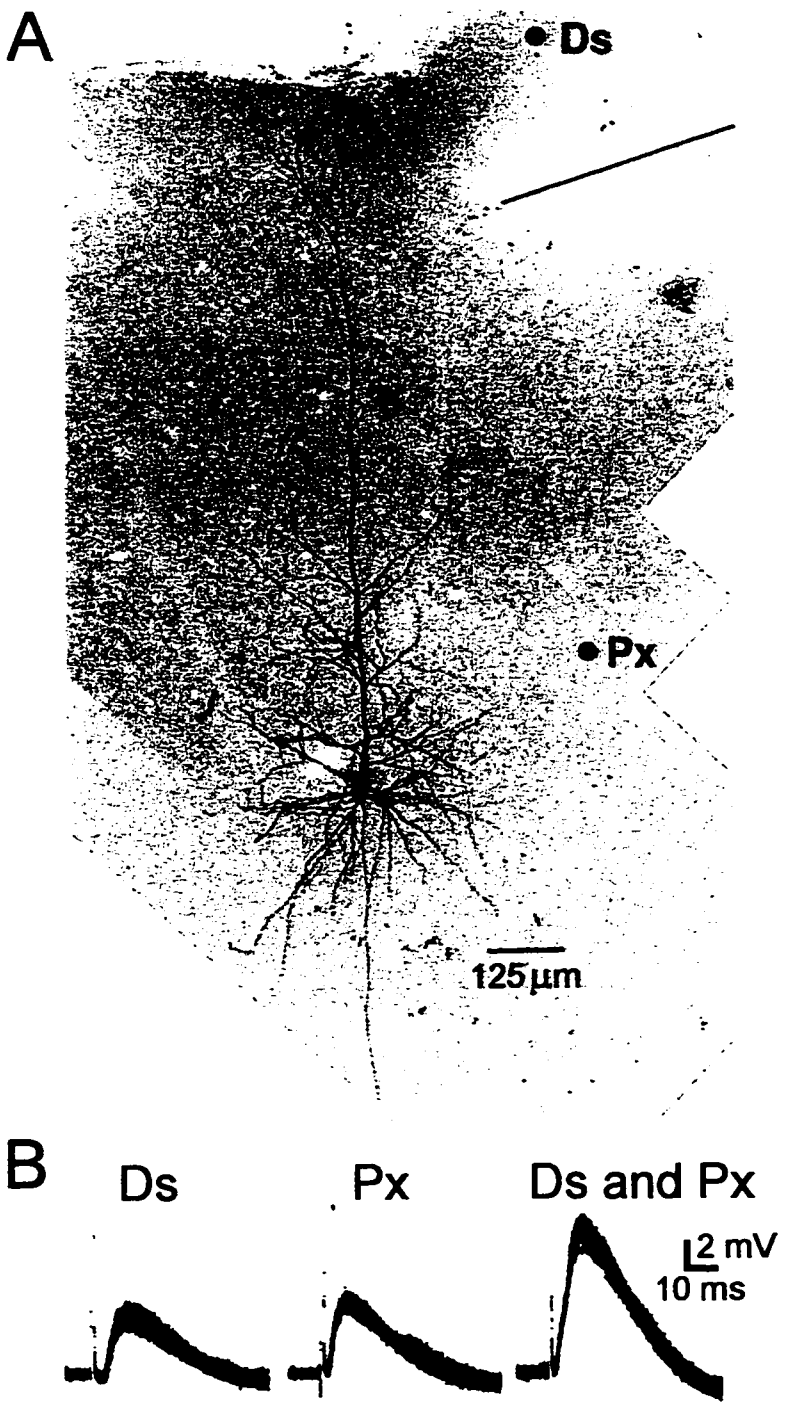
A
Ds
Px
125 µm
B
Ds
Px
Ds and Px
2 mV
10 ms

Figure 4. Block of EPSPs by DNQX

EPSPs in experimental protocol were completely blocked by DNQX demonstrating that they were AMPA mediated. Both Px EPSPs (*A*) and Ds EPSPs (*B*) were blocked over time by the addition of 20 μM DNQX to the bath solution. *A*, Px EPSPs were from a 1 ms, 3.3 μA stimulus pulse. *B*, Ds EPSPs were from a 1 ms, 60 μA stimulus pulse. The traces are the average of 4-9 responses. The calibration bar is for all traces.

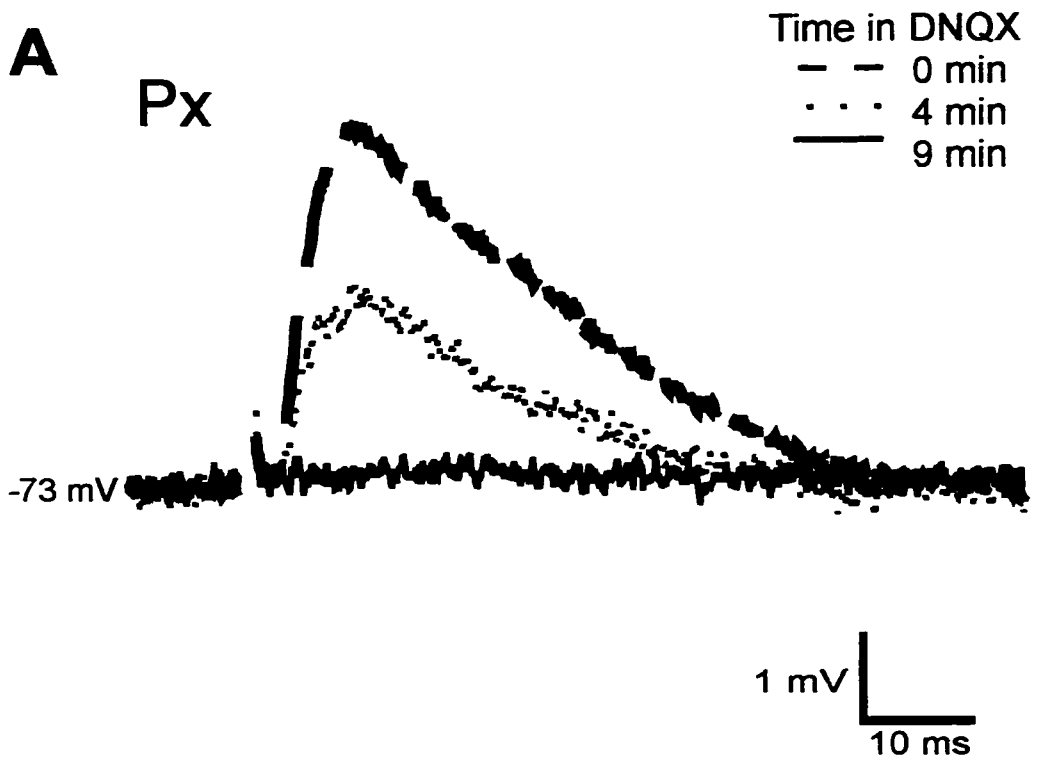
A
Px
Time in DNQX
0 min
4 min
9 min
-73 mV
1 mV
10 ms
B
Ds
-73 mV

Figure 5. Paired-Pulses

A. Averaged response to two proximal stimuli (2.9 μA) spaced 50 ms apart showing paired-pulse depression of the Px EPSPs. The dashed line is the first Px EPSP offset 50 ms for comparison with the second Px EPSP. B. Averaged response to a proximal stimulus (2.9 μA) followed 50 ms later by a distal stimulus (13 μA). For comparison the response to the distal stimulus alone is shown as a dashed line and is offset to line up with the second Ds EPSP. In both A and B, the traces are the average of 9 to 15 individual responses.

A. Paired Pulses Px + Px

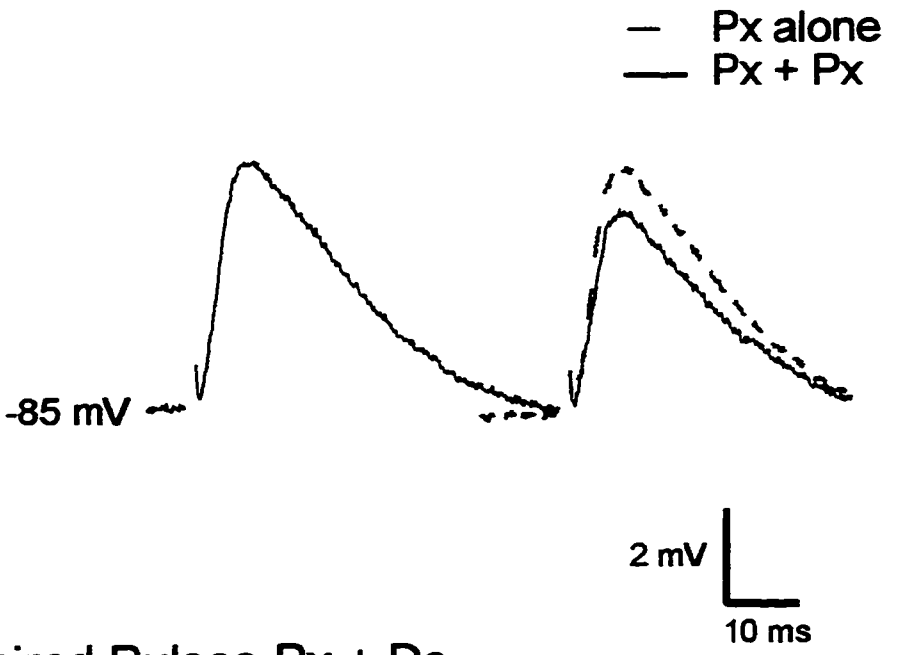

B. Paired Pulses Px + Ds

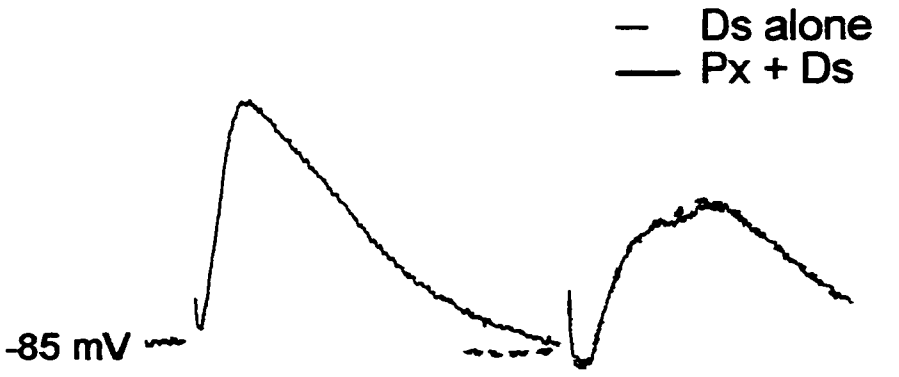

Figure 6. Rise and Latency of EPSPs.

Example EPSPs from the same cell demonstrating that distally evoked EPSPs (Ds) were delayed compared to proximally evoked EPSPs (Px). Latency of Ds EPSP was 4.4 ms compared to 2.6 ms for Px EPSP. Additionally, the time to peak of the Ds EPSP (8.5 ms) was longer compared to the Px EPSP (4.8 ms) although both EPSPs had similar 20-80 % rates of rise (1.3 mV/ms for Px, 1.1 mV/ms for Ds). Traces are the average of 15 individual EPSPs from 1 ms pulses of 3.0 μA for the Px EPSPs and 7.0 μA for the Ds EPSPs.

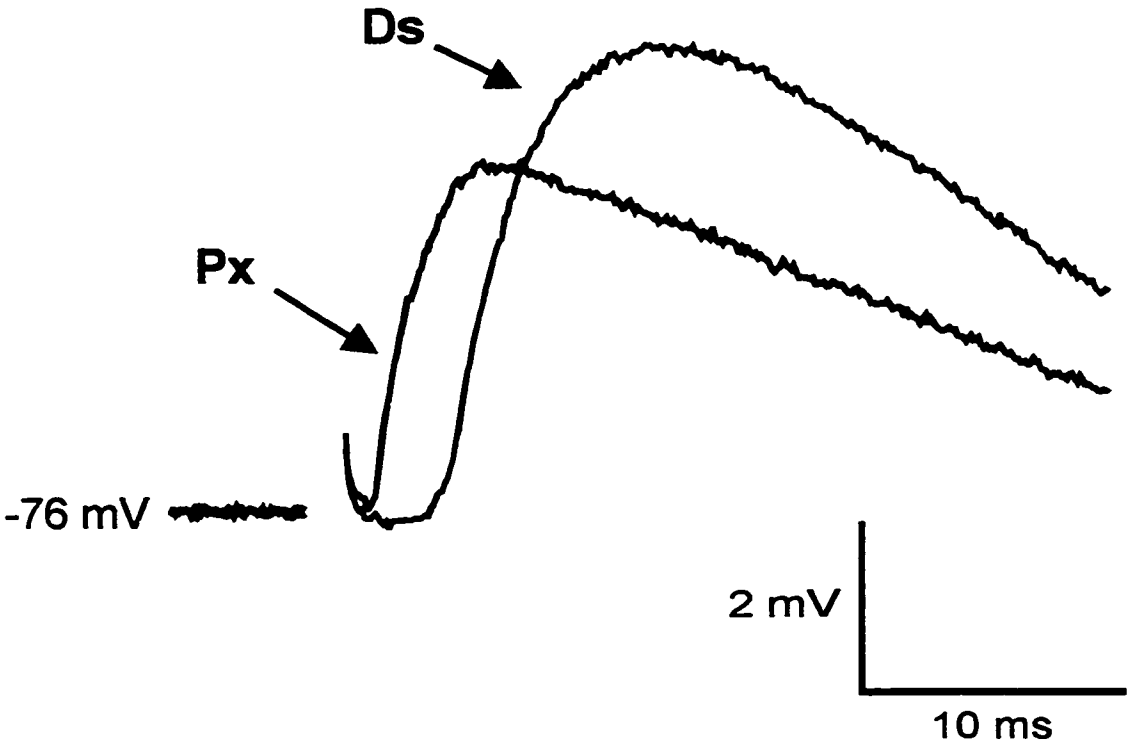
Ds
Px
-76 mV
2 mV
10 ms

Figure 7. Stimulation protocol

Stimulation protocol used showing stability of EPSPs. *A*, Sequential EPSP traces from one summation experiment from which one SR value will be determined. First, a 3.3 μA proximal stimulus (Px1) was given followed by a 12.3 μA distal stimulus (Ds1) and then both stimuli were given simultaneously (Px and Ds). This was followed by the same distal stimulus (Ds2) followed by the same proximal stimulus (Px2) being given again. For clarity, only the first 10 traces from each stimulus group are shown and the time between EPSPs has been removed. In the experiment itself stimuli were given 3 sec apart. *B*, Areas of each EPSP are shown over the course of the experiment. The area is limited to the first 15 ms after the start of the EPSP.

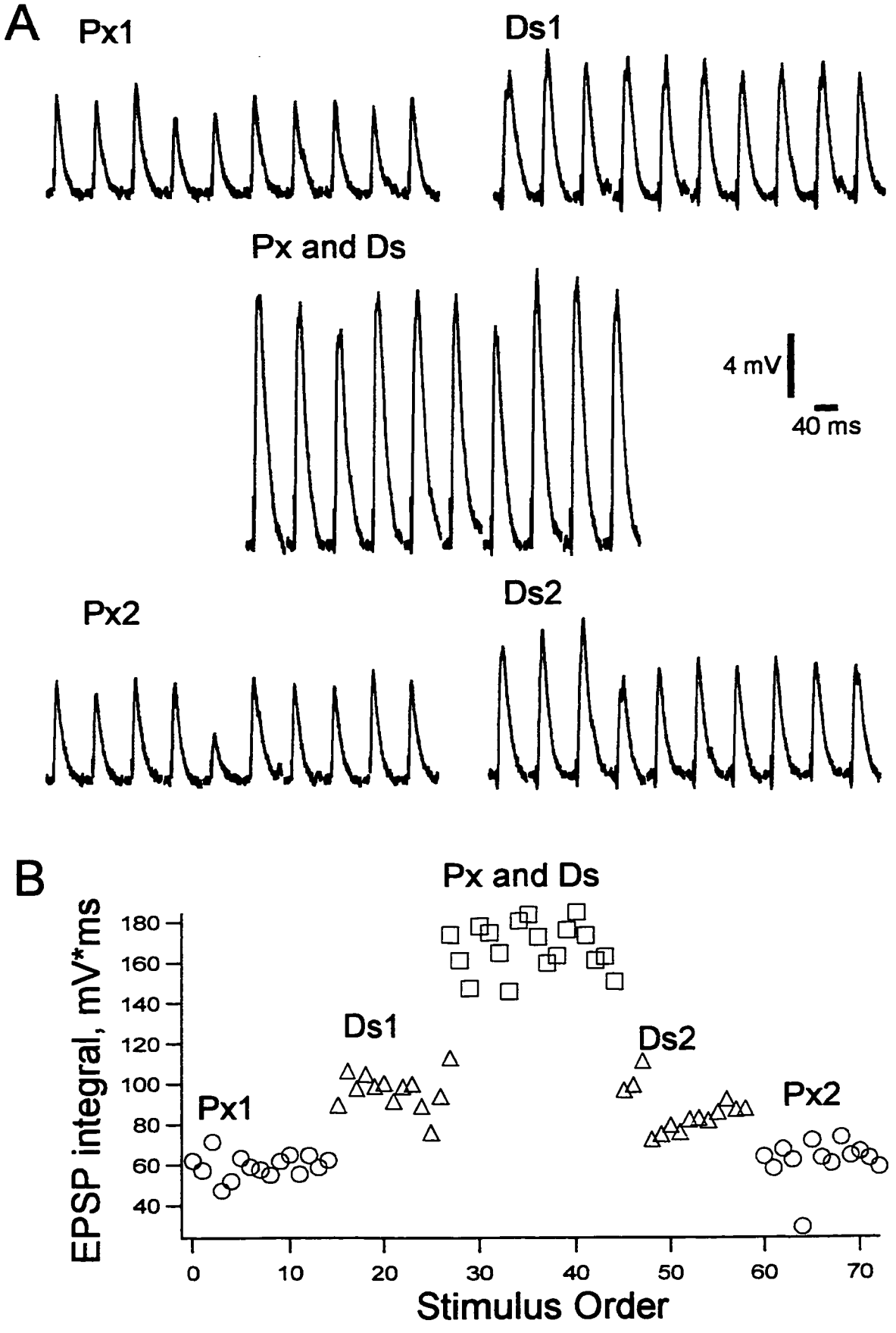
A
Px1
Ds1
Px and Ds
4 mV
40 ms
Px2
Ds2
B
Px and Ds
Ds1
Ds2
Px1
Px2
EPSP integral, mV*ms
180
160
140
120
100
80
60
40
0
10
20
30
40
50
60
70
Stimulus Order

CHAPTER 2: NON-LINEAR SUMMATION IS QX-314 SENSITIVE.

INTRODUCTION

The Rall model and other linear cable models based on passive dendrites predict that synaptic inputs will sum linear or sublinearly. Sublinear summation is expected if there is decrease in the synaptic driving force (Rall, 1977) or a transient decrease in the membrane resistance due to synaptic conductance changes (Bernander, et al., 1991). Other studies have found that summation of synaptic inputs will depend upon voltage-sensitive conductances (Cash and Yuste, 1998). To test whether passive or active dendritic properties affected EPSP summation, I first determined if EPSPs in layer V summed linearly or nonlinearly. The next goal was to demonstrate that the nonlinear summation was due to active conductances by blocking postsynaptic voltage-sensitive conductances with intracellular QX-314.

MEASUREMENT OF SUPERLINEAR SUMMATION

As shown in Figure 3, two stimulating sites, (one distally, Ds, and the other proximally, Px, located) were used to measure EPSP summation in layer V pyramidal neurons. To determine if the Ds and Px evoked EPSPs summed linearly, the method shown in Figure 8 was used. The integral of the EPSP generated in response to the simultaneous stimulation at the Px and Ds sites was divided by the integral of the

algebraic sum of the individual Px and Ds evoked EPSPs to give a summation ratio (SR). As discussed in the previous chapter, the latency of the Ds EPSP was longer than the latency of the Px EPSP (4.9±0.2 ms compared to 2.9±0.2 ms). The integrals were limited to a 15 ms interval beginning 1 ms after the start of the distal EPSP so that late occurring polysynaptic events were not included. These late polysynaptic events were likely to occur due to presynaptic interactions between the two stimuli. Since these late events may not have been presynaptically isolated from each other, they were excluded from analysis.

Figure 10C shows the distribution of SR values measured in normal neurons (i.e., recorded with KCl electrodes). For these cells the mean SR of 1.12±0.02 (n =74 SR measurements from 23 cells) was significantly greater than 1, the expected SR value of linear summation. There was also a wide range of SR values (0.81 – 1.73) in these neurons and the distribution was skewed to the right. Excluding the lower and upper 10% of SR measurements, the remaining 80% of SR values were from 0.98 to 1.31 indicating that the majority of EPSPs summed linearly to superlinearly.

EFFECTS OF QX-314

A goal was to determine if postsynaptic conductances contributed to non-linear summation of synaptic inputs. Therefore, the SR was also determined for a set of neurons filled with QX-314. Figure 9 shows the effects of QX-314 on layer V pyramidal neurons. QX-314, a permanently charged lidocaine derivative has been shown to internally block several voltage-sensitive conductances: Na^+ (Strichartz, 1973), some

types of K^+ (Andreasen and Hablitz, 1993), Ca^{2+} (Talbot and Sayer, 1996), and I_h (Perkins and Wong, 1995). In the presence of QX-314, neurons ceased firing action potentials. The effects of QX-314 were time dependent. The input resistance increased and the IV relationship changed for the first 40 minutes after impalement (Figure 9C) indicating that QX-314 may take time to diffuse into the dendrites. Because of this time dependence of QX-314, EPSP summation was measured after cells had been recorded from for at least 40 minutes. The 22 cells recorded with QX-314 electrodes had significantly higher input resistance (67±11 MΩ, measured after 40 minutes recording). Resting membrane potential was also significantly more depolarized in the QX-314 loaded cells (69±1 mV) compared to cells recorded without QX-314 (-74 ± 1 mV). The more depolarized resting membrane potential in QX-314 loaded cells was correlated with the higher input resistance caused by QX-314. QX-314 loaded cells with input resistances less than 50MΩ did not have significantly different holding potentials (-72±1, n=9) compared to KCl recorded cells. The IV relationship was also more linear with the loss of hyperpolarization-activated inward rectification consistent with previous studies (Perkins and Wong, 1995). By blocking many of the postsynaptic conductances thought to be responsible for nonlinear summation, this method allowed me to determine how a neuron's intrinsic conductances affect EPSP summation. One limitation is that these experiments may not account for all non-linear summation, particularly sublinear summation, since QX-314 does not necessarily block all voltage-sensitive conductances.

Additionally, QX-314 would not block any sublinear summation caused by changes in driving force or synaptic conductance change (e.g., shunting).

The distribution of SR values obtained with QX-314 in the recording electrode is shown in Figure 10. On average the EPSPs summed linearly with a mean SR of 1.00±0.02 (n = 34 SR values from 14 cells) which was significantly smaller than the SR values measured with KCl electrodes (1.12±0.02). For both groups of neurons, SR values were measured under the same range of EPSP sizes and holding potentials (see also Figure 11 and Figure 12). Comparing the distribution of SR values measured in neurons with and without QX-314 revealed other differences. First, the range of SR values measured with QX-314 electrodes was smaller (0.82 - 1.33) and the middle 80% of SR values fell around 1 between 0.88 and 1.09. Second, the distribution of SR values from QX-314 loaded cells was well fit by a Gaussian curve with a peak at SR = 0.99 similar to the mean (Figure 10D). In comparison, the distribution of SR values from cells recorded with KCl electrodes was skewed to the right.

To understand what factors may underlie the skewed SR distribution measured for neurons recorded with KCl electrodes, the SR values were split into two groups using the distribution of SR values measured for QX-314 filled neurons as a baseline for linearity. Based on the Gaussian fit to the data from QX-314 filled cells, an upper 95% confidence limit of 1.16 was determined. From the SR values in neurons recorded with KCl electrodes, 23% were above the 95% cutoff limit and were thus

considered to show clear cut superlinear summation. Figure 10A shows an example of EPSPs with a large amount of superlinear summation measured with KCl electrodes, while Figure 10B shows EPSP summation from a typical QX-314 loaded cell.

It should be noted that the SR values above the 95% confidence limit are not the only ones contributing to superlinear summation. When the SR distribution from neurons recorded without QX-314 was normalized by removing SR values greater than 2 standard deviations from the mean, the SR values were still significantly larger than SR values obtained from QX-314 filled cells. When fit to a Gaussian curve, the SR values measured with KCl electrodes that were within two standard deviations of the mean had a peak SR of 1.07. This peak was 0.08 SR units higher than the peak SR measured using QX-314 electrodes. The smaller mean and more restricted range of SR values found in QX-314 filled neurons indicate that QX-314 sensitive conductances are contributing to superlinear summation.

SUMMARY

EPSPs summed in a greater than linear fashion. QX-314 reduced the amount of superlinear summation indicating that a postsynaptic mechanism was responsible. Unlike previous measurements in spinal motoneurons and pyramidal hippocampal neurons that measured sublinear to linear summation of EPSPs (Burke, 1967, Cash and Yuste, 1998), I observed linear to superlinear summation. Succeeding

chapters will focus on how other factors (i.e., membrane potential, time and dendritic conductances) contribute to EPSP summation.

Figure 8. Measurement of Summation Ratio.

Deviation from linearity of EPSP summation is quantified using the summation ratio, SR. The SR was calculated for summed EPSPs using the equation shown in the figure. The algebraic sum (dashed line) was calculated as the linear sum of the averaged proximally (Px) evoked EPSP with the averaged distally (Ds) evoked EPSP (the individual average Px and Ds evoked EPSPs are shown as thin solid lines). The cell's sum (thick solid line) was the average response evoked by simultaneous stimulation of both the Px and Ds stimulation sites. SR was then calculated as the area under the cell's sum divided by the area under the algebraic sum. The area used to calculate SR was limited to the first 15 ms beginning 1 ms after the start of the second EPSP or the Ds evoked EPSP when the Ds and Px were evoked simultaneously.

$$SR = \frac{\text{area of cell's sum ( )}}{\text{area of algebraic sum ( )}}$$

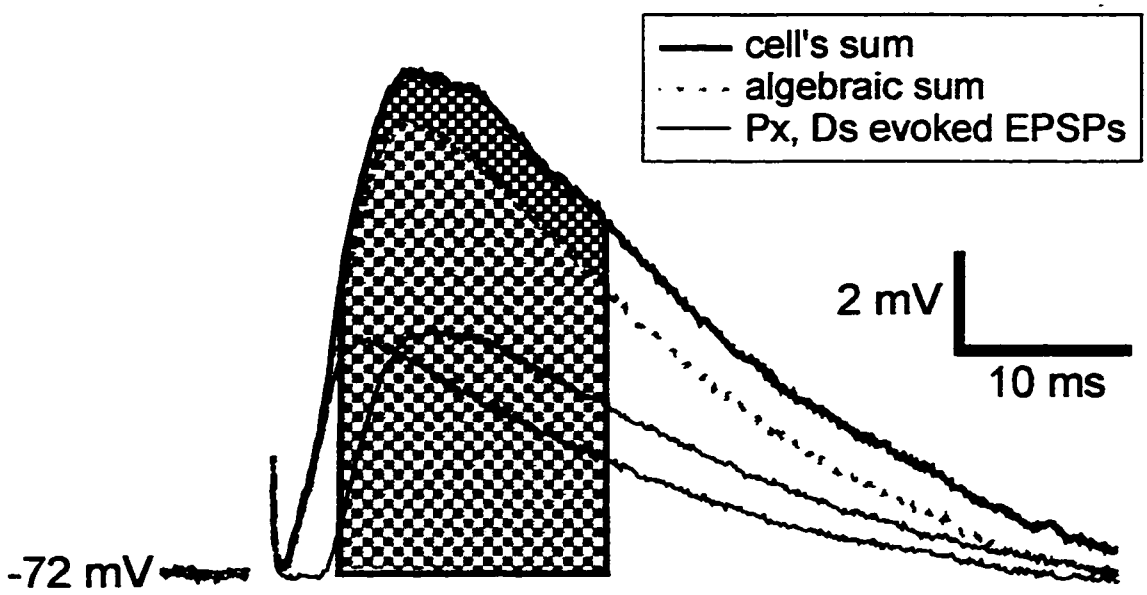

Figure 9. QX-314 blocks post-synaptic conductances

A, Steady state IV relationship in a cell recorded with KCl electrodes (example traces shown in *B*), and in a cell recorded with QX-314 electrodes at 15 minutes after impalement (traces shown in *C*) and at 38 minutes after impalement (traces shown in *D*). In *B-D*, voltage responses are above the corresponding current pulses. The scale bars are for all traces in *B-D*. Note that in the presence of QX-314 the cell ceased firing indicating block of Na^+ current and that the sag and rebound typical of layer V pyramidal cells reduces over time in the QX-314 loaded cell. Baseline holding potential for all traces was -72 mV.

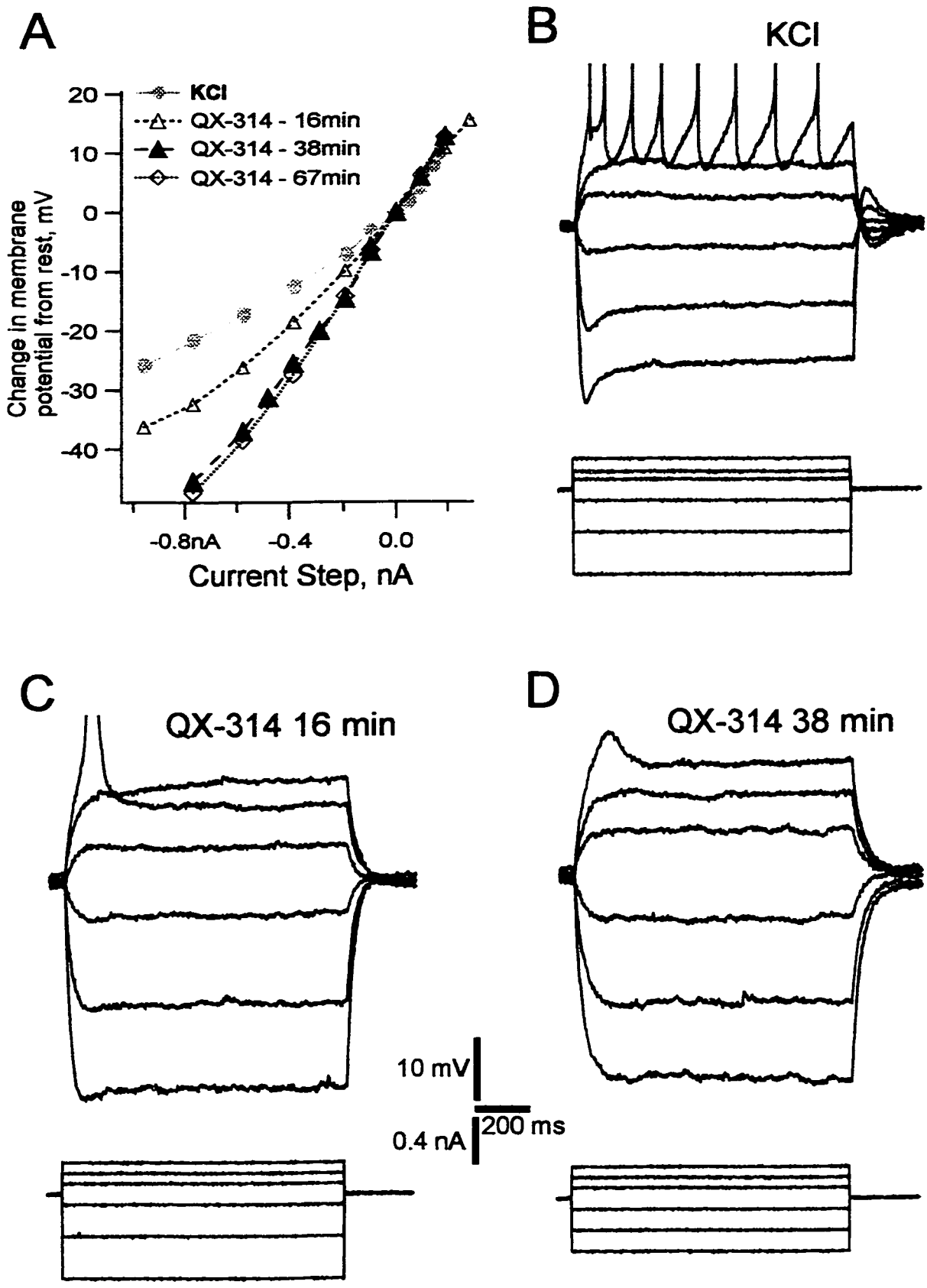
A
KCl
QX-314 - 16min
QX-314 - 38min
QX-314 - 67min
20
10
0
-10
-20
-30
-40
Change in membrane potential from rest, mV
-0.8nA
-0.4
0.0
Current Step, nA
B
KCl
C
QX-314 16 min
D
QX-314 38 min
10 mV
0.4 nA
200 ms

Figure 10. Summation of EPSPs with and without QX-314.

Superlinear summation of EPSPs is due to QX-314 blockable conductances. *A*, An example of superlinear summation of EPSPs evoked in a neuron recorded with only KCl in the electrode (KCl). *B*, A typical example of linear summation of EPSPs evoked in a neuron recorded with an electrode that also contained QX-314 (QX-314). *C*, Histogram distribution of all SR values measured from neurons recorded with KCl electrodes (KCl). *D*, Histogram distribution of all SR values from neurons filled with QX-314. The histogram was fit to a Gaussian curve (solid line) and the upper 95% confidence limits were determined (dashed vertical lines). For both *C* & *D*, all SR values were obtained from summed EPSPs where the Px and Ds stimuli were delivered simultaneously. Bin width for both histograms was 0.04 SR units. More than one SR value may be from the same cell but under different conditions (e.g., holding potential, or stimulus intensity; KCl: 74 SR values measured in 23 neurons, QX-314: 34 SR values measured in 14 neurons). For both types of cells, the range of conditions used to gather the data was similar (see Figures 4 & 5). The non-normal nature of the data from neurons recorded with KCl electrodes was not extreme enough to prevent use of a Student's t-test. A Mann-Whitney U test yielded similar results

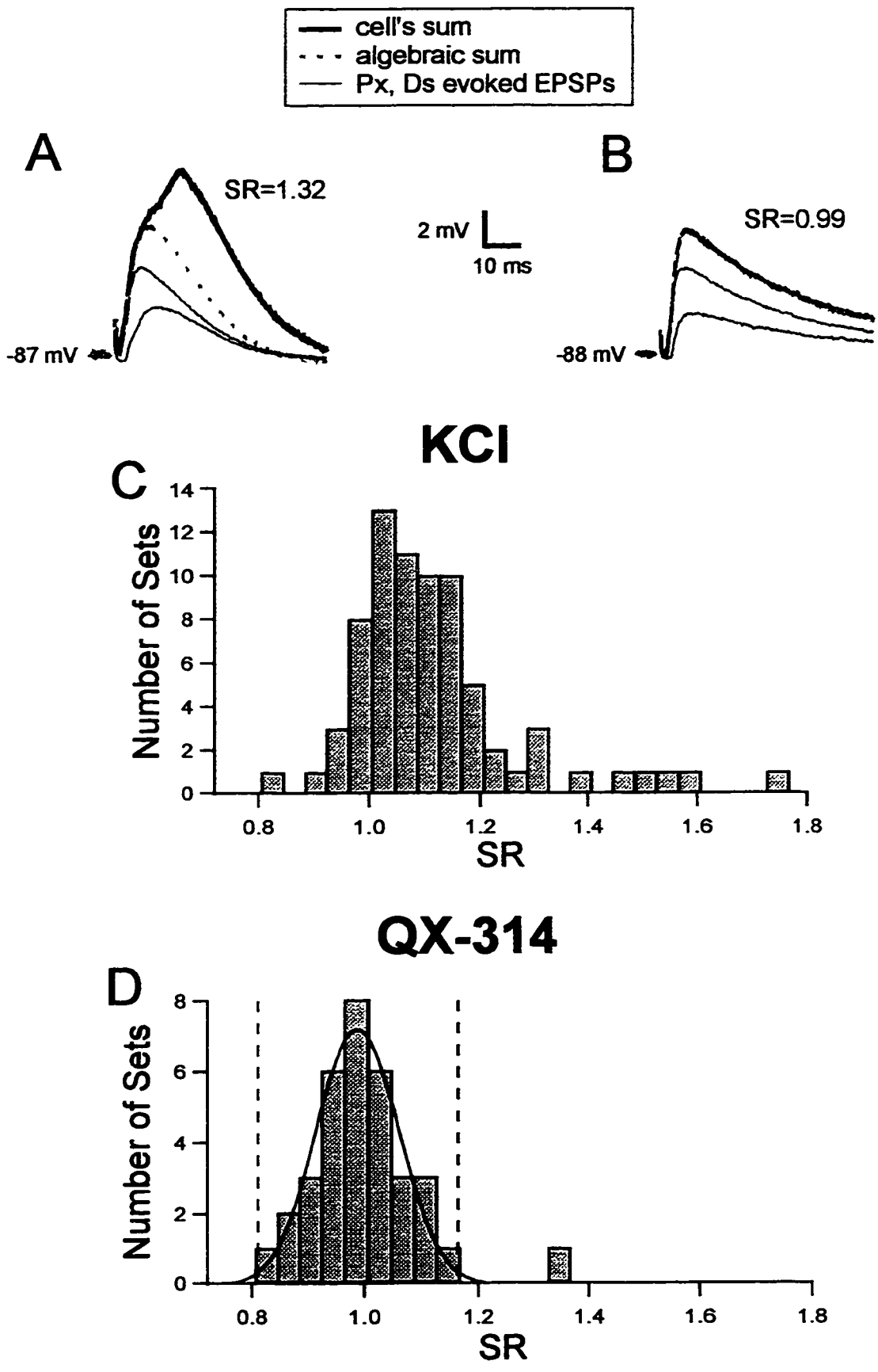
cell's sum
algebraic sum
Px, Ds evoked EPSPs
A
SR=1.32
-87 mV
2 mV
10 ms
B
SR=0.99
-88 mV
KCl
C
Number of Sets
SR
QX-314
D
Number of Sets
SR

CHAPTER 3: SUMMATION RATIO DEPENDENCE ON MEMBRANE POTENTIAL AND EPSP SIZE

INTRODUCTION

In the first chapter, I determined that EPSPs summation in layer V pyramidal neurons had a wide range of SR values (0.81 to 1.73) with most EPSPs summing linearly to superlinearly. Since the amount of superlinear summation was significantly reduced in QX-314 loaded cells, one conclusion is that one or more QX-314 sensitive conductances (Na^+, Ca^{2+}, K^+, and I_h) are responsible for superlinear summation of EPSPs. In this case, we would expect that EPSP summation should be affected by conditions that change the activation state of QX-314 sensitive conductances. I therefore looked for relationships between SR and holding potential and EPSP size, which could either activate or inactivate the Na^+, Ca^{2+}, K^+, and I_h conductances blocked by QX-314. Another possibility is that the summation of EPSPs is cell-dependent with some cells able to sum their EPSPs more non-linearly than others are.

CELL DEPENDENT EFFECTS ON SUMMATION RATIO

Layer V neocortical pyramidal cells have been categorized into two firing types, bursters and regular firing neurons (Connors and Gutnick, 1990). Bursting neurons are classified according to their ability to fire a burst of 3 or more action potentials and

are sometimes able to burst repetitively throughout a prolonged current pulse (Chagnac-Amitai, et al., 1990). Bursting neurons are also thought to have different complement of ionic conductance than regular firing neurons (Connors and Gutnick, 1990; Kim and Connors, 1993; Larkman and Mason, 1990). In particular, Kim et al (1993) postulated that dendrites of bursting cells could generate large-amplitude, prolonged spikes or plateaus. In contrast, dendrites of regular cells were postulated to only generate small, fast spikes (Kim and Connors, 1993). Kim et al. (1993) suggested that the observed difference in dendritic spikes was due to more high-voltage activated Ca^{2+} conductances in the bursting cells' dendrites than in regular-firing cells' dendrites. If burster neurons have more dendritic high-voltage activated Ca^{2+} conductances compared to regular firing neurons, than one expectation would be more superlinear summation in bursting neurons than in regular firing neurons. Contrary to this expectation, there was no significant dependence of SR on firing type. In these experiments, cells could not be clearly classified as bursters or regular firing cells. Eight cells were clearly bursters, 15 were clearly regular firing, and 9 cells varied in their firing pattern. The mean SR values among the three groups were not significantly different (burster neurons: 1.05 ± 0.02, n=12; regular firing neurons: 1.10 ± 0.03, n=23; not classified 1.04 ± 0.03, n = 13; for all SR values holding potential > -85 mV).

Typically, cells could not be grouped according to their ability to perform superlinear or sublinear summation. Instead, a wide range of SR values was obtained for different experimental conditions (i.e., changes in holding potential, EPSP amplitude)

within a given neuron. I observed that for cells with at least 3 SR measurements, the within cell variation of SR was at least half the total population variance in SR. Additionally, although only 23% of all SR values were > 1.16, 35% of all cells recorded with KCl electrodes had a least one SR value > 1.16. Therefore, the most superlinear SR values did not belong to a subset of cells. Since there did not appear to be a strong cell specific effect on SR values, all measurements were pooled for further analysis with some cells contributing more than one SR value.

EFFECT OF HOLDING POTENTIAL ON SUMMATION RATIO

In individual neurons, SR frequently increased with hyperpolarization. Figure 11A shows an example from one neuron for which SR increased from 1.10 to 1.28 while the holding potential was hyperpolarized from -71 mV to -82 mV, and the Px and Ds stimuli strengths were held constant. In the 10 cells for which the stimuli were held constant while the holding potential was hyperpolarized from between -71 and -81 mV to between -82 and -97 mV, SR values increased by 0.008±0.003 for every 1 mV hyperpolarization (Range: increase of 0.026 SR units to a decrease of 0.004 SR units for every mV of hyperpolarization). Moreover, EPSPs with more hyperpolarized holding potentials were more likely to show clear-cut superlinear summation (i.e. SR greater than 1.16). Of EPSPs with a holding potential more negative than -84 mV, 42% had SR > 1.16, while for more depolarized EPSPs only 10% were in this category. Additionally, the average holding potential for those EPSPs with SR > 1.16 was significantly more

negative (-89±2 mV, n=17) than the average holding potential for all remaining EPSPs (-80±1 mV, n=57). The entire population of SR values is shown graphically in Figure 11B where SR values are plotted as a function of the membrane holding potential. The data from neurons recorded with KCl electrodes is fit to a linear regression with a slope of -0.009±0.002 SR/mV, similar to what was found for individual cells. The slope of the regression is significantly different from zero with an R value of 0.48 indicating that 23% of the variation in SR values was due to changes in holding potential. Therefore, SR values from neurons recorded with KCl electrodes increase with membrane hyperpolarization.

In contrast, SR values from neurons recorded with QX-314 electrodes did not vary significantly with holding potential in individual cells (n=5). Likewise, for all EPSPs recorded with QX-314 (Figure 11B), the linear regression of SR versus holding potential was not significantly different from zero. The slope of -0.0005±0.0017 SR units/mV measured for the QX-314 group was significantly different from the slope measured using KCl electrodes. Therefore, one conclusion is that the increase of SR with increasing hyperpolarization is not simply due to a change in the driving force for AMPA- mediated conductance but results from QX-314 blockable voltage-dependent conductance.

EFFECT OF EPSP SIZE ON SUMMATION RATIO

The amplitude of EPSPs would also be expected to affect the amount of nonlinear summation, since larger EPSPs will activate voltage-dependent conductances to a different degree than smaller EPSPs. Unlike holding potential, EPSP amplitude had no clear effect on SR over the range of amplitudes shown in Figure 12. In individual cells where the stimulus strength of either the Px or the Ds stimuli was increased while the other was held constant, the dependence of SR on size of EPSPs was variable. Figure 12A shows summed EPSPs from two different cells whose SR values were differently affected by EPSP size. In the first cell (Figure 12A, top row), the SR decreased when the proximal stimulus increased but then increased when the distal stimulus was increased. In the second cell (Figure 12A, bottom row), the exact opposite was observed. The SR increased when the proximal stimulus increased but then decreased when the distal stimulus was increased. In the 5 cases where the Px stimulus strength was increased while holding potential and Ds stimulus strength were held constant, 4 showed an increase in SR while one decreased (average change: 0.031±0.025 AR/mV; range: -0.059 to 0.093 AR/mV). In 4 cases where Ds stimulus strength was systematically increased, the SR was not significantly changed (0.004±0.007 AR/mV, range: -0.019 to 0.016 AR/mV).

One limitation of trying to determine the effect of EPSP size on SR was that the EPSP amplitude could only be varied over a narrow range in any one neuron. This was due to inhibition being largely blocked, so small increases in stimulus strength resulted in large polysynaptic potentials as has been observed previously (Chagnac-

Amital and Connors, 1989). The relationship between SR and all EPSP amplitudes is shown in Figure 12B-D where all SR values are pooled and plotted as a function of Px amplitude, Ds amplitude and Px plus Ds amplitudes. For all three plots, linear regression reveals slopes of 0.016±0.009, -0.008±0.008 and 0.001±0.005 SR units/mV, respectively. None of these slopes is significantly different from zero. Additionally, EPSPs with SR above the QX-314 95% limit (i.e. SR > 1.16) do not have significantly different summed Px and Ds amplitudes (9.6±1.2 mV, n=17) compared to those with SR ≤ 1.16 (9.5±0.4 mV, n=57). The same is true for Ds amplitudes (Ds peak = 4.6±0.7 for SR > 1.16 compared to 5.2±0.3 for SR<=1.16) and for the peak Px amplitudes (Px peak = 5.0±0.7 mV for SR> 1.16 compared to 4.4±0.2 mV for SR<=1.16).

Since, the effect of holding potential could have masked an effect of EPSP size on SR, multiple regression was also used to determine SR's dependence on holding potential and/or EPSP amplitude. Multiple regression analysis revealed that only holding potential had any significant effect on SR in neurons recorded with KCl electrodes. Using multiple regression the linear dependence on holding potential, Px amplitude and Ds amplitude was found to be -0.008±0.002 SR/mV, 0.015±0.009 SR/mV, and -0.013±0.07 SR/mV, respectively for neurons recorded with KCl electrodes. Additionally, holding potential was not correlated with EPSP size, indicating that the effect of holding potential on SR was not due to any changes in EPSP size with holding potential. For cells recorded with QX-314 electrodes, multiple regression reveled no significant dependence of SR on holding potential or peak EPSP amplitude. Therefore, another conclusion is that the

amount of superlinear summation is not dependent on the amplitude of EPSPs when measured at the soma, but does show an inverse correlation with somatic membrane potential.

Although, there did not appear to be a cell-specific effect based on previous analysis, the relationship between SR and holding potential or EPSP amplitude could have been affected by some cells having many large SR values. To assess this, I randomly selected one SR value from each neuron, and then plotted these SR values against holding potential and summed EPSP size (Figure 13). For this subset of the original data, SR was again found to be significantly dependent on holding potential for cells recorded with KCl electrodes (-0.009±0.003 SR/mV), but not for QX-314-loaded cells (-0.003±0.003 SR/mV). There was no significant relationship found between SR and the sum of Px and Ds amplitudes for either group of cells. These results confirm that for cells recorded with KCl electrodes, there is a significant relationship between SR and holding potential that is not dependent upon a particular type of cell.

SUMMARY

Changes in holding potential, but not EPSP amplitude or cell type affected EPSP summation in cells recorded with KCl electrodes. The effect of holding potential was absent in QX-314 loaded cells indicating that postsynaptic conductances affecting EPSP summation are voltage-dependent. Although EPSP amplitude would also be expected to change the activation state of voltage-dependent conductances, changes in

EPSP amplitude had no consistent effect upon EPSP summation. Possible explanations for this lack of correlation are in the discussion. In these experiments, the amount of non-linear EPSP summation was not related to a particular type of cell. Both intrinsic burst firing and regular spiking neurons summed EPSPs equivalently. Additionally, SR values were not highest or lowest in a particular group of cells; instead, individual cells showed a wide variation in SR values as either holding potential or EPSP amplitude was changed. In these experiments, all neurons recorded with KCl electrodes appeared to be capable of summing EPSPs in a linear to superlinear fashion with holding potential having the most consistent effect on EPSP summation.

Figure 11. Summation Ratio increases with hyperpolarization

Superlinear summation of EPSPs decreased with membrane depolarization. *A*, Two examples from the same cell showed an increase in SR as membrane potential was hyperpolarized from rest (-71 mV) to -82 mV. *B*, Plot of SR as a function of holding potential for KCl recorded neurons (●) and QX-314 recorded neurons (ρ). Linear regression revealed a significant decrease of SR with membrane depolarization for neurons recorded with KCl electrodes (solid line; Student's t-test $P<0.001$; slope = -0.09±0.02 SR units/mV, R = 0.48) but not for neurons recorded with QX-314 (dashed line; slope = -0.01±0.01). The two slopes were also significantly different from each other (Student's t-test $P<0.05$). All data points are the same as those used for the histograms in Figure 10.

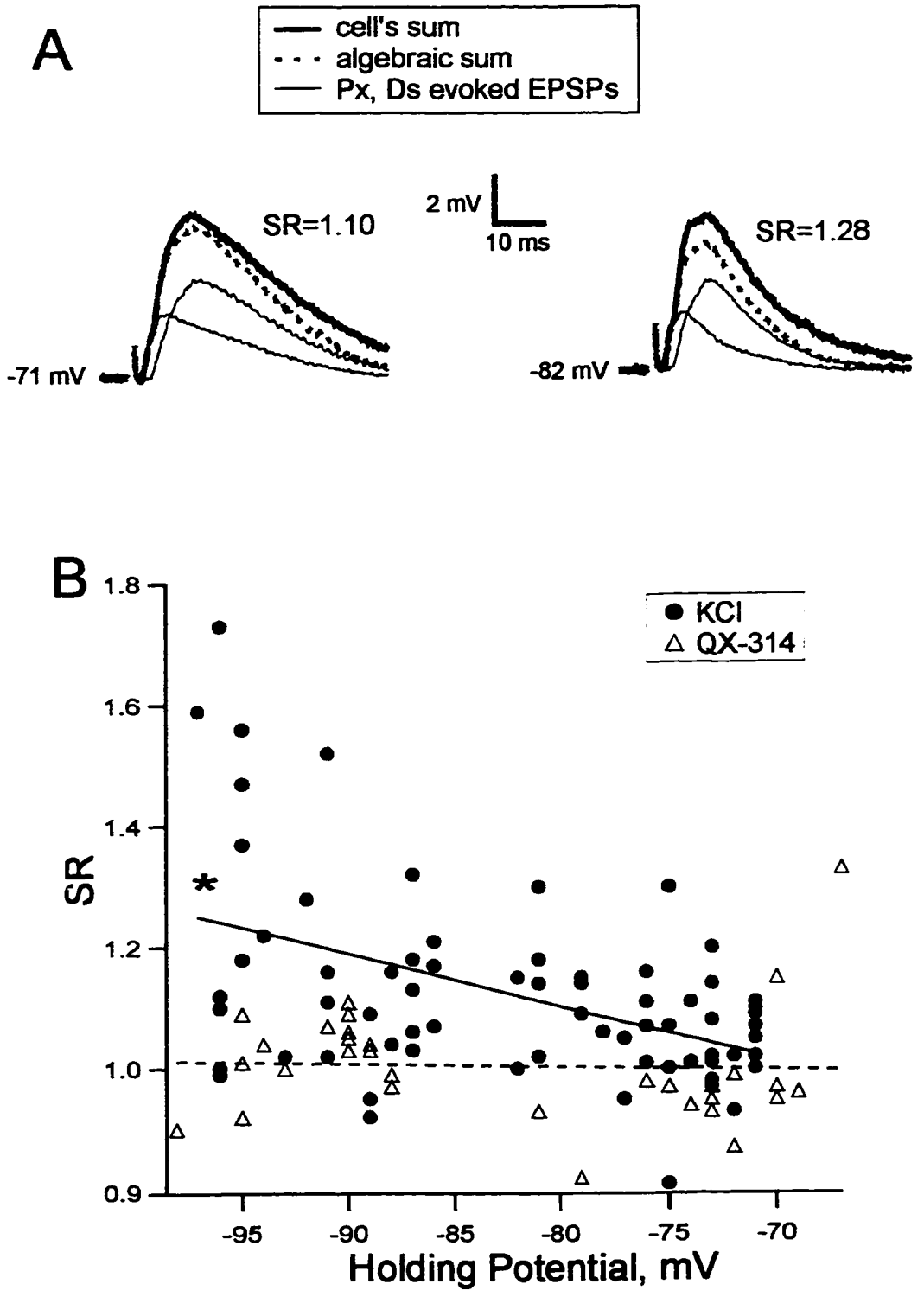
A
cell's sum
algebraic sum
Px, Ds evoked EPSPs
2 mV
10 ms
SR=1.10
-71 mV
SR=1.28
-82 mV
B
KCl
QX-314
SR
1.8
1.6
1.4
1.2
1.0
0.9
-95
-90
-85
-80
-75
-70
Holding Potential, mV

Figure 12. Summation ratio is not dependent on EPSP size

A, Examples from 2 different cells in which SR showed no clear relationship with EPSP size. *B-D*, Plots of SR as a function of EPSP amplitude: *B*, Px evoked EPSP amplitude; *C*, Ds evoked EPSP amplitude; *D*, algebraic sum of the peak Px and peak Ds evoked EPSP amplitudes for cells recorded with KCl electrodes (●) and for cells recorded with QX-314 filled electrodes (ρ). In all cases, the fit to a linear regression was not significantly different from zero for neurons recorded with KCl electrodes (solid lines) or with QX-314 electrodes (dashed lines). For data from QX-314 loaded cells in *B* and *D*, the one large SR value is excluded from the regression as it alone altered the significance of the slope. All data points are from the same as those used for the histograms in Figure 10.

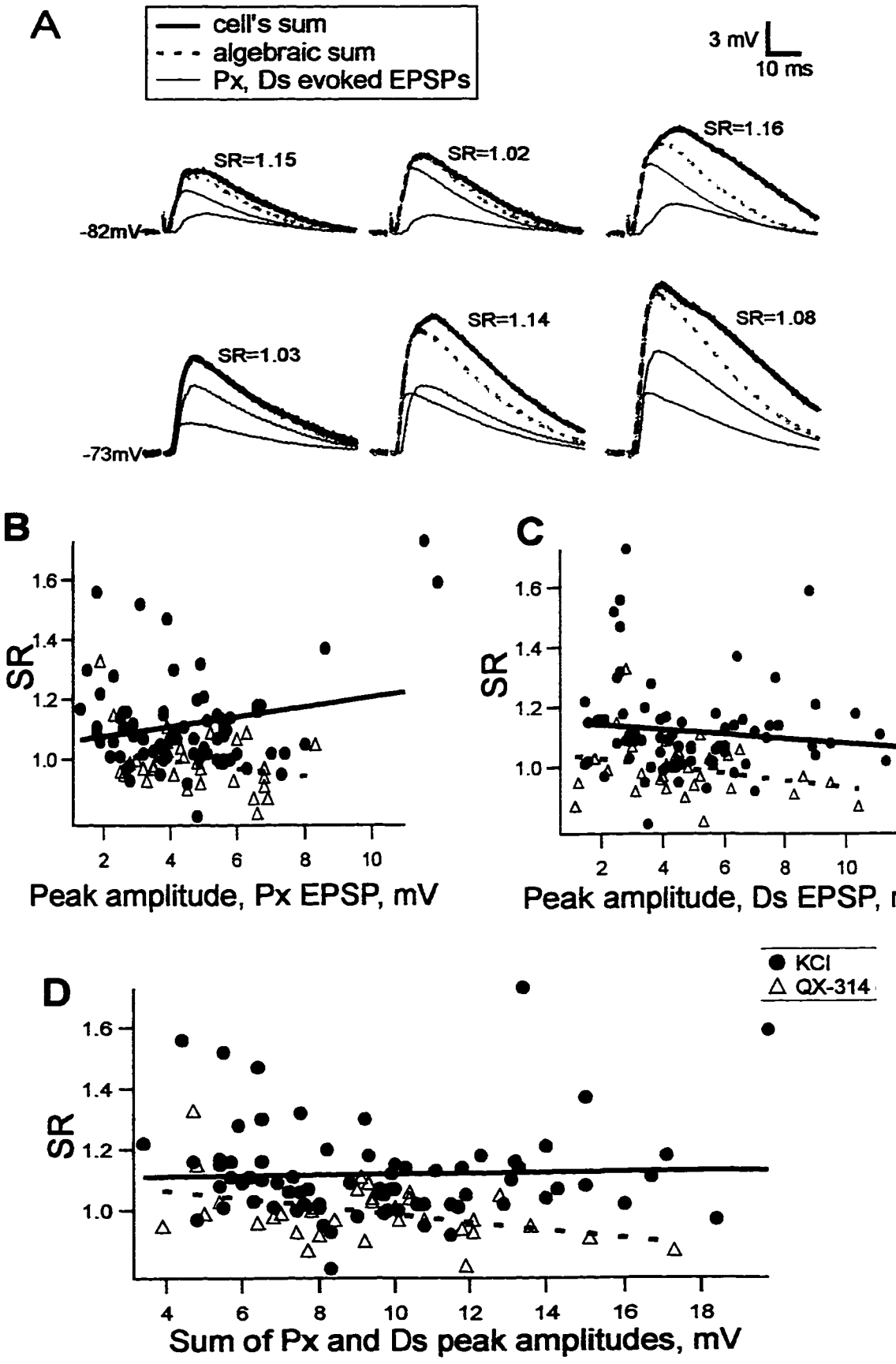
A
cell's sum
algebraic sum
Px, Ds evoked EPSPs
3 mV
10 ms
SR=1.15
SR=1.02
SR=1.16
-82mV
SR=1.03
SR=1.14
SR=1.08
-73mV
B
SR
Peak amplitude, Px EPSP, mV
C
SR
Peak amplitude, Ds EPSP, mV
D
KCl
QX-314
SR
Sum of Px and Ds peak amplitudes, mV

Figure 13. SR is not cell-dependent

For these two plots, one SR value from each cell was randomly chosen. The same points are used in both A and B. Data from neurons recorded with KCl electrodes (●) and with QX-314 electrodes (ρ) were plotted against holding potential (*A*) and the sum of Px and Ds amplitudes (*B*). The data was then fit by linear regression for neurons recorded with KCl electrodes (solid lines) and QX-314 electrodes (dashed lines). Linear regression revealed that in cells recorded with KCl electrodes, SR was found to depend significantly upon holding potential (A-solid line). No other slopes were significant.

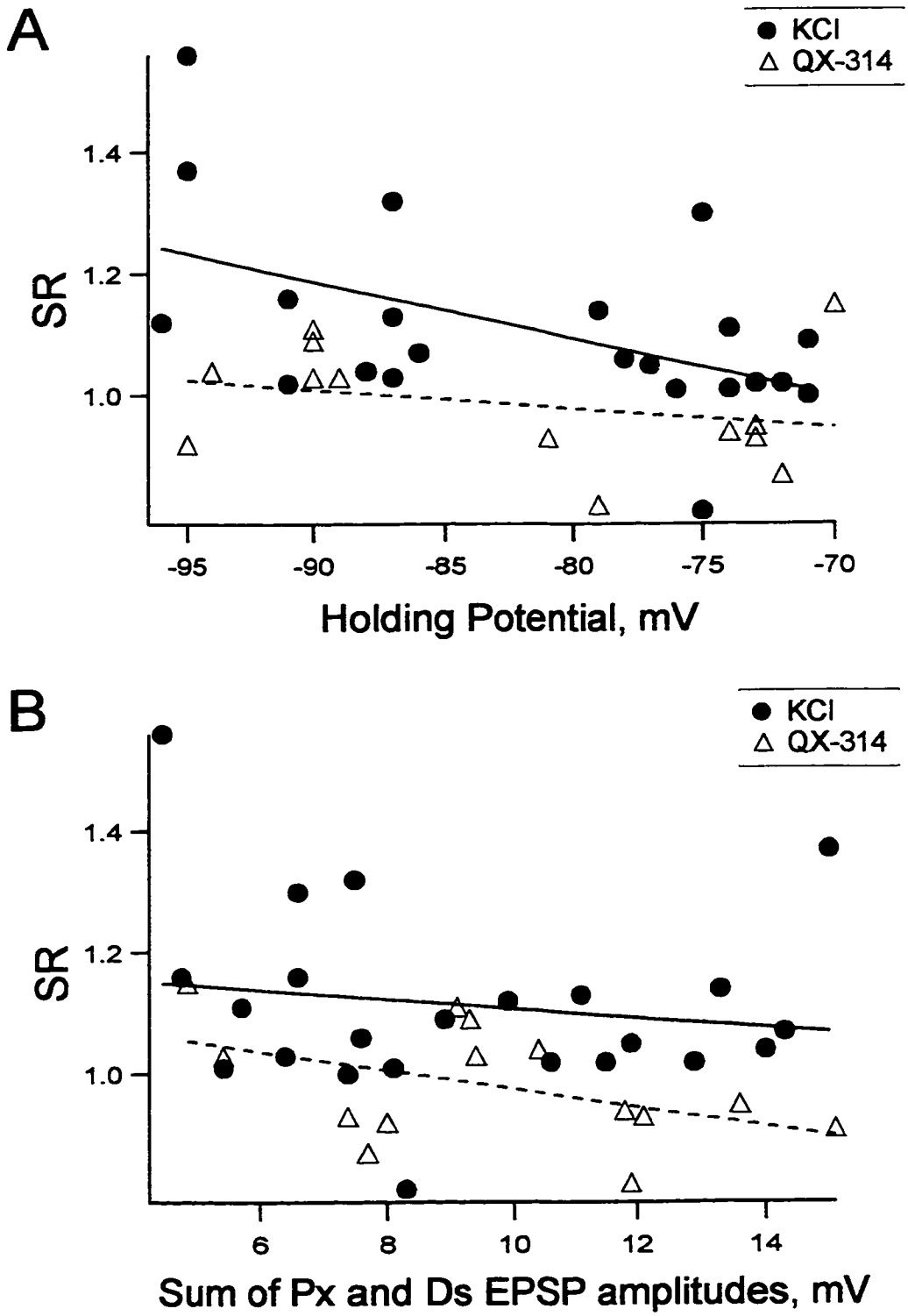
A
KCl
QX-314
SR
1.4
1.2
1.0
-95
-90
-85
-80
-75
-70
Holding Potential, mV
B
KCl
QX-314
SR
1.4
1.2
1.0
6
8
10
12
14
Sum of Px and Ds EPSP amplitudes, mV

CHAPTER 4: THE EFFECT OF TIME BETWEEN INPUTS ON SUMMATION RATIO

INTRODUCTION

Activation of voltage-dependent conductances by EPSPs could either improve coincidence detection (Bernander, et al., 1991; Konig, et al., 1996; Softky and Koch, 1993) or favor temporal summation depending on the characteristics of the conductance. For example, a conductance with rapid activation and inactivation kinetics would cause superlinear summation mainly to EPSPs that are nearly coincident. In contrast, a noninactivating inward conductance with slow deactivation kinetics could favor superlinear summation of EPSPs separated in time and thus enhance temporal summation. Therefore, I measured SR as a function of the time between the Ds and Px stimuli.

SUMMATION RATIO INCREASES AS TIME BETWEEN INPUTS DECREASES

Examples of experiments to determine the effect of a delay between synaptic inputs on SR are shown in Figure 14A. For the neuron recorded with a KCl electrode, the SR decreased from 1.13 to 1.05 as the time (Δt) between the Px and Ds stimuli increased from 5 to 30 ms. On the other hand, in a QX-314 recorded neuron, the SR was close to linear (1.0) for all Δt. In 9 individual KCl recorded neurons in which

EPSPs size and holding potential were held constant while Δt was increased. 6 had the largest SR at 0 or 5 ms, 1 had the a peak SR at 10 ms, and 2 neurons had SR values that were independent of changes in Δt.

Figure 14 B-D show the SR distribution histograms for all KCl and QX-314 recorded neurons in which the two inputs were separated by 5, 10 and 30 ms. A majority of summed EPSPs (80%) had the Px EPSP preceding the Ds EPSP. In the remaining, the Ds stimulus was given first. Both groups were analyzed together since no correlation between stimulus order and EPSP summation was observed. Similar to what was observed for Δt=0 (e.g. Figure 10), the distribution of SR values in neurons recorded with KCl electrodes were clearly skewed to the right for Δt's equal to 5 and 10 ms. For QX-314 loaded neurons at the same Δt, the distribution of SR values was relatively normal and the upper 95% confidence limit was determined, (1.19, 1.15, and 1.12 for Δt= 5, 10, and 30 ms, respectively). For Δt=5 ms, 19% of SR values were found to lie above 1.19, while for Δt=10 ms 18% of all SR values were above 1.15. When Δt=30 ms, the distribution of SR values was close to normal for both groups of neurons although 9% of neurons recorded with KCl electrodes were above 1.12. At all Δt's and for both groups of neurons, measurements were taken over the same range of holding potentials and EPSP sizes (see also Figure 12). As the time between inputs decreased, the difference between the SR distributions from the two types of cells increased, indicating that a QX-314 sensitive conductance caused SR to increase in a time-dependent fashion. Figure 15

shows the dependence of SR on holding potential and EPSP amplitude for each Δt. As for simultaneous inputs (Δt=0), there was no significant relationship between SR and EPSP amplitude. Unlike simultaneous inputs, there was no significant dependence of SR on holding potential for Δt=5, 10 or 30 ms. The lack of any relationship between SR and holding potential for non-simultaneous indicates that the effects of voltage-sensitive conductances may lessen as time between input increases.

EFFECTS OF TIME AND VOLTAGE ON SUMMATION RATIO

Since holding potential was shown to affect SR summation at Δt=0, the relationship between SR and Δt for EPSPs with holding potentials positive to -85 mV (depolarized EPSPs) was examined separately from EPSPs with holding potentials equal to or more negative to -85 mV (hyperpolarized EPSPs). Figure 16A and Figure 16B show plots of the relation of SR to Δt for all depolarized and hyperpolarized EPSPs respectively. At hyperpolarized potentials, SR decreased more dramatically with time between inputs than at potentials closer to rest. Such results imply that there is a time-dependent component to superlinear summation that is more pronounced at more hyperpolarized holding potentials (≤ -85 mV).

While QX-314 sensitive conductances contribute to SR values greater than 1, there are other possible factors affecting the relationship between SR and time. Factors such as synaptic conductance change, presynaptic interactions between the stimuli, or

post-synaptic conductances not blocked or only partially blocked by QX-314 might affect how EPSPs sum in QX-314 loaded cells. Consistent with this idea, I observed that cells recorded with QX-314 electrodes did not sum linearly at all Δt's. In particular, the mean SR peaked at Δt = 5 ms for both the hyperpolarized EPSPs and the EPSPs closer to resting membrane potential. Such behavior would be consistent with a non-QX-314 blockable component contributing to superlinear summation when the inputs are within 5 ms of each other combined with a reduction in driving force and/or a synaptic conductance change decreasing EPSP summation when the inputs are simultaneous.

To examine only the contribution of the QX-314 blockable conductances to the SR vs. Δt relationship, I plotted the difference in mean SR, (ΔSR), between cells recorded in KCl and QX-314 electrodes as a function of Δt (Figure 16C). At both hyperpolarized and depolarized potentials, there was a clear decrease in ΔSR with Δt. At membrane potentials more positive than -85 mV, SR decreased linearly (slope = -0.0018± 0.0010 AR/ms) as time between inputs increased, until at Δt=30 ms ΔSR was not significantly different from zero. For hyperpolarized EPSPs, the decrease in ΔSR with time between stimuli was well fit by a single exponential with a time constant of 15± 8 ms. These results indicate that there is a QX-314 sensitive, time-dependent component to superlinear summation that is altered by changes in holding potential.

SUMMARY

Summation of EPSPs depended upon time between inputs. SR values decreased as time between inputs increased for cells recorded with KCl electrodes. In contrast, SR values measured in cells recorded with QX-314 electrodes did not depend on time between inputs indicating that the postsynaptic conductances underlying superlinear summation of EPSPs were time dependent. Additionally, SR dependence on the time between stimuli was affected by changes in holding potential. More depolarized EPSPs were able to sum over a longer time course while more hyperpolarized EPSPs summed over a shorter time course. This is consistent with time- and voltage-conductances underlying summation of EPSPs. The functional implications as well as the possible ionic conductances underlying EPSP summation are discussed in more detail in Chapter 6.

Figure 14. Superlinear summation depends on the time between inputs

A, Examples of EPSP summation from two neurons (left recorded with a KCl electrode and right with a QX-314 electrode) in which the time between Px and Ds stimuli (Δt) was increased from 5 ms (top) to 10 ms (middle) to 30 ms (bottom). In these examples, the Px stimulus preceded the Ds stimulus. Holding potential is -75 mV for the neuron recorded with a KCl electrode and -70 mV for the neuron recorded with a QX-314 electrode. *B-D*. Histograms of SR values for Δt of 5 ms (*B*), 10 ms (*C*) and 30 ms (*D*) in neurons recorded with KCl electrodes (top graphs) and neurons recorded with QX-314 electrodes (bottom graphs). Bin width = 0.04 SR units. As in Figure 3, the histograms of SR values measured in QX-314 loaded cells were fit to a Gaussian curve (solid line) and the upper and lower 95% confidence limits were determined (dashed vertical lines).

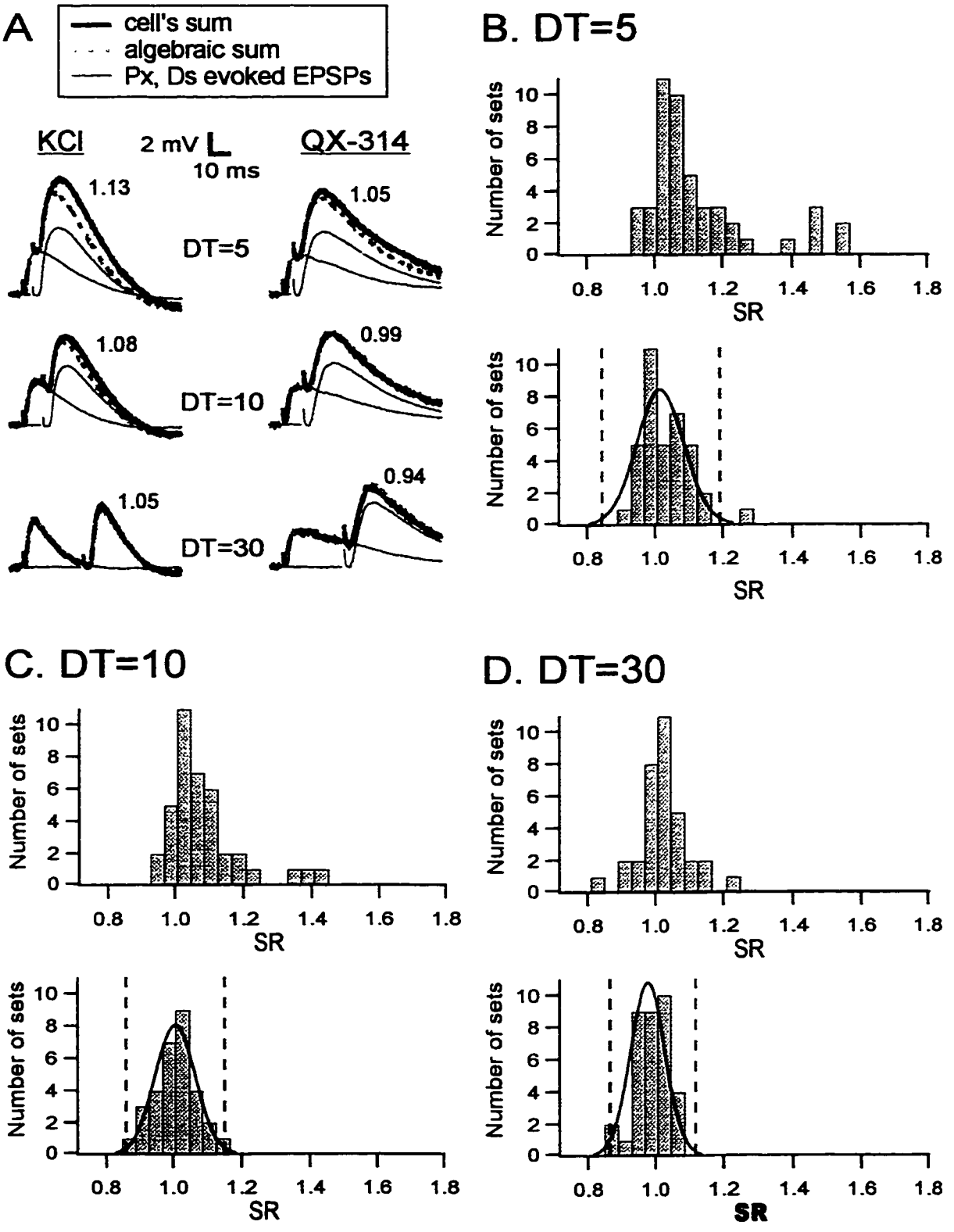
A
cell's sum
algebraic sum
Px, Ds evoked EPSPs
KCl
2 mV
10 ms
QX-314
1.13
1.05
DT=5
1.08
0.99
DT=10
1.05
0.94
DT=30
B. DT=5
C. DT=10
D. DT=30
Number of sets
SR
0.8
1.0
1.2
1.4
1.6
1.8
0
2
4
6
8
10

Figure 15. Dependence of SR on membrane potential for increasing Δt's

Plots of SR against holding potential (left panels) and SR against sum of Px and Ds peak amplitudes (right panels) for Δt=5 (A), Δt=10 (B) , Δt=30. Data used in these figures is the same as those used to create histograms in Figure 14. Solid lines are the linear regression of data from cell recorded with KCl electrodes, while the dashed lines are the linear regression of data points from QX-314 loaded cells. None of the linear regressions in these plots were found to be significantly different from zero.

A. DT=5

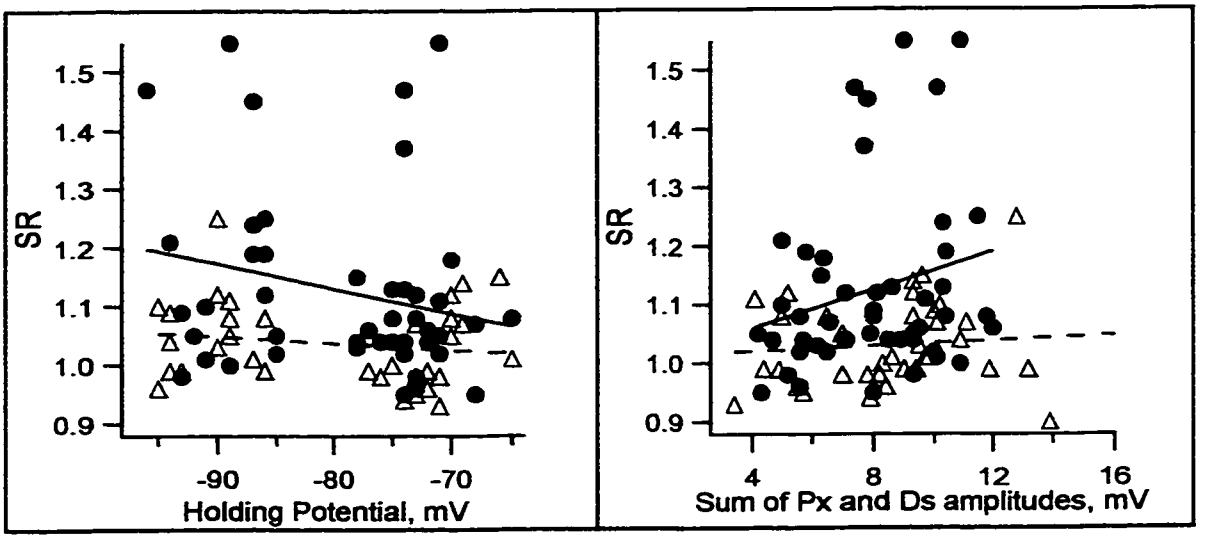

B. DT=10

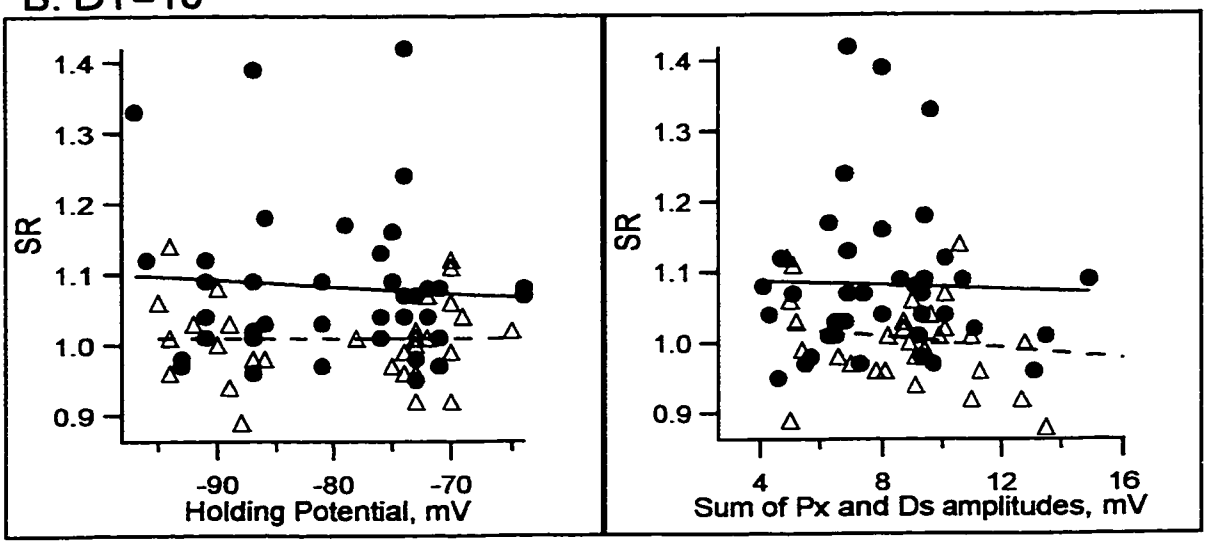

C. DT=30

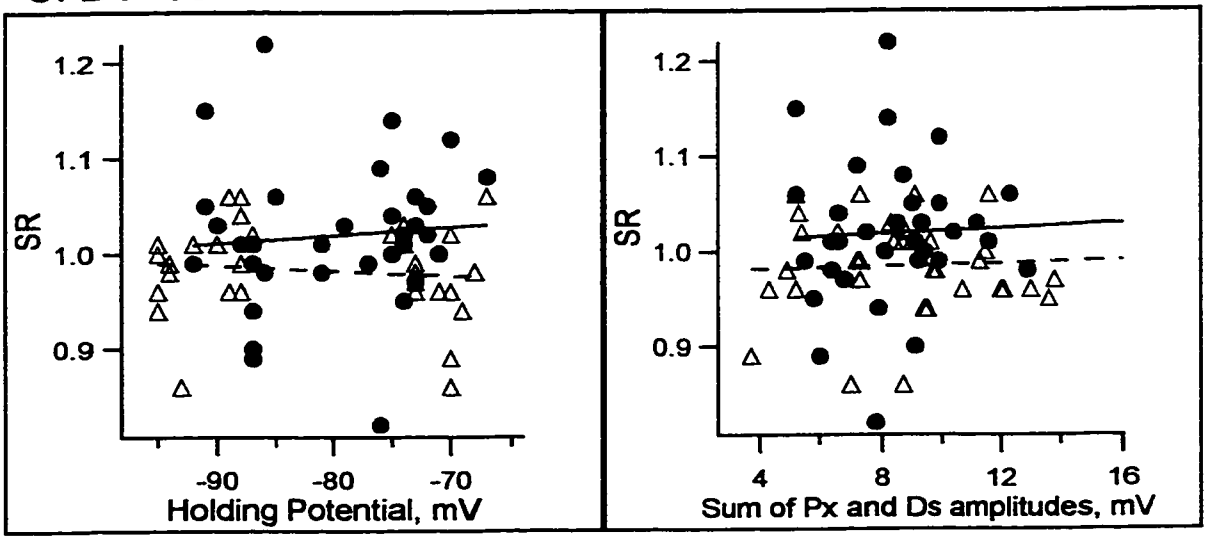

Figure 16. SR depends on both the time between inputs and holding potential.

A, Plots of mean SR as a function of the time between the proximal and distal stimuli (Δt) for EPSPs with holding potentials positive to -85 mV. Each point is the mean of 18 to 43 SR values (filled circles - neurons recorded with KCl; open circles - neurons recorded with QX-314). At $\Delta t = 0$, 5, and 10 but not 30 ms, SR was significantly larger in neurons recorded with KCl electrodes than in QX-314 loaded neurons. *B*, Similar to *A* but for EPSPs in which the holding potential was $\leq$ -85 mV. Each point is the mean of 12 to 31 SR values (filled squares - neurons recorded with KCl electrodes; open squares - neurons recorded with QX-314 electrodes). At $\Delta t = 0$ ms and $\Delta t = 5$ ms, SR was significantly larger in neurons recorded with KCl electrodes than in QX-314 loaded neurons. *C*, The data in A and B is used to calculate the QX-314 blockable component of the SR (ΔSR) for each Δt. ΔSR is equal to the mean SR measured in cells recorded with KCl electrodes minus the mean SR measured in cells recorded with QX-314 electrodes. The plot of ΔSR vs. Δt from more hyperpolarized EPSPs (squares) was best fit to an exponential function, $Ae^{-\Delta t/\tau}$, where the intercept (A) = 0.16±0.04 SR units, and the time constant (τ) = 15±8 ms. The plot of ΔSR vs. Δt from the more depolarized EPSPs (circles) was best fit to a line with a slope of -0.002±0.001 SR units/ms and y-intercept = 0.093±0.020 SR units. All comparisons were done as a one-way ANOVA, $P<0.05$. Error bars represent the SEM in SR.

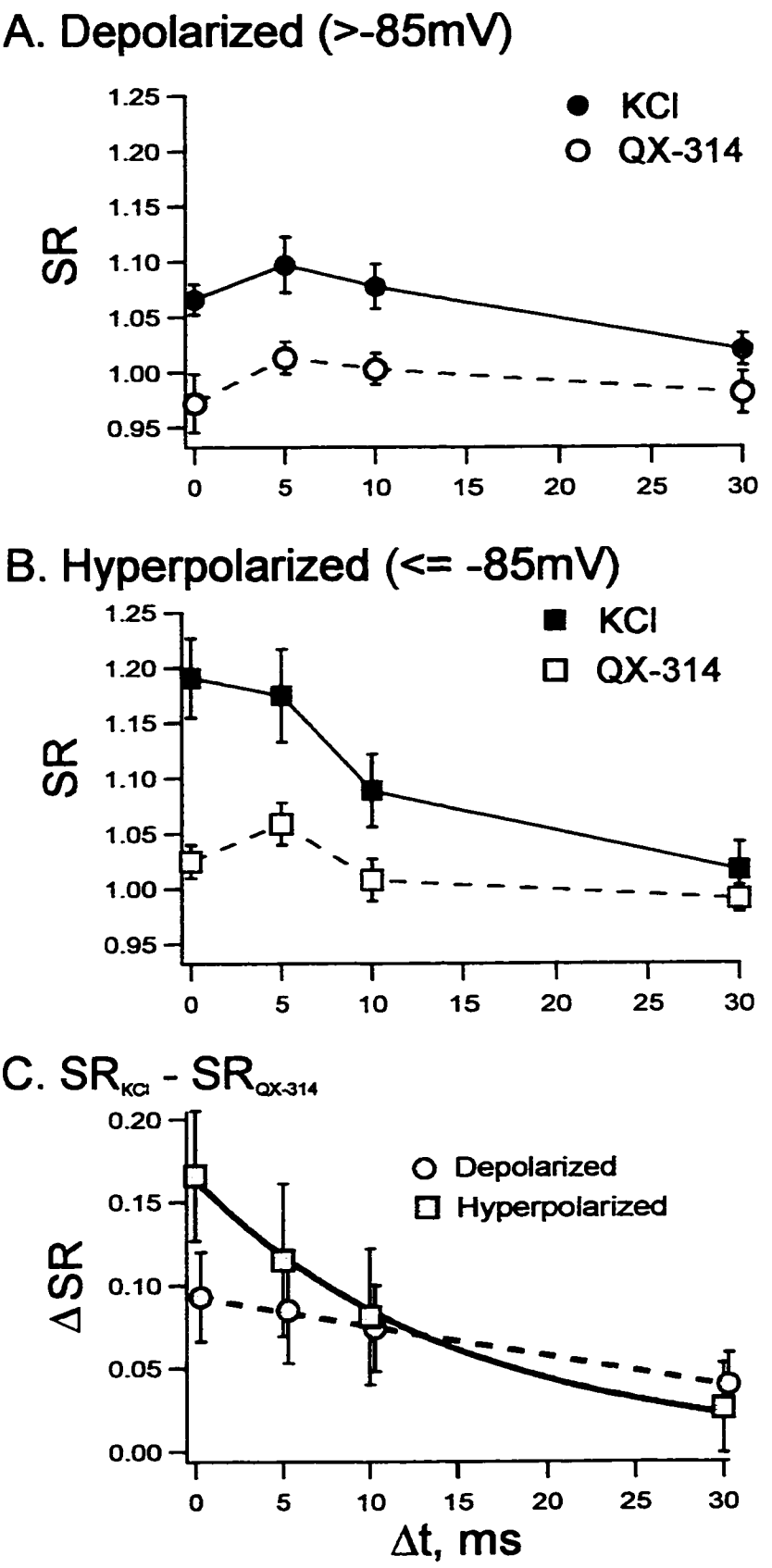
A. Depolarized (>-85mV)
KCl
QX-314
SR
1.25
1.20
1.15
1.10
1.05
1.00
0.95
0
5
10
15
20
25
30
B. Hyperpolarized (<= -85mV)
KCl
QX-314
SR
1.25
1.20
1.15
1.10
1.05
1.00
0.95
0
5
10
15
20
25
30
C. SR$_{KCl}$ - SR$_{QX-314}$
Depolarized
Hyperpolarized
ΔSR
0.20
0.15
0.10
0.05
0.00
0
5
10
15
20
25
30
Δt, ms

CHAPTER 5: DENDRITIC CONDUCTANCES CAUSE SUPERLINEAR SUMMATION OF EPSPS

INTRODUCTION

Previous studies indicate that voltage-sensitive conductances on the dendrites play an important role in synaptic integration (see Introduction and also Johnston, et al., 1996; Yuste and Tank, 1996 for reviews). Both electrical recordings from and calcium imaging of the apical dendrite of pyramidal cells indicate that even subthreshold EPSPs activate ionic conductances in the apical dendrite (Hoffman, et al., 1997; Markram, et al., 1995; Schiller, et al., 1997). In this section, the role dendrites play in EPSP summation is examined using simulated EPSPs. In addition, I was able to compare summation of EPSPs in intact cells with summation of EPSPs in cells whose distal apical tuft was missing. The cells with missing apical tufts occurred because in some cases the cut used to isolate the two stimulus sites also cut off the most distal portion of the recorded neuron's apical tuft. These experiments allowed me to determine the potential role of the apical dendrite and tuft in superlinear summation of EPSPs.

CREATING SIMULATED EPSPS

The hypothesis that dendritic conductances cause superlinear summation of EPSPs was tested by generating simulated EPSPs with current pulses injected through

the recording electrode at the soma. In these experiments simulated EPSPs were created by intracellular current injection, I, as a function of time, t, according to the equation (from Otis, et al., 1993):

$$I(t) = K*(1-e^{-t/t_1})^4 e^{-t/t_2}$$

The amplitude was adjusted by changing K, and changing t_1 and t_2 altered the rise and decay of the injected current. The current pulse was adjusted until the time course and amplitude of the evoked voltage response (simulated EPSP) approximated by eye an evoked EPSP in the same neuron (Figure 17). Simulated EPSPs were then substituted for evoked EPSPs in the experimental protocol as described previously (Reyes and Fetz, 1993). For all SR values measured using simulated EPSPs there was no delay between the two stimuli.

Simulated EPSPs were used to differentiate between the dendritic and somatic contributions to non-linear summation of EPSPs. One possible explanation for the results presented in the three previous chapters is that EPSPs are passively conducted to the soma. Only when the EPSPs reach the soma do they activate voltage-sensitive conductances. If somatic voltage-sensitive conductances cause nonlinear summation of EPSPs, then simulated EPSPs created by current pulses at the soma should cause as much superlinear summation as evoked dendritic EPSPs. If dendritic conductances contribute to

superlinear summation of EPSPs, then simulated EPSPs and evoked EPSPs should display different amounts of non-linear summation.

EVOKED EPSPS HAVE LARGER SR VALUES THAN MATCHED SIMULATED EPSPS

Figure 18A shows an example of a neuron in which the simulated EPSPs closely approximated the time course and amplitude of the evoked EPSPs. The evoked EPSPs summed superlinearly with a SR of 1.18. When simulated EPSPs were substituted for either the Px, Ds, or both evoked EPSPs, SR values were close to linear (0.99, 1.05, and 1.02 respectively). For the 12 neurons in which simulated EPSPs were used, the amount of summation did not depend upon whether the simulated EPSPs were substituted for either the Px or Ds or both the evoked EPSPs. There was no significant difference among the mean SR measured for each of the three groups: (simulated Px with evoked Ds: 1.04±0.01, n=30, evoked Px with simulated Ds: 1.02±0.01, n=13, and both Px and Ds simulated: 1.06±0.02 n=22). In the same group of neurons, two evoked EPSPs were found to have significantly larger SR: 1.16± 0.04, n=30 (only SR values from EPSPs that were at the same holding potentials as the simulated EPSPs were included in this mean; one-way ANOVA for all group comparisons).

Figure 18B compares the SR values measured from two evoked EPSPs to SR values from well-matched simulated EPSPs. In the 5 cases where the two evoked EPSPs yielded SR values above the QX-314 limit of 1.16, their matched simulated EPSPs

yielded SR values closer to linear. For the remaining SR measurements, evoked EPSPs yielded larger or equivalent SR values compared to those SR values measured using simulated EPSPs. This demonstrates that dendritic and somatic EPSPs do not exhibit the same amount of superlinear summation indicating that dendritic conductances are contributing to superlinear summation of evoked EPSPs.

EFFECT OF QX-314 ON SUMMATION OF SIMULATED EPSPS

Conductances near or in the soma may also contribute to superlinear summation. To assess this effect, simulated EPSPs' SR values were measured in neurons recorded with and without QX-314. (Examples are shown in Figure 19A and Figure 19B). Figure 19 shows the distribution of all simulated EPSP SR values from cells recorded with KCl electrodes (Figure 19C) compared to the distribution of all simulated EPSP SR values from cells recorded with QX-314 electrodes (Figure 19D). As seen for evoked EPSPs (Figure 10), the SR values obtained from neurons recorded with KCl electrodes are skewed to the right while SR values obtained from QX-314 filled neurons have a normal distribution. Since SR values did not depend upon which or both EPSPs were simulated, all SR values measured using simulated EPSPs were pooled. In QX-314 filled neurons, simulated EPSPs combined with an evoked or another simulated EPSP had an average SR value of 0.98± 0.01 (n=20) while in neurons recorded without QX-314, the average SR was significantly larger (1.04±0.01, n=65). Thus, QX-314 sensitive conductances near or in the soma also contribute to superlinear summation.

Some insight into the relative contribution of somatic versus dendritic conductances can be gained by comparing the data from Figure 11 with the data from Figure 19 (shown replotted in Figure 20). In cells recorded with KCl electrodes, the overall mean SR measured when using two evoked EPSPs (1.12±0.02, n=74) was significantly larger than the mean SR measured when using one or more simulated EPSPs (1.04±0.01, n =65) demonstrating that dendritic conductances contribute to larger SR values. In contrast, QX-314 filled cells had a mean SR for evoked EPSPs (1.00±0.02) that was not significantly different from the mean SR for simulated EPSPs (0.98±0.01). Thus, QX-314 eliminated both the somatic and dendritic conductances responsible for superlinear summation. Such a difference indicates that postsynaptic dendritic conductances are responsible for a majority of the superlinear summation observed in these experiments.

EPSP SUMMATION IN NEURONS MISSING THE APICAL DENDRITIC TUFT

Recent studies indicate that the apical tuft of pyramidal neocortical neurons can generate Ca^{2+} action potentials separately from the soma (Schiller, et al., 1997). If this mechanism is contributing to superlinear summation, then neurons lacking their apical tuft may show less superlinear summation. In support of this idea, SR values in neurons where the most distal portion of the apical dendrite was missing were significantly smaller than SR values in intact neurons. Figure 21A shows an example of a neuron whose apical tuft was cut off by the cut made to isolate the two stimulating sites.

Also shown is an example of EPSP summation from that cell (Figure 21B) compared to an example of EPSP summation from an intact cell (Figure 21C). Overall, the distribution of SR values from cells missing their distal apical tufts (Figure 20D) was closer to 1 than SR values from intact cells (Figure 20E). For cells missing the distal apical tuft, the mean SR was 1.03±0.01 (n=16, 6 cells) which is significantly smaller than the mean SR for intact cells, 1.10±0.03 (n = 30 from 14 cells). For all EPSPs in both types of cells, the time between stimuli was equal to 5 ms and the holding potential was more positive than -85 mV. The data in figure 19D is a subset of the data in Figure 14B. One explanation for the larger SR values in intact cells compared to cells missing an apical dendritic tuft is that conductances in the apical tuft are causing superlinear summation of EPSPs. One problem is that for cells missing their distal tufts, it is not clear how the distal stimuli were able to elicit EPSPs that reach the apical dendrite of the recorded neuron. For an intact cell, the distal stimulus presumably elicits EPSPs by stimulating the horizontal pathways to the apical tuft. Without a distal apical tuft to stimulate, the distal stimulus may be stimulating pathways that cross laminae and then impinge on the upper part of the apical dendrite (Ichinose and Murakoshi, 1996). Support for this idea comes from the fact that the strength of the distal stimulus was significantly larger for neurons without apical dendritic tufts than for intact neurons (14±1μA for intact cells, 23±2μA for cells without apical dendritic tufts).

While this result suggests an important role for the apical dendritic tuft, there are alternative explanations for the observed larger SR values in intact cells than in

cut cells. First, getting the apical dendrite cut off may have slightly damaged the cell and thus the smaller SR values reflect EPSP summation in a less healthy cell. However, neither input resistance nor resting membrane potential was significantly different for cells missing an apical dendritic tuft (IR = 18±3 MΩ, RMP=-75±1 mV) compared to intact cells (IR= 21±1 MΩ, RMP = -73±1 mV). Additionally, cells without a distal apical dendritic tuft had action potentials that overshot 0 mV. Another possibility is that the two inputs were interacting presynaptically. Since the distal stimulus cannot be acting through horizontal pathways, it may be activating other pathways also affected by the proximal stimulus. One possibility is that this presynaptic interaction invokes a depressed response via paired-pulse depression.

DIFFUSION OF QX-314 INTO DENDRITES

If the apical dendritic tuft is important for superlinear EPSP summation, QX-314 must be able to diffuse from the soma to the distal portion of the apical dendritic tuft before its effect can be observed. Assuming that QX-314 must diffuse down an essentially one-dimensional apical dendrite, the one-dimensional diffusion equation can be used (from Hille, 1992, pg. 264):

$$r^2 = 2Dt \quad \text{-or-} \quad t = r^2/2D$$

In this equation, D is the diffusion coefficient of the compound, and t is the time it will take the compound to diffuse a mean-squared distance of r^2. Unfortunately, the QX-314

diffusion coefficient is not known. One estimate for the diffusion coefficient for QX-314 would be twice the diffusion coefficient for TEA. The rationale for using this estimate is based on QX-314's similarity in structure to TEA. QX-314 consists of a benzene ring attached to a TEA molecule. Using $D = 1.7 \times 10^{-5}$ cm^2/s (from Hille, 92 pg. 268 Table 1), QX-314 will travel 1.4 mm in 40 minutes. The distance from the soma to the apical tuft in these experiments was 1 to 1.5 mm. Therefore, QX-314 should have diffused to the apical tuft during the time allotted for QX-314 diffusion into the dendrites (40 minutes).

Given that QX-314 takes time to diffuse to the apical tuft, we might expect to see an effect of time on SR in QX-314 loaded cells. Contrary to this expectation there was only a small effect of time on SR in QX-314 loaded cells. Figure 20 shows the average SR for QX-314 at increasing times. There is no significant difference among the times, nor does linear regression of SR versus time reveal a slope significantly different from zero. One explanation for this effect is that in 20 minutes, the earliest time I was able to take reliable EPSP summation measurements in QX-314 recorded cells, QX-314 would have already diffused 1 mm according to the equation and estimates used above. Thus, QX-314 may already be blocking postsynaptic conductances in the dendrites by the time SR values were being measured.

SUMMARY

Dendritic conductances were found to play an important role in EPSP summation. Evoked dendritic EPSPs in cells recorded with KCl electrodes had

significantly larger SR values that simulated somatic EPSPs. If EPSPs were passively conducted to the soma where they then summed, we would expect that simulated EPSPs and evoked EPSPs would have the same amount of superlinear summation. Instead, I observed that evoked dendritic EPSPs are able to interact with each other and had significantly more superlinear summation. This superlinear summation appeared to be due to postsynaptic conductances. The SR values from both evoked and simulated EPSPs in QX-314 loaded cells were significantly smaller compared to SR values from cells recorded with KCl electrodes. Where in the dendrites these EPSPs interact is not clear, but the smaller SR values measured in cells missing their distal apical dendritic tuft indicate that the distal apical tuft may play an important role.

Figure 17. Matching Evoked EPSPs with Current Pulses

Simulated EPSPs were created by current pulses that yielded voltage responses matching evoked EPSPs in both types of cells, those recorded with KCl electrodes (*A*) and those recorded with QX-314 electrodes (*B*). *A*, The solid line represents the average of 15 responses to a 1 ms, 2.8 μA pulse. The dashed line is the averaged response (n=10) from the current pulse shown below. Current pulse created using equation in text with K = 1.6 nA, $t_1 = 0.3$ ms, $t_2 = 4$ ms. *B*, Same as *A*, except the stimulus was 3.4 μA, and K = 1.6 nA, $t_1 = 1$ ms, and $t_2 = 5$ ms.

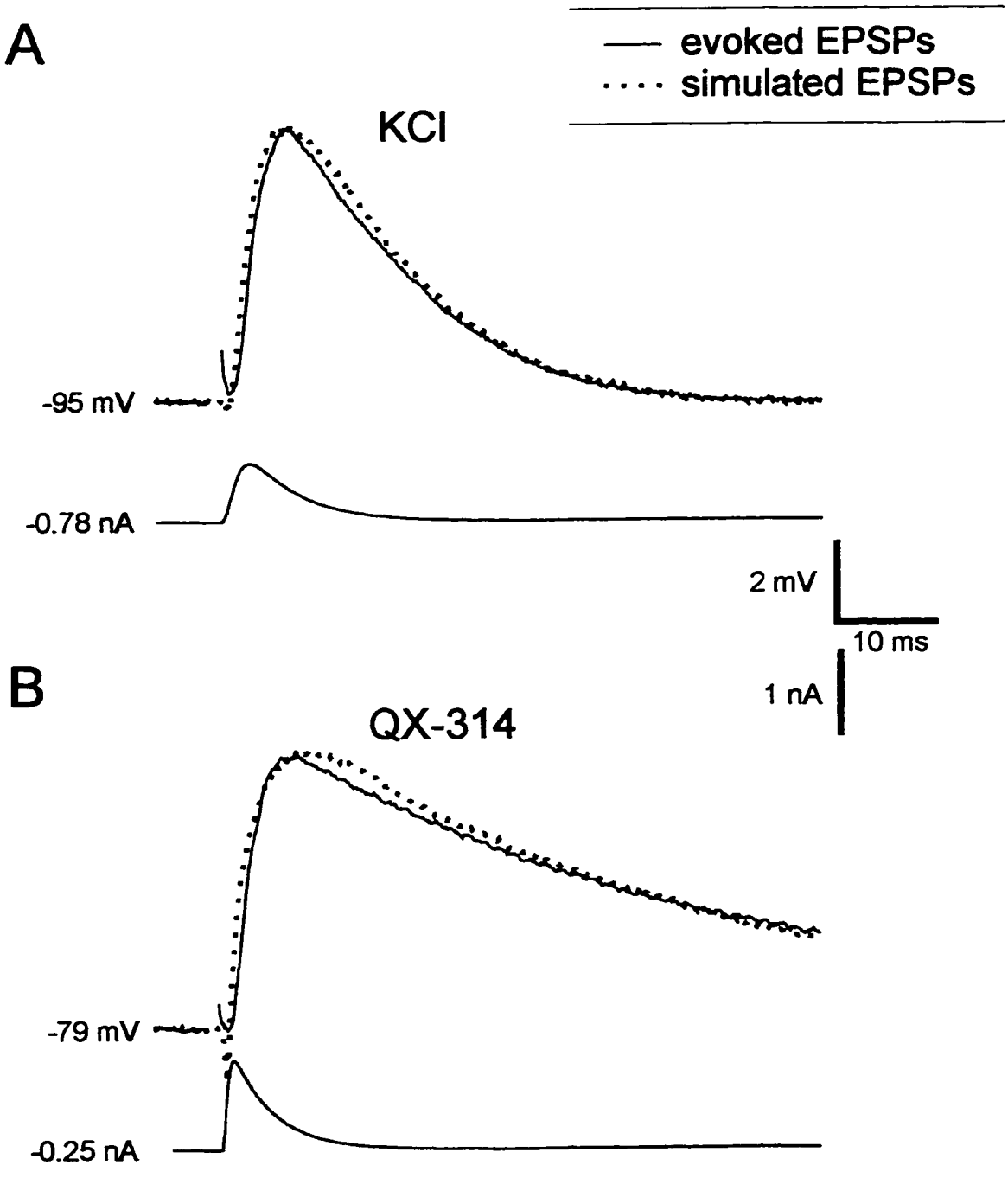
A
evoked EPSPs
simulated EPSPs
KCl
-95 mV
-0.78 nA
2 mV
10 ms
B
1 nA
QX-314
-79 mV
-0.25 nA

Figure 18. EPSP summation using matched simulated EPSPs.

A, Four examples from one neuron comparing EPSP summation for two evoked EPSPs (top left) to EPSP summation in which a simulated EPSP is substituted for: the Px evoked EPSP (top right), the Ds EPSP (bottom left) and both the Px and Ds evoked EPSPs (bottom right). Below each set of voltage traces are the traces of the current injected into the soma to generate simulated EPSPs (shown as dotted lines). *B*, Comparison of SR values from summation of evoked EPSPs to summation with their matched simulated EPSPs. To be considered matched, the simulated EPSPs and the evoked EPSPs had to be of similar size, time course and done at the same holding potential. In cases where error bars are shown, 2 to 5 SR values were measured under similar conditions; however, the size of the simulated EPSP was adjusted to bracket the size of the evoked EPSP or SR values were measured (as in *A*) where a simulated EPSP was first substituted for one and then for the other (or both) evoked EPSPs. The numbers at the bottom indicate the cell in which the data was gathered. In two cells, there was more than one group of matched EPSPs. The first 3 data points (306.1A-C) are from the same neuron but with different sized EPSPs. In another cell, two data groups were measured at -71 mV (714.2A) and -87 mV (714.2B). The example shown in *A* corresponds to neuron 714.1 in *B*.

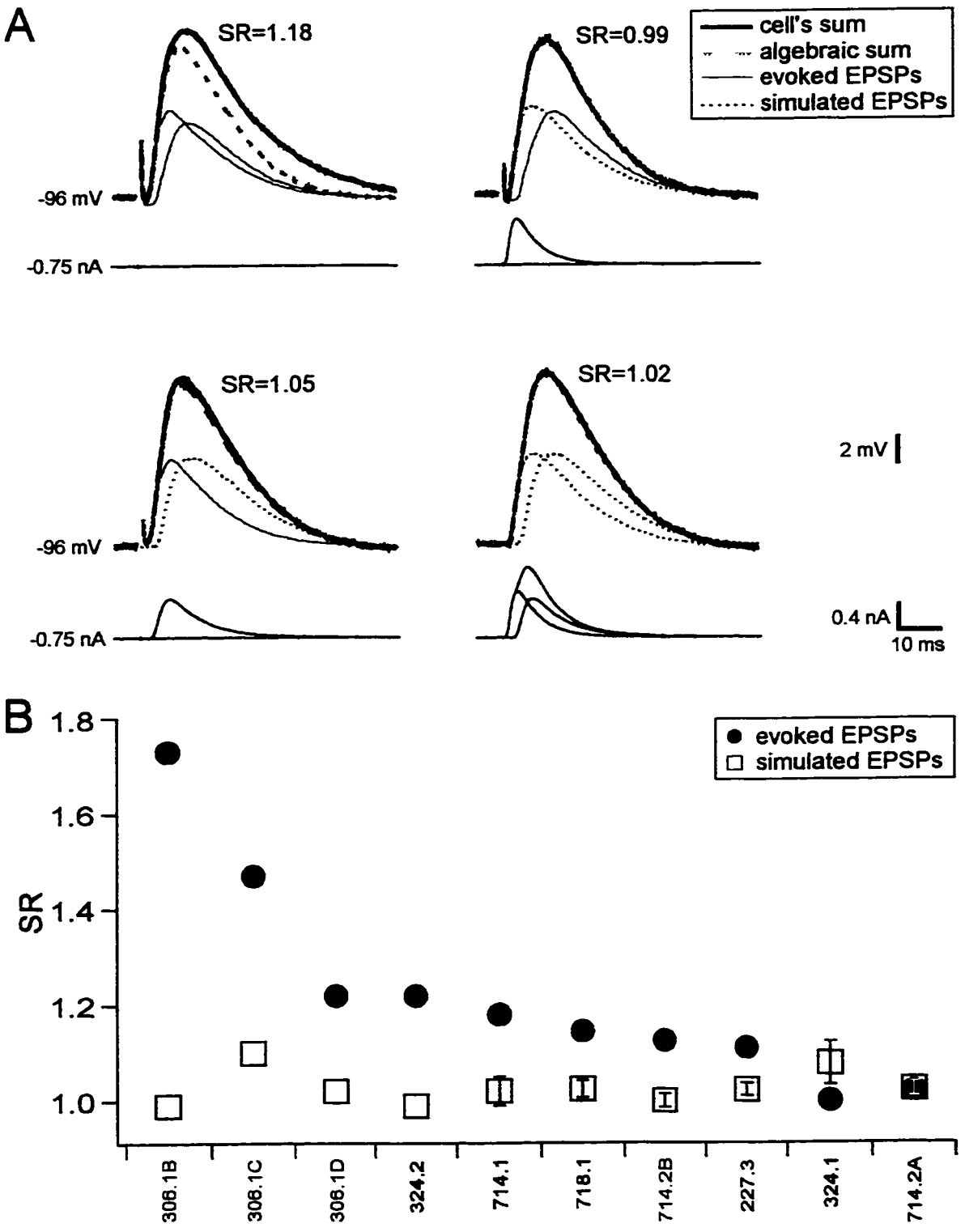
A
SR=1.18
SR=0.99
cell's sum
algebraic sum
evoked EPSPs
simulated EPSPs
-96 mV
-0.75 nA
SR=1.05
SR=1.02
2 mV
-96 mV
-0.75 nA
0.4 nA
10 ms
B
1.8
1.6
1.4
1.2
1.0
SR
evoked EPSPs
simulated EPSPs
306.1B
306.1C
306.1D
324.2
714.1
718.1
714.2B
227.3
324.1
714.2A

Figure 19. QX-314 reduces superlinear summation of simulated EPSPs

Left: examples from two neurons in which a simulated EPSP is substituted for the Px EPSP. In *A*, the neuron recorded without QX-314 (KCl) has a higher SR than the neuron in *B* which was recorded with QX-314 filled electrodes. Below each set of voltage traces are the traces of the current injected into the soma to generate the simulated EPSPs. Right: Distribution of SR values measured using a simulated EPSPs in place of either or both the proximal and distal stimuli for neurons recorded without QX-314 (*C*, KCl) and with QX-314 (*D*). Bin width = 0.02 SR units. As in Figure 10, the QX-314 histogram was fit to a Gaussian curve (solid line) and the upper and lower 95% confidence limits were determined (dashed vertical lines).

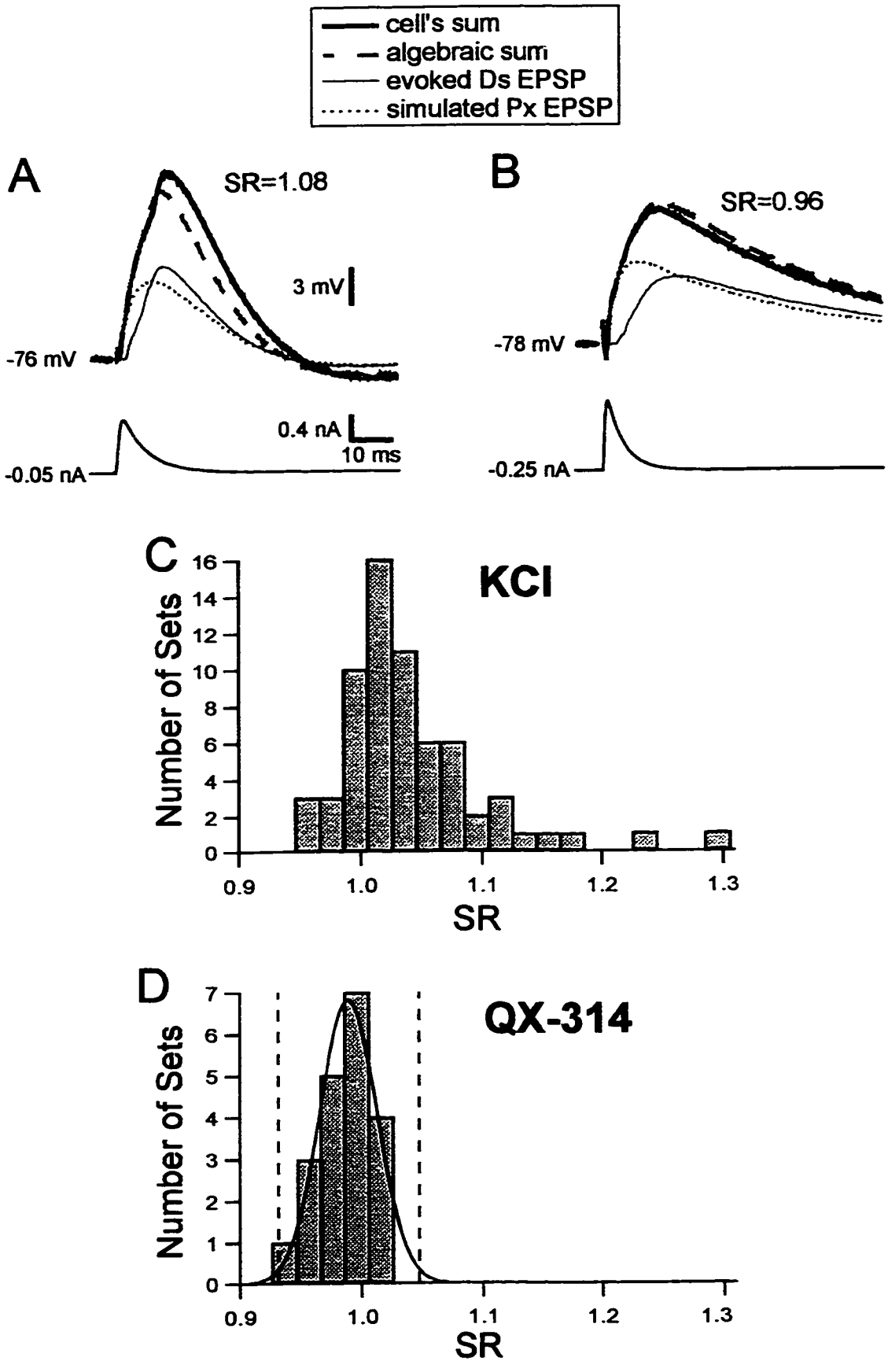
cell's sum
algebraic sum
evoked Ds EPSP
simulated Px EPSP
A
SR=1.08
3 mV
-76 mV
0.4 nA
10 ms
-0.05 nA
B
SR=0.96
-78 mV
-0.25 nA
C
KCl
Number of Sets
SR
D
QX-314
Number of Sets
SR

Figure 20. SR values for evoked and simulated EPSPs

SR distributions comparing evoked EPSPs in neurons recorded with KCl electrodes (*A*) and neurons recorded with QX-314 electrodes (*B*) to simulated EPSPs in both types of cells (*C*, *D*). Data in this figure is the same data used to create Figures 10 and 19. Histograms created using bin width of 0.04 SR units for all histograms.

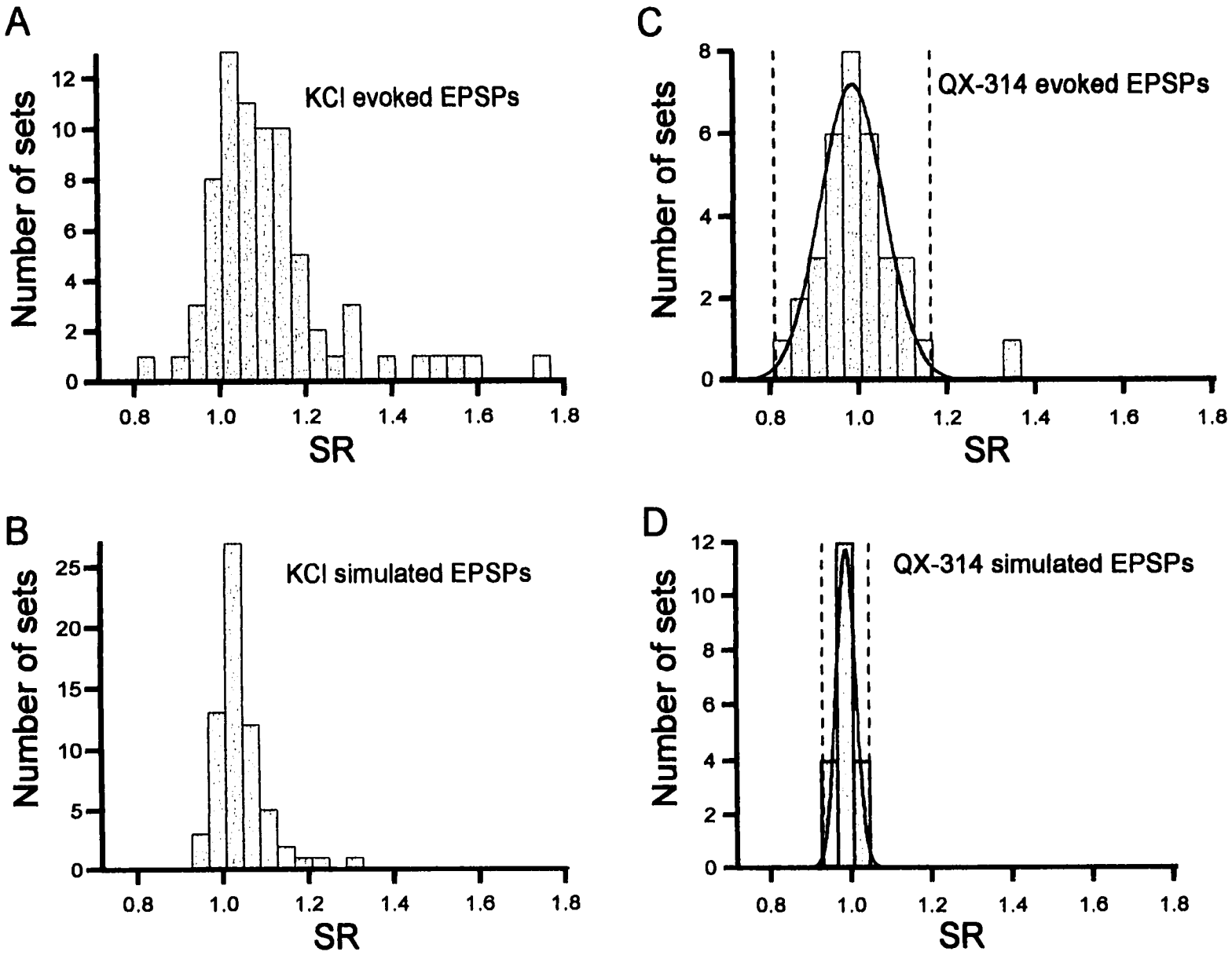
A
KCl evoked EPSPs
Number of sets
SR
B
KCl simulated EPSPs
Number of sets
SR
C
QX-314 evoked EPSPs
Number of sets
SR
D
QX-314 simulated EPSPs
Number of sets
SR

Figure 20. SR values from neurons without apical tuft

A, Photomicrograph of florescently labeled neuron whose apical dendritic tuft is missing beyond the cut made to isolate the two stimuli. *B*, Example from cell in A showing linear summation of EPSPs. *C*, Example from intact cell showing large amount of superlinear summation. Histogram distribution of SR values from cells with missing apical dendrtic tufts (*D*) compared to SR values from intact cells (*E*). Only summed EPSPs with Δt=5 ms and holding potentials > -85 mV were used in these histograms, since there was not enough data under other conditions to do a statistical comparison. The data in *E* is a subset of the data in Figure 14. The binwidth for both histograms is 0.04 SR units.

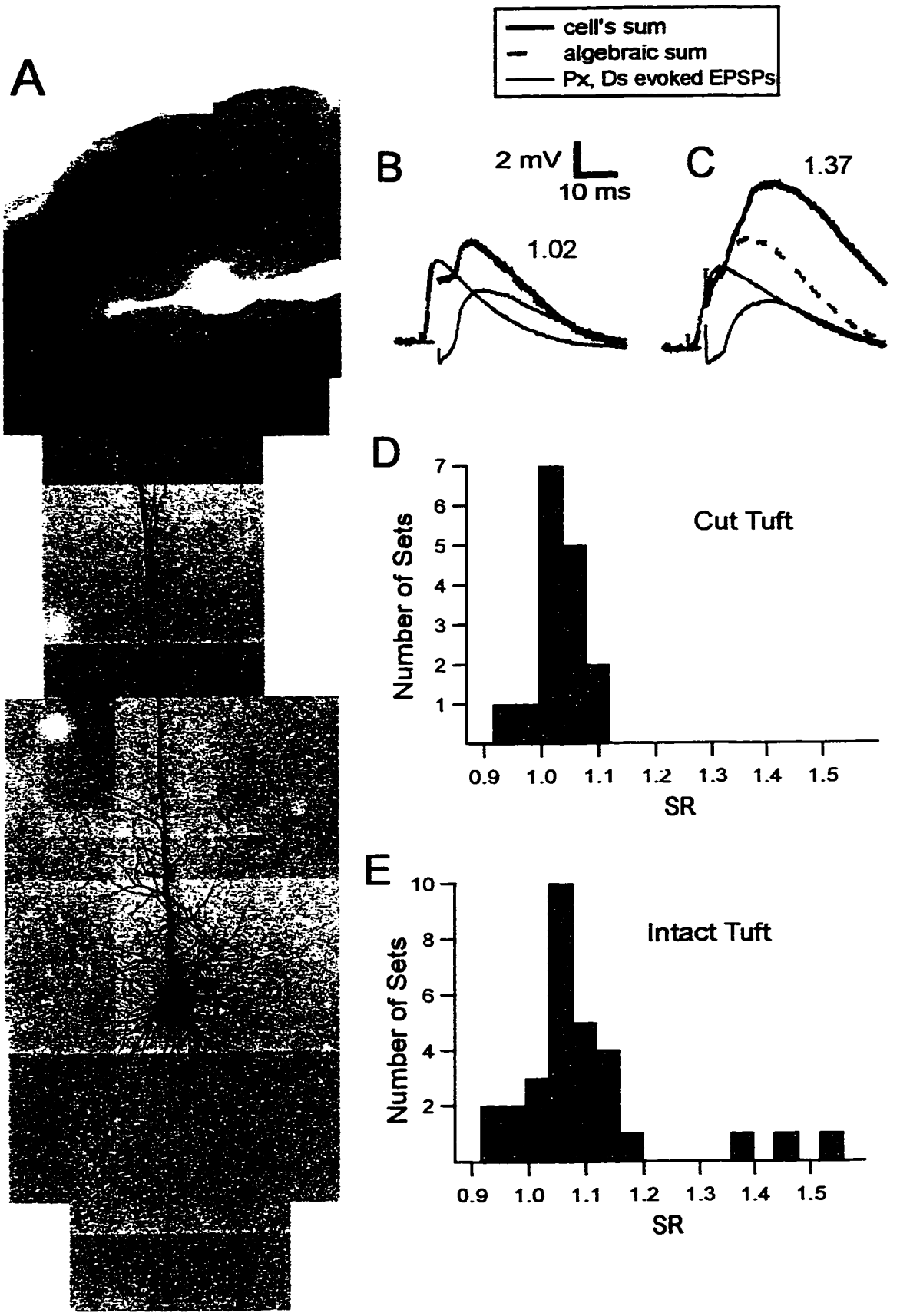
A
cell's sum
algebraic sum
Px, Ds evoked EPSPs
B
2 mV
10 ms
1.02
C
1.37
D
Cut Tuft
Number of Sets
SR
E
Intact Tuft
Number of Sets
SR

Figure 21. Effect of time on SR in cells recorded with QX-314 electrodes

Mean SR versus time in QX-314 loaded cells. Each point is the mean of 5 to 9 SR values measured in cells recorded with QX-314 electrodes with $\Delta t=0$ and holding potentials of more depolarized than -85 mV. Bars represent the SEM of each point.

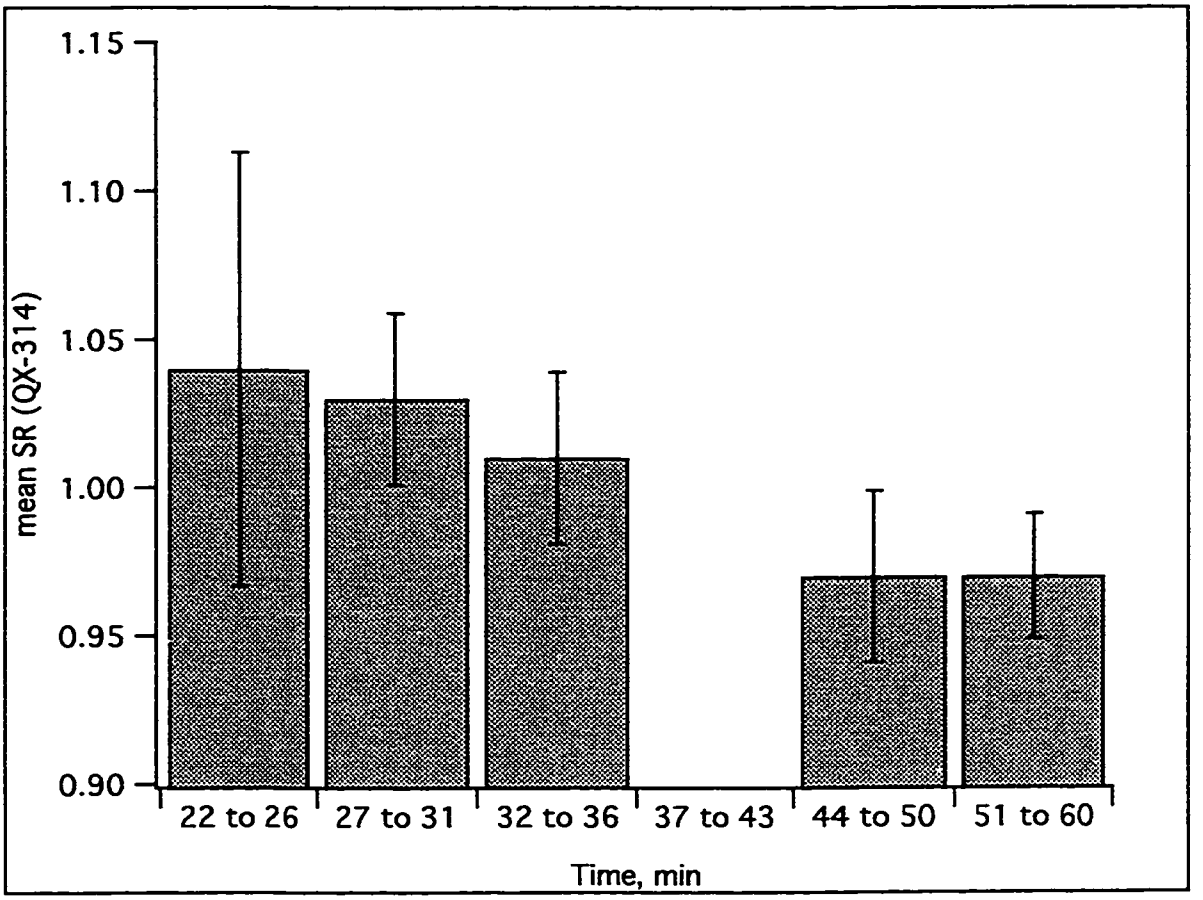
1.15
1.10
1.05
1.00
0.95
0.90
mean SR (QX-314)
22 to 26
27 to 31
32 to 36
37 to 43
44 to 50
51 to 60
Time, min

CHAPTER 6: GENERAL DISCUSSION

The results described in this dissertation support the idea that voltage-sensitive conductances in the dendrites play an important role in EPSP summation in layer V pyramidal neurons. Models of passive dendrites predict that synaptic inputs will sum sublinearly if the signal from one input affects the synaptic driving force of other inputs (Rall, 1977; Rall, et al., 1967), or if synaptic conductance changes cause a reduction in input resistance (Bernander, et al., 1991). Early support for the effects of synaptic driving force came from measurements of sublinear EPSP summation in motoneurons (Burke, 1967). There is now, however, substantial evidence that many types of neurons contain voltage-sensitive conductances throughout their dendritic trees (for review see Johnston, et al., 1996; Yuste and Tank, 1996). Here I have demonstrated that postsynaptic conductances can cause superlinear summation of AMPA-receptor mediated synaptic inputs in neocortical layer V pyramidal neurons. The amount of nonlinear summation was affected by the time interval between inputs and the holding potential of the postsynaptic neuron. Using simulated EPSPs, I showed that superlinear summation primarily occurs in the dendrites, although the somatic conductances also contributed to superlinear summation of inputs.

SUPERLINEAR SUMMATION IS DUE TO POSTSYNATPIC MECHANISMS.

Superlinear summation could result from either postsynaptic mechanisms or presynaptic interactions between the two stimulating sites. In these experiments, superlinear summation appears to be primarily due to postsynaptic mechanisms. First, intracellular QX-314 reduced the neurons ability to sum EPSPs in a greater than linear fashion. If superlinear summation were due to presynaptic interactions instead of postsynaptic conductances, superlinear summation would have been observed in neurons recorded with and without QX-314 in the electrode. Additionally, in QX-314 filled neurons, summation using simulated EPSPs was similar to summation with physiologic EPSPs. If presynaptic interactions were affecting summation, simulated EPSPs would have had a different mean SR than evoked EPSPs. Finally, paired-pulses indicated that the two stimuli were stimulating separate sets of fibers (See Chapter 1). There is the possibility that a small amount of presynaptic interactions may be contaminating my measurements since I did observe that SR's in cells recorded with QX-314 electrodes were not linear for all Δt's (see Figure 16). However, a majority of the superlinear summation measured was blocked by QX-314 indicating it was due to postsynaptic conductances.

DENDRITIC CONDUCTANCES CONTRIBUTE TO SUPERLINEAR SUMMATION.

These results suggest that the dendritic QX-314 sensitive conductances contribute to the superlinear summation observed in these experiments. If the soma

region itself contributed to large amounts of superlinear summation, we would expect the SR values measured with simulated EPSPs to be similar to SR values measured with evoked EPSPs. Instead, evoked dendritic EPSPs had larger SR values than simulated EPSPs. One explanation for this result is that the amplitude of the evoked EPSPs in the dendrites is larger than the amplitude that would be recorded at the soma (Stuart and Sakmann, 1995, Stuart and Spruston, 1998). Thus, simulated EPSPs at the soma may not have activated the same amount of Na^+ or Ca^{2+} conductances as the evoked EPSPs in the dendrites. Additionally, in these experiments there is not necessarily a proportional relationship between EPSP size measured at the soma and EPSP size in the dendrites since the inputs may be coming from various regions of the dendrite. The true relationship between SR and EPSP amplitude may be obscured due to measurements being taken from the soma. This could explain why I was unable to find a significant correlation between EPSP size and SR.

Evoked dendritic EPSPs may also have larger SR values compared to simulated somatic EPSPs due to the somatic shunt created by microelectrode impalement (Clements and Redman, 1987; Spruston and Johnston, 1992). This shunt would create a leak conductance that could counteract other conductances contributing to superlinear summation in the soma (Clements and Redman, 1987; Spruston and Johnston, 1992). In these experiments, the input resistance of layer 5 pyramidal cells from 3-5 week old rats using sharp electrodes was found to be 22±2 MΩ, while whole-cell recording from the same aged rats with patch electrodes yielded an input resistance of 77 ± 5MΩ (from

Cerne and Spain, (1997); temperature = 33±1° C). The 3.5 fold difference between the two groups is indicative of a somatic shunt resulting from the use of sharp electrodes (Spruston and Johnston, 1992). Due to this shunt, the soma may contribute less to EPSP summation than it would normally. Under these experimental conditions, only the superlinear summation in the dendrites is readily apparent, while the somatic component is minimal.

These results are consistent with mutual interaction between the proximal and distal inputs leading to superlinear summation. Although it is not known exactly where the inputs will occur in these studies, they do not seem to be impinging on the same area. The distal stimulus likely stimulated the apical tuft while the proximal stimulus likely stimulated the proximal portion of the apical dendrite and/or parts of the basal dendrites due to horizontal cortical pathways (Cauller and Connors, 1994; Ichinose and Murakoshi, 1996; Thomson and Deuchars, 1994; White and Keller, 1989). Despite the fact that the proximal and distal EPSPs stimulate different areas of the apical dendrite, SR values did not appear to depend more on one type of EPSP or the other. For both Px and Ds EPSPs, the size of EPSP did not significantly affect SR. Additionally, the order of the two EPSPs did not affect EPSP summation.

How could the proximal and distal EPSPs affect the size and shape of each other if the two inputs are impinging on very different areas of the apical dendrite? One possibility is that very distal synaptic events are affected by conductances elsewhere in

the neuron. Several studies have shown that the apical dendrite has a nonhomogeneous distribution of calcium channels, which if activated by one input would affect the size and shape of subsequent inputs (Schiller, et al., 1995; Seamans, 1997; Yuste, et al., 1994). Another possibility is that although one input cannot elicit a Ca^{2+} spike by itself, when combined with another input a Ca^{2+} spike is elicited. In my experiments, there were a few cases in which the response to both stimuli elicited a large voltage deflection reminiscent of a Ca^{2+} spike and resulted in SR values > 1.30 (See Figure 10A and Figure 20C). On the other hand, there were many cases of superlinear summation for which no such large responses were observed. Another possibility is that layer 1 inputs are amplified by more proximal active conductances (Cauller and Connors, 1994). Stuart and Sakmann (1995) demonstrated that Na^+ conductances in the soma and initial segment can boost EPSPs in the apical dendrite. However, if conductances in the soma and initial segment were causing superlinear summation, I would have expected that simulated EPSPs would cause similar amounts of superlinear summation as real EPSPs. These studies imply that a QX-314 sensitive conductance somewhere in the apical dendrite is responsible for superlinear summation.

WHAT CONDUCTANCES UNDERLIE SUPERLINEAR SUMMATION?

Since QX-314 blocks many conductances, Na^+, Ca^{2+}, I_h and possibly other K^+ conductances (Andreasen and Hablitz, 1993; Issac and Wheal, 1993; Nuñez and Buño, 1992; Perkins and Wong, 1995; Stafstorm, et al., 1985; Talbot and Sayer, 1996), it is

uncertain what conductance or conductances are responsible for superlinear summation. Since greater than linear summation was predominately observed, a regenerative current such as Na^+ or Ca^{2+}, particularly a low-voltage activated T-like calcium current, could be responsible for boosting EPSP summation. Paradoxically, hyperpolarization could increase the amount of superlinear summation by partially removing inactivation of the Na^+ or Ca^{2+} conductances particularly in the more proximal dendrites. Both types of conductances have been shown to be affected by subthreshold EPSPs (Magee, et al., 1995; Magee and Johnston, 1995a, Magee and Johnston, 1995b). The low-voltage activated T-type Ca^{2+} channels have been shown to have a higher density in the apical tuft of CA1 hippocampal pyramidal neurons (Magee and Johnston, 1995b). If neocortical neurons have a similar distribution of Ca^{2+} channels, they may cause inputs in the tuft to be substantially amplified as found by Schiller et al. (1997). A higher density of Ca^{2+} conductances in the tuft could also create superlinear summation of EPSPs. In support of this idea, I observed that SR values were reduced in neurons that were missing the apical tuft.

K^+ currents will also affect EPSPs summation (Cash and Yuste, 1998; Schwindt and Crill, 1997). For instance, Cash and Yuste, (1998) measured predominately sublinear summation of AMPA-receptor mediated glutamatergic synaptic inputs onto cultured hippocampal cells due to I_A. In contrast to this, I did not observe sublinear summation in my experiments, which may indicate that there was less I_A in my preparation than in theirs. Another conductance that would influence EPSP summation is

the hyperpolarization-activated cation conductance, I_h. This conductance could affect EPSP summation in two opposing ways. First, I_h might decrease SR by shunting EPSPs. Alternatively, if I_h deactivates during the rise of an EPSP, the conductance decrease could result in an increase of EPSP amplitude and thus create superlinear summation. Further studies designed to determine the contribution of different types of conductances would aid in determining the factors underlying summation of EPSPs.

FUNCTIONAL IMPLICATIONS.

Layer V pyramidal neurons have been postulated to act as coincidence detectors, meaning neurons will preferentially respond to synchronized inputs (Konig, et al., 1996). In these experiments, superlinear summation occurred with 5 ms and in some cases 10 ms between stimuli. These results are not consistent with layer V pyramidal neurons performing as coincidence detectors on a 1 ms or less timescale as proposed (Softky, 1995). When comparing results across studies, it is important to keep in mind that other presynaptic factors could affect the time course of EPSP summation. One possibility is that inhibition could potentially cause neurons to act as coincident detectors by shortening the length of the EPSP and shunting subsequent EPSPs (Cauller and Connors, 1994, Koch, et al., 1983). If indeed inhibitory input always occurs with excitatory input as some studies indicate (Ferster and Jagadeesh, 1992), the time course of EPSP summation could be reduced. In this case, superlinear summation over an extended time course may only occur when inhibition is reduced. Additionally, recent studies both

in vivo and using computer-simulated neurons have postulated that the amount of synaptic background activity will affect the time course of EPSPs and their ability to interact with other EPSPs (Bernander, et al., 1991, Paré, et al., 1997). In this case, the background synaptic activity reduces the input resistance of the cell and thus shortens the time course of synaptic inputs (Koch, et al., 1996). One prediction of these studies is that in the absence of background activity such as in these experiments, synaptic inputs will be able to affect each other over a longer time course (Agmon-Snir and Segev, 1993).

In the described experiments, my primary interest was the effect that intrinsic voltage-sensitive conductances would have on superlinear summation. In this case, where there is boosting of synaptic potentials by active postsynaptic conductances, the time course over which boosting occurs will set limits on the independence of synaptic events separated in time. Long-lasting boosting would favor temporal integration whereas boosting by conductances with a rapid time course would favor coincidence detection. In my studies, I found the time course of superlinear summation was voltage-dependent. When the holding potential was relatively depolarized (membrane potential >-85 mV) neurons favored temporal integration with superlinear summation occurring even at 10 ms between inputs. At hyperpolarized potentials (≤ -85 mV), neurons were more like coincidence detectors with the only significant amounts of superlinear summation at Δt=0 ms and Δt=5 ms.

Based on simultaneous dual dendritic and somatic recordings from pyramidal cells using patch-pipettes, hyperpolarizing the soma by 15 mV would roughly

result in a potential change of -5 mV, 500μm from the soma (Stuart and Spruston, 1998). A distance of 500 μm from the soma corresponds to halfway between the distal and proximal stimulating electrodes. (Stuart and Spruston, 1998). Since I used sharp microelectrodes in these experiments, hyperpolarizing the soma would be expected to have even less effect on the dendritic membrane potential due to the somatic shunt created by microelectrode impalement (Clements and Redman, 1987; Spruston and Johnston, 1992). Thus, a hyperpolarization of 5 mV represents the greatest change in dendritic membrane potential possible in these experiments. This suggests that under a physiological relevant change in membrane potential, the time range over which synaptic inputs interact can change from one that favors temporal integration to one that favors coincident detection.

In these experiments, I predominately observed linear to superlinear summation for EPSPs that occurred either simultaneously or 5 ms apart. The middle 80% of all SR values were between 0.98 and 1.31 for simultaneously evoked EPSPs ($\Delta t=0$), and between 0.98 and 1.45 for EPSPs evoked 5 ms apart. On average, SR was around 1.1, which represents a 10% amplification over linear summation. While 10% is not large, it would affect neuronal output by raising membrane potential closer to firing threshold. In addition, I did not observe any sublinear summation of EPSPs as predicted by models of passive dendrites. This indicates that the active, voltage-sensitive properties of dendrites play an important role in EPSP summation and can compensate for the effect of passive properties of dendrites.

FUTURE STUDIES

These experiments demonstrate that the dendrites of layer V pyramidal neurons are capable of summing their inputs in a superlinear fashion due to time and voltage dependent postsynaptic conductances. What remains unknown is how the different types of ionic conductances, Na^+, Ca^{2+}, K^+, and I_h, affect EPSP summation. One way to address this question would be to measure EPSP summation using microiontophoresis to apply glutamate directly to specific areas of the dendritic tree. This method would allow pharmacological isolation of individual types of conductances without affecting synaptic response. By being able block ionic conductances separately, the effect of each type of conductances on the amount and time course of nonlinear EPSP summation could be determined. Iontophoretically applied glutamate would also allow control over which areas of the dendrite are being stimulated, thus determining location dependent effects.

Another question raised by these experiments is how other components of the postsynaptic potential will affect synaptic summation. In this study, summation was restricted to AMPA-receptor mediated EPSPs in order to focus on the postsynaptic role of EPSP summation. During normal activity, neurons would be receiving NMDA-receptor mediated EPSPs as well as IPSPs mediated by GABA receptors. As discussed above, these other components may affect EPSP summation by changing the shape of EPSPs. The NMDA-receptor mediated component amplifies and lengthens EPSPs (Jones and

Baughman, 1988). Cash and Yuste (1998) demonstrated than the NMDA-receptor mediated conductance can increase the amount of EPSP summation in hippocampal neurons. On the other hand, GABAergic IPSPs, particularly $GABA_A$ would shorten the EPSP and thus decrease the time course of EPSP summation (Cauller and Connors, 1994, Koch, et al., 1983).

Another intriguing question deals with what would be the effect of neuromodulators such as serotonin, norepinephrine, or acetylcholine. I observed a shift from coincident-like summation to more integrate-and-fire-like summation with changes in holding potential. Presumably, this shift is due to a change in the activation state of one or more ionic conductances. One expectation is that neuromodulators known to affect the activation of ionic conductances will also affect the amount of and time-course of EPSP summation. For instance, Skydsgaard and Hounsgaard (1994) observed superlinear summation of iontophoretically applied glutamate responses in the presence of muscarine. Muscarine may have this effect because it blocks a slow outward K^+ conductance, the m-current, and it increases low-threshold Ca^{2+} currents (Brown and Adams, 1980; Fisher and Johnston, 1990; Nishikawa, et al., 1994; Nowak and Macdonald, 1983; Schwindt, et al., 1992). By their ability to affect the activation of various ionic conductances, neuromodulators may also play an important role in determining how EPSPs sum.

The results in this dissertation demonstrate that the summation of EPSPs in layer V pyramidal cells is linear to superlinear and is affected by postsynaptic

conductances. The dendrites are not passive but instead allow for amplification of EPSP summation. Future studies that determine how various conditions, such as the level of activation of different ionic conductances or the relative amount of inhibition and excitation, affect EPSP summation will further our understanding of what underlies synaptic integration.

BIBLIOGRAPHY

Agmon-Snir H, Segev I (1993) Signal delay and input synchronization in passive dendritic structures. J Neurophysiol 70:2066-2085

Amitai Y, Friedman A, Connors BW, Gutnick MJ (1993) Regenerative activity in apical dendrites of pyramidal cells in neocortex. Cereb Cortex 3:26-38

Andreasen M, Hablitz JJ (1993) Local anesthetics block transient outward potassium currents in rat neocortical neurons. J Neurophysiol 69:1966-1975

Barrett JN (1975) Motoneuron dendrites: role in synaptic integration. Fed Proc 34:1398-1407

Barrett JN, Crill WE (1974) Specific membrane properties of cat motoneurones. J Physiol (Lond) 239:301-324

Benardo LS (1994) Separate activation of fast and slow inhibitory postsynaptic potentials in rat neocortex *in vitro*. J Physiol (Lond) 476:203-215

Benardo LS, Masukawa LM, Prince DA (1982) Electrophysiology of isolated hippocampal pyramidal dendrites. J Neurosci 2:1614-1622

Bernander O, Douglas RJ, Martin KAC, Koch C (1991) Synaptic background activity influences spatiotemporal integration in single pyramidal cells. Proc Natl Acad Sci USA 88:11569-11573

Brown DA, Adams PR (1980) Muscarinic suppression of a novel voltage-sensitive K^+ current in a vertebrae neurone. Nature 283:673-6

Burke RE (1967) Composite nature of the monosynaptic excitatory postsynaptic potential. J Neurophysiol 30:1114-37

Cash S, Yuste R (1998) Input summation by cultured pyramidal neurons is linear and position-independent. J Neurosci 18:10-15

Cauller LJ, Connors BW (1994) Synaptic physiology of horizontal afferents to layer I in slices of rat SI neocortex. J Neurosci 14:751-762

Cerne R, Spain WJ (1997) $GABA_A$ mediated afterdepolarization in pyramidal neurons from rat neocortex. J Neurophysiol 77:1039-1045

Chagnac-Amitai Y, Luhmann HJ, Prince D (1990) Burst generating and regular spiking layer V pyramidal neurons of rat neocortex have different morphological features. J Comp Neurol 296:598-613

Chagnac-Amital Y, Connors BW (1989) Horizontal spread of synchronized activity in neocortex and its control by GABA-mediated inhibition. J Neurophysiol 61:747-758

Clements JD, Redman SJ (1987) Cable properties of cat spinal motoneurones measured by combining voltage clamp, current clamp and intracellular staining. J Physiol 409:63-87

Connors BW, Gutnick MJ (1990) Intrinsic firing patterns of diverse neocortical neurons. Trends Neurosci 13:99-103

Cook EP, Johnston D (1997) Active dendrites reduce location-dependent variability of synaptic input trains. J Neurophysiol 78:2116-2128

Coombs JS, Curtis DR, Eccles JC (1959) The electrical constants of the motoneurone membrane. J Physiol (Lond) 145:505-528

Deisz RA, Fortin G, Zieglgansberger W (1991) Voltage dependence of excitatory postsynaptic potentials of rat neocortical neurons. J Neurophysiol 65:371-382

Del Castillo J, Katz B (1954) Quantal Componets of the End-Plate Potential. J Physiol 124:560-573

Eccles JC (1957) The Physiology of Nerve Cells. Baltimore: John Hopkins Press

Ferster D, Jagadeesh B (1992) EPSP-IPSP interactions in cat visual cortex studied with *in vivo* whole-cell patch recording. J Neurosci 12:1262-1274

Fisher R, Johnston D (1990) Differential modulation of single voltage-gated calcium channels by cholinergic and adrenergic agonists in adult hippocampal neurons. J Neurophysiol 64:1291-302

Gil Z, Connors BW, Amitai Y (1997) Differential regulation of neocortical synapses by neuromodulators and activity. Neuron 19:679-686

Hille B (1992) Ionic Channels of Excitable Membranes. Sunderland, MA: Sinauer Associates, Inc.

Hodgkin AL, Rushton WAH (1946) The electrical constraints of a crustacean nerve fibre. Proc R Soc Lond B 133:444-479

Hoffman DA, Magee JC, Colbert CM, Johnston D (1997) K^+ channel regulation of signal propagation in dendrites of hippocampal pyramidal neurons. Nature 387:869-875

Horikawa K, Armstrong WE (1988) A versatile means of intracellular labeling: injection of biocytin and its detection with avidin conjugates. J Neurosci Methods 25:1-11

Huguenard JR, Hamill OP, Prince DA (1989) Sodium channels in dendrites of rat cortical pyramidal neurons. Proc Natl Acad Sci USA 86:2473-2477

Ichinose T, Murakoshi T (1996) Electrophysiological elucidation of pathways of intrinsic connections in rat visual cortex. Neurosci 73:25-37

Issac JT, Wheal HV (1993) The local anaesthetic QX-314 enables enhanced whole-cell recordings of excitatory synaptic currents in rat hippocampal slices *in vitro*. Neurosci Lett 150:227-230

Jack JJB, Noble D, Tsien RW (1975) Electrical current flow in excitable cells. Oxford: Clarendon Press

Johnston D, Magee JC, Colbert CM, R. CB (1996) Active properties of neuronal dendrites. Annu Rev Neurosci 19:165-186

Jones KA, Baughman RW (1988) NMDA- and non-NMDA-receptor components of excitatory synaptic potentials recorded from cells in layer V of rat visual cortex. J Neurosci 8:3522-34

Kelvin WT (1855) On the theory of the electric telegraph. Proc Roy Soc 7:392-399

Kim HG, Connors BW (1993) Apical dendrites of the neocortex: correlation between sodium- and calcium- dependent spiking and pyramidal cell morphology. J Neurosci 13:5301-5311

Koch C, Poggio T, Torre V (1983) Nonlinear interactions in a dendritic tree: localization, timing, and role in information processing. Proc Natl Acad Sci USA 80:2799-2802

Koch C, Rapp M, Segev I (1996) A brief history of time (constants). Cerb Cortex 6:93-101

Konig P, Engel AK, Singer W (1996) Integrator or coincidence detector? The role of the cortical neuron revisited. Trends Neurosci 19:130-137

Kuno M, Miyahara JT (1969) Non-linear summation of unit synaptic potentials in spinal motorneurons of the cat. J Physiol (Lond) 201:465-477

Larkman A, Mason A (1990) Correlations between morphology and electrophysiology of pyramidal neurons in slices of rat visual cortex. II. Electrophysiology. J Neurosci 10:1407-1414

Llinas R, Sugimori M (1980) Electrophysiological properties of in vitro Purkinje cell dendrites in mammalian cerebellar slices II. J Physiol (Lond) 305:197-213

Lorente de Nó R, Condouris GA (1959) Decremental conduction in peripheral nerve. Integration of stimuli in the neuron. Proc Natl Acad Sci 45:592-617

Lux HD, Schubert P, Kreutzberg GW (1970) Direct matching of morphological and electrophysiological data in cat spinal motoneurones. In: Excitatory Synaptic Mechanisms (P. Andersen and J. K. S. Jansen, ed), pp189-198. Olso: Scandinavian University Books, Universitetsforlaget

Magee JC (1998) Dendritic hyperpolarization-activated currents modify the integrative properties of hippocampal CA1 pyramidal neurons. J Neurosci 18:7613-24

Magee JC, Christofi G, Miyakawa H, Christie B, Lasser-Ross N, Johnston D (1995) Subthreshold synaptic activation of voltage-gated Ca^{2+} channels mediates a localized Ca^{2+} influx into dendrites of hippocampal pyramidal neurons. J Neurophysiol 74:1335-1342

Magee JC, Johnston D (1995b) Characterization of single voltage-gated Na^{+} and Ca^{2+} channels in apical dendrites of rat CA1 pyramidal neurons. J Physiol (Lond) 487:67-90

Magee JC, Johnston D (1995a) Synaptic activation of voltage-gated channels in the dendrites of hippocampal pyramidal neurons. Science 268:301-304

Major G, Larkman AU, Jones P, Sakmann B, Jack JJB (1994) Detailed passive cable models of whole-cell recorded CA3 pyramidal neurons in rat hippocampal slices. J Neurosci 14:4613-4638

Markram H, Helm PJ, Sakmann B (1995) Dendritic calcium transients evoked by single back-propagating action potentials in rat neocortical pyramidal neurons. J Physiol Lond 485:1-20

Markram H, Sakmann B (1994) Calcium transients in dendrites of neocortical neurons evoked by single subthreshold excitatory postsynaptic potentials via low-voltage calcium channels. Proc Natl Acad Sci USA 91:5207-5211

Nicoll A, Larkmore A, Blakemore C (1993) Modulation of EPSPs shape and efficacy by intrinsic membrane conductances in rat neocortical pyramidal neurons *in vitro*. J Physiol (Lond) 468:693-710

Nishikawa M, Munakata M, Akaike N (1994) Muscarinic acetylcholine response in pyramidal neurones of rat cerebral cortex. Br J Pharmacol 112:1160-6

Nowak LM, Macdonald RL (1983) Muscarine-sensitive voltage-dependent potassium current in cultured murine spinal cord neurons. Neurosci Lett 35:85-91

Nuñez A, Buño W (1992) Intracellular effects of QX-314 and Cs^+ in hippocampal pyramidal neurons *in vivo*. Experimental Neurology 115:266-270

Otis TS, DeKonick Y, Mody I (1993) Characterization of synaptically elicited $GABA_B$ responses using patch-clamp recordings in rat hippocampal slices. J Physiol (Lond) 463:391-407

Paré D, Lebel E, Lang EJ (1997) Differential impact of miniature synaptic potentials on the soma and dendrites of pyramidal neurons in vivo. J Neurophysiol 78:1735-39

Perkins KL, Wong RKS (1995) Intracellular QX-314 blocks the hyperpolarization-activated inward current I_q in hippocampal CA1 pyramidal neurons. J Neurophysiol 73:911-915

Pockberger H (1991) Electrophysiological and morphological properties of rat motor cortex neurons in vivo. Brain Res 539:181-190

Rall W (1977) Core conductor theory and cable properties of neurons. In: Handbook of Physiology: the Nervous System. Cellular Biology of Neurons. ed), pp39-97. Bethesda, MD: Am. Physiol. Soc.

Rall W (1967) Distinguishing theoretical synatpic potentials computed for different soma-dendritic distributions of synaptic input. J Neurophysiol 30:1138-1193

Rall W (1964) Theoretical significance of dendritic trees for neuronal input-output relations. In: Neural Theory and Modeling: Proceedings of the 1962 Ojai Symposium (R. F. Reiss, ed), Stanford, CA: Stanford University Press

Rall W (1962) Theory of physiological properties of dendrites. Ann NY Acad Sci 96:1071-1092

Rall W, Burke RE, Smith TG, Nelson PG, Frank K (1967) Dendritic location of synapses and possible mechanisms for the monosynaptic EPSP in motoneurons. J Neurophysiol 30:1169-93

Ramon-Moliner, E (1962) An attempt at classifying nerve cells on the basis of their dendritic patterns. J Comp Neurol 119:211-227

Ramón y Cajal S (1937) Recolections of My Life. Cambridge, MA: MIT Press

Redman S, Walmsley B (1983) The time course of synaptic potentials evoked in cat spinal motoneurones at identified group Ia synapses. J Physiol 343:117-133

Reyes AD, Fetz EE (1993) Two modes of interspike interval shortening by brief transient depolarizations in cat neocortical neurons. J Neurophysiol 69:1661-1672

Schiller J, Helmchen F, Sakmann B (1995) Spatial profile of dendritic calcium transients evoked by action potentials in rat neocortical pyramidal neuron. J Physiol (Lond) 487:583-600

Schiller J, Schiller Y, Stuart G, Sakmann B (1997) Calcium action potentials restricted to distal apical dendrites of rat neocortical pyramidal neurons. J Physiol (Lond) 505:605-616

Schwindt PC, Crill WE (1995) Amplification of synaptic current by persistent sodium conductance in apical dendrite of neocortical neurons. J Neurophysiol 74:2220-2224

Schwindt PC, Crill WE (1997) Modification of current transmitted from apical dendrite to soma by blockade of voltage- and Ca^{2+} -dependent conductances from rat neocortical pyramidal neurons. J Neurophysiol 78:187-198

Schwindt PC, Spain WJ, Crill WE (1992) Calcium-dependent potassium currents in neurons from cat sensorimotor cortex. J Neurophysiol 67:216-225

Seamans JK (1997) Contributions of voltage-gated Ca^{2+} channels in the proximal versus distal dendrites to synaptic integration in prefrontal cortical neurons. J Neurosci 17:5936-5948

Shadlen MN, Newsome WT (1994) Noise, neural code and cortical organization. Curr Opin Neurobiol 4:569-579

Skydsgaard M, Hounsgaard J (1994) Spatial integration of local transmitter responses in motoneurones of the turtle spinal cord in vitro. J Physiol (Lond) 479:233-46

Softky W (1994) Sub-millisecond coincidence detection in active dendritic trees. Neuroscience 58:13-41

Softky WR (1995) Simple codes versus efficient codes. Curr Opin Neurobiol 5:239-247

Softky WR, Koch C (1993) The highly irregular firing of cortical cells is inconsistent with temporal integration of random EPSPs. J Neurosci 13:334-350

Spain WJ, Schwindt PC, Crill WE (1987) Anomalous recification in neuons from cat sensorimotor cortex in vitro. J Neurophysiol 57:1555-1576

Spruston N, Jaffe DB, Johnston D (1994) Dendritic attenuation of synaptic potentials and currents: the role of passive membrane properties. Trends Neurosci 17:161-6

Spruston N, Jaffe DB, Williams SH, Johnston D (1993) Voltage- and space-clamp errors associated with the measure of electronicIly remote syanaptic events. J Neurophysiol 70:781-802

Spruston N, Johnston D (1992) Perforated patch-clamp analysis of the passive membrane properties of three classes of hippocampal neurons. J Neurophysiol 67:508-29

Spruston N, Schiller Y, Stuart G, Sakmann B (1995) Activity-dependent action potential invasion and calcium influx into hippocampal CA1 dendrites. Science 268:297-300

Stafstorm CE, Schwindt PC, Chubb MC, Crill WE (1985) Properties of persistent sodium conductance and calcium conductance of layer V neurons from cat sensorimotor cortex in vitro. J Neurophysiol 53:153-169

Strichartz GR (1973) The inhibition of sodium current in myelinated nerve by quaternary derivatives of lidocaine. J Gen Physiol 62:37-57

Stuart GJ, Sakmann B (1994) Active propagation of somatic action potentials into neocortical pyramidal cell dendrites. Nature 367:69-72

Stuart GJ, Sakmann B (1995) Amplification of EPSPs by axosomatic sodium channels in neocortical pyramidal neurons. Neuron 15:1065-1076

Stuart GJ, Spruston N (1998) Determinants of voltage attenuation in neocortical pyramidal neuron dendrites. J Neurosci 18:3501-3510

Talbot MJ, Sayer RJ (1996) Intracellular QX-314 inhibits calcium currents in hippocampal CA1 pyramidal neurons. J Neurophysiol 76:2120-2124

Thomson AM, Deuchars J (1994) Temporal and spatial properties of local circuits in neocortex. Trends Neurosci 17:119-126

Thurbon D, Luscher HR, Hofstetter T, Redman SJ (1998) Passive electrical properties of ventral horn neurons in rat spinal cord slices. J Neurophysiol 79:2485-2502

Turner DA (1988) Waveform and amplitude characteristics of evoked responses to dendritic stimulation of CA1 guinea-pig pyramidal cells. J Physiol (Lond) 395:419-439

van Brederode JFM, Spain WJ (1995) Differences in inhibitory synaptic input between layer II-III and layer V in cat neocortex. J Neurophysiol 74:1149-1166

White EL, Keller A (1989) Cortical circuits : synaptic organization of the cortex -- structure, function, and theory. Boston: Birkhauser

Yuste R, Gutnick MJ, Sarr D, Delaney KR, Tank DW (1994) Ca^{2+} accumulations in dendrites of neocortical pyramidal neurons: an apical band and evidence for two functional compartments. Neuron 13:23-43

Yuste R, Tank DW (1996) Dendritic integration in mammalian neurons a century after Cajal. Neuron 16:701-716

Zilles KJ (1985) The cortex of the rat : a stereotaxic atlas. Berlin: Springer-Verlag

APPENDIX A: COMPUTER PROGRAMS WRITTEN AND USED FOR DATA ACQUISITION AND ANALYSIS

All computer programs were written using IgorPro versions 2 and 3 (WaveMetrics, Inc., Lake Oswego, OR) and with the using of ITC16_XOP version (Instrutech, Great Neck, NY) for communicating between IgorPro and the ITC16 computer interface.

DATA ACQUISITION PROCEDURES

```
#pragma rtGlobals=1          // Use modern global access method.

//****DATA ACQUISITION PROCEDURES********

//Global Variables:
//****************Constant Variables (rarely if ever changed)
// CU_scale = 3.2                              Computer units/mV
// Stim_DAC_scale = 100                        Scales stim output. (mV/nA) -> (Current Clamp)
// Voltgain= 100, AmpGain= 1000      Gains for data read in  (mV/mV, mV/nA)
// Tl=1,TTb= CU_scale*5500   Width (ms) and height (V) for TTL pulses
// InVC=0                    Switch for Being in VC Default is 0 (i.e. not in voltage clamp!)
// Stime= datetime           Time experiment started
// ***************Variables for data aquisition
//per,sweeplength,cycleperiod   Acquistion parameters: time between points, points in wave,
time (s) between stims
// amp=-0.3, plen=4          Pulse (stim3) amplitude (nA) and length (ms)
// tm1=0, tm2=0, tm3=10            Delays for stim1, stim2, stim3
// flag=3, SaveWaves=0       Switches for data aquisition,
// nwaves=0, maxn=500        num waves digitized so far, max number of waves to digitize

//***********PreMade waves*******************
// Stimwv, Sampwv      Sent directly to, Read directly from ITC16 board: data is in computer
units
// stimT, stim1, stim2, stim3      Stimulus waved used to make Stimwv, for TTL output 0, &DAC
1,2,3
// v0, c0                Data waves Created from sampwv, have meaningful scale


//@@@@@@@**********VISIBLE MACROS AND PANALS**********@@@@@@

// Do at start of experiment or when want to restart entire experiment
Macro StartRestart()
SetDataFolder root:DataAcq
```

```
        StimReset()
        SaveWaves=0; flag=3
        nwaves=0; maxn=500
        ::raw:stime=datetime    // Moved to raw data folder 5/10/97
        MonitorResistance()
End

// Get stim waves back to orginal position, doesn't reset entire experiment
Macro StimReset()

        silent 1
         reset                          //resets board
        seq "D123","0101"               //4 Dacs and 2 ADC- For VoltageClamp
        Button ClampSwitch title="C C", proc=VoltClamp
SetDataFolder root:DataAcq
        PauseUpdate
                stim1=0; stim2=0; stim3=0; stimT=0
        StimT:=(x<tl)                   // Trigger Pulse, Beginning of each output wave
        stim1:=(tm1 != 0)*( (x>= tm1) %& (x< (tm1+tl) ) )       //Actually a ttL pulse
        stim2:=(tm2 !=0)*( (x>= tm2) %& (x< (tm2+tl) ) )        // Another TTL pulse
        stim3:= amp*( (x>= tm3) %& (x< (tm3+plen)) )            // Step pulse
End

Window StimGr_Con() : Graph
        PauseUpdate; Silent 1           | building window...
        String fldrSav= GetDataFolder(1)
        SetDataFolder root:DataAcq:
        Display /W=(388,218,806,466)/R stim2,stim1
        Append stim3
        SetDataFolder fldrSav
        ModifyGraph lSize(stim1)=2
        ModifyGraph rgb(stim2)=(3,52428,1),rgb(stim1)=(1,16019,65535)
        ModifyGraph axOffset(left)=-0.571429
        ControlBar 64
        SetVariable setk,pos={227,40},size={175,17},title="Step Amp, nA "
        SetVariable setk,limits={-10,10,0.1},value= root:DataAcq:amp
        SetVariable seta,pos={193,21},size={185,17},title="Time length, ms (a)"
        SetVariable seta,limits={0,INF,10},value= root:DataAcq:plen
        SetVariable setm3,pos={214,3},size={170,17},title="Delay, ms (tm3)"
        SetVariable setm3,limits={0,INF,5},value= root:DataAcq:tm3
        SetVariable setm1,pos={14,24},size={170,17},title="Time stim1, ms"
        SetVariable setm1,limits={0,INF,10},value= root:DataAcq:tm1
        SetVariable setm2,pos={14,41},size={170,17},title="Time stim2, ms"
        SetVariable setm2,limits={0,INF,10},value= root:DataAcq:tm2
        Button load,pos={103,1},size={80,20},proc=LoadStim,title="Load Stim"
        Button b2,pos={15,1},size={80,20},proc=StartProc,title="Send Stim"
```

```
EndMacro

//Digitizing_Panal
//control digitizing parameters:  Per, CyclePeriod ,sweeplength ,maxn
//Displays:       n, "Wavelength, ms" (gives length in ms of in/out waves)
//Procedures              ButtonProc() (Resets Board)
        //SaveCheck()   ( If checked creates new waves from v0, c0. v0, c0 are always latest read
in waves)
        //ButtonDigitize()        (Start Data aquisition but waits for trigger. Data aquistion is
NOT done as backgroud task)

Window Digitizing_Panal() : Panel
        PauseUpdate; Silent 1           | building window...
        NewPanel /W=(367,45,777,147)
        ShowTools
        SetDrawLayer UserBack
        SetDrawEnv linefgc= (29524,1,58982)
        DrawRect 2,24,198,83
        DrawRect 142,86,152,86
        SetDrawEnv linefgc= (65535,16385,36045)
        DrawRect 202,83,362,24
        SetVariable setvar0,pos={52,26},size={140,17},title="SampPer, us"
        SetVariable setvar0,limits={10,10000,100},value= root:DataAcq:per
        ValDisplay valdisp0,pos={211,62},size={130,17},title="num wvs dig"
        ValDisplay valdisp0,limits={0,0,0},barmisc={0,1000}
        ValDisplay valdisp0,value= #"Root:Dataacq:nwaves"
        SetVariable maxnum,pos={208,43},size={150,17},title="Max num wvs"
        SetVariable maxnum,limits={0,INF,1},value= root:DataAcq:maxn
        SetVariable swlnvar,pos={13,45},size={180,17},title="Sweeplength(pnts)"
        SetVariable swlnvar,limits={0,INF,512},value= root:DataAcq:SweepLength
        Button ResetCon,pos={4,1},size={100,20},proc=ButtonProc,title="Reset Stims"
        ValDisplay wvlength,pos={22,64},size={170,17},title="Wavelength, ms"
        ValDisplay wvlength,limits={0,0,0},barmisc={0,1000}
        ValDisplay wvlength,value=#"root:dataacq:per/1000*root:dataacq:Sweeplength"
        SetVariable setvarCyPer,pos={114,3},size={130,17},title="CyclePer, sec"
        SetVariable setvarCyPer,limits={0,INF,1},value= root:DataAcq:CyclePeriod
        CheckBox CheckSav,pos={232,25},size={100,20},proc=SaveCheck,title="Save
Waves",value=1
        Button ClampSwitch,pos={274,2},size={70,20},proc=CurClamp,title="C C"
EndMacro

Window Graph_v0() : Graph
        PauseUpdate; Silent 1           | building window...
        String fldrSav= GetDataFolder(1)
        SetDataFolder root:DataAcq:
        Display /W=(13,40,379,423) v0
```

```
	SetDataFolder fldrSav
	ModifyGraph live=1
	SetAxis left -50,40
	SetAxis bottom 0,1300
EndMacro


//@@@@@@@**********BUTTONANDCHECKFUNCTIONS********@@@@@

	//LoadStim()  DEPENDENT
	//updates scaling and redimensions all In/Out waves (sampwv, stimwv, v0, c0, stimT,
stim1, stim2, stim3)
	//Creates stimwv based on current stim* waves and sends to board
	//Reads GV: sweeplength, per, TLb, stim_Dac_scale, CU_scale
Function LoadStim(ctrlname) : ButtonControl //Remakes stimwv after changed parameters!
	String ctrlname

Execute "StimClear 0"
SetDataFolder root:DataAcq
// Global variables, *********
	nVar per= per
	nVar npnts= sweeplength
	nVar TLb= TLb
	nVar stim_scale= stim_DAC_scale
	nVar CUscale = CU_scale

//waves  used**************
	wave stwv= stimwv, spwv= sampwv	//Waves directly from and to ITC16 board
	wave stimT= stimT, stim1= stim1, stim2= stim2, stim3= stim3
	wave v0=v0, c0=c0				//Read in waves

// Real code ******************
	stwv=0
	Redimension/N=(npnts) spwv, stwv

	Redimension/N=(npnts/4) stim1, stimT, stim2, stim3
	Redimension/N=(npnts/2) v0, c0

	SetScale/P x 0, (per*2/1000), "ms", v0, c0
	SetScale/P x 0,(per*4/1000), "ms", stim1, stimT, stim2, stim3
	stwv[0,npnts-4;4]=stimT[p/4]*2*TLb	//needs to be full scale to get Trigger
	stwv[1,npnts-3;4]=stim1[(p-1)/4]*TLb
	stwv[2,npnts-2;4]=stim2[(p-2)/4]*TLb
	stwv[3,npnts-1;4]=stim3[(p-3)/4]*stim_scale*CUscale
	Execute "stim stimwv"
End
```

```
Function ButtonProc(ctrlName) : ButtonControl
        String ctrlName

Execute "StimReset()"
End

Function SaveCheck(ctrlName,checked) : CheckBoxControl
        String ctrlName
        Variable checked                //Makes Waves during stim if checked

SetDataFolder root:DataAcq:
Nvar save= savewaves
        If (checked)
                save=1
          else
                save=0
          endif
End

Function StartProc(ctrlName) : ButtonControl
        String ctrlName

SetDataFolder root:DataAcq
//Globals & Waves
        nVar  CP=cyclePeriod
        nvar flag=flag, n=nwaves, maxn=maxn

        If (flag==7)
        do
                AcqData()       //Calls main digitization procedure
                DoUpdate                //Updates waves, so can observe digitization
                Sleep /B/C=2/S CP       //Waits for cyclePeriod before looking for next trigger
        while(n<=maxn)
        else
                SetBackground AcqData()
                CtrlBackground start, period=(CP*60.15)
                Button b2, title="StopStim", proc=StopProc
        endif
END

Function StopProc(name)
        String name

        CtrlBackground stop
        Button b2, title ="StartStim", proc=StartProc
```

```
END

Function CurClamp(ctrlName) : ButtonControl
        String ctrlName

NVAR Stim_DAC_scale=root:Dataacq:Stim_DAC_scale
NVAR InVC= root:Dataacq:InVC
        Execute "seq \"D120\",\"0101\""          //4 Dacs C Command out 3 and 2 ADC- For
Curent Clamp
        Stim_DAC_scale = 100          //Scales stim output. (mV to Axodata/nA out electrode)
        InVC=0
        Print "Now set for Current Clamp"
        Button ClampSwitch title="C C", proc=VoltClamp
End

Function VoltClamp(name)
        String name

NVAR Stim_DAC_scale=root:Dataacq:Stim_DAC_scale
NVAR InVC= root:Dataacq:InVC
        Execute "seq \"D120\",\"0101\""          //4 Dacs: V Command out 0  and 2 ADC- For
VoltageClamp
        Stim_DAC_scale = 50  //Scales stim output. (mV to Axodata/mV out electrode)
        InVC=1
        Print "Now set for Voltage Clamp"
        Button clampSwitch title="V C", proc=CurClamp
End


Function AcqData()
// Digitizes triggered current and voltage waves through ITC16 board

// Global variables, *********
        nVar per=per, flag=flag, Save=SaveWaves
        nVar npnts= sweeplength
        nVar CUscale = CU_scale
        nVar VG= VoltGain, AG=AmpGain
        nVar n=nwaves, maxn=maxn

//waves  used**************
        wave  spwv= sampwv   //Waves directly from and to ITC16 board
        wave v=v0, c=c0

// Real code *************
        Execute "startacq "+num2str(per)+"," +num2str(flag)
```

```
        Execute "samp sampwv"
                                //Reads raw data in board buffer to wave sampwv
        v[0,(npnts/2-1)]=spwv[2 * p]/(CUscale*VG)              // puts data with correct scale
into
        c[0,(npnts/2-1)]=spwv[2 * p + 1]/(CUscale*AG) // named data waves

If (Save)
        String cn, vn              //raw data is translated into current and voltage traces
        n +=1                                          // Increase n for successive waves
        cn="root:raw:c"+num2str(n)                     // name of current wave (string)
        vn="root:raw:v"+num2str(n)                     // name of voltage wave (string)
        Duplicate/o v $vn        ; Duplicate/o c $cn
                //creates waves or will overwrite old waves!

        If (n>=maxn)
                DoAlert 0, "You may be exceeded Igor's memory limits. Check before
continuing. To continue increase \"Max num of waves\" value."
                StopProc("b2")
                DoUpdate
                Return 1  //Tells program to stop if specified wave limit reached
          else
                Return 0          //Otherwise keep going!
          endif
  else
        RETURN 0      //need to have this for Background Task, otherwise irrelevant
endif
End


Window GainsPanal() : Panel
        PauseUpdate; Silent 1              // building window...
SetDataFolder root:DataAcq
        NewPanel /W=(379,259,627,337)
        SetDrawLayer UserBack
        SetDrawEnv linethick= 0,fillfgc= (44253,29492,58982)
        DrawRect 0,0,252,80
        SetVariable SetGainV,pos={50,6},size={170,17},title="VoltGain mV/mV"
        SetVariable SetGainV,limits={10,100000,100},value= VoltGain
        SetVariable StimVar,pos={11,52},size={210,17},title="Stim Out gain (mV/nA)"
        SetVariable StimVar,limits={0,INF,100},value= stim_DAC_scale
        SetVariable
SetAmpGain,pos={50,29},size={170,17},proc=UpdateSweep,title="AmpGain mV/nA"
        SetVariable SetAmpGain,limits={0,INF,100},value= AmpGain
EndMacro
```

```
#pragma rtGlobals=1             // Use modern global access method.

// Procedures used to set variables for DataAcquisition
Menu "Macros"
        Submenu "Stimulus Protocols"
                "MonitorResistance"
                "ActionPotentials"
                "SubThreshold"
                "FiringRates"
                "EPSPs"
        End
End

Macro MonitorResistance()

        Silent 1; PauseUpdate
SetDataFolder root:DataAcq
        per=30; sweeplength=512; cycleperiod= 0.5
        plen= 4; amp=-0.3; tm3= 2
        StimReset()
        tm1=0; tm2=0
        LoadStim("load")
        DoWindow /F graph_v0
        SetAxis bottom 0, 15
        SetAxis left -50,100
End //MonRes

Macro ActionPotentials()

        Silent 1; PauseUpdate
SetDataFolder root:DataAcq
        per=30; sweeplength = 1024 ; cycleperiod = 1
        plen= 4; amp= 2; tm3=2
        StimReset()
        tm1=0; tm2=0
        LoadStim("load")
        DoWindow /F graph_v0
        SetAxis bottom 0, 30
        SetAxis left -50,100
End lAP

Macro SubThreshold()
        Silent 1; PauseUpdate
SetDataFolder root:DataAcq
        per= 1000; sweeplength= 1536
        plen=1000;  tm3=  50
```

```
        amp=-0.2
        cycleperiod = 5
        tm1=0; tm2=0
        StimReset()
        LoadStim("load")
        DoWindow /F graph_v0
        SetAxis bottom 0, 1300
        SetAxis left -50,40
End !SubThres

Macro FiringRates()
        Silent 1; PauseUpdate
SetDataFolder root:DataAcq
        per= 300; sweeplength = 4096
        plen=1000; tm3=  50;    amp=0.5
        cycleperiod=15
        tm1=0; tm2=0
        StimReset()
        LoadStim("load")
        DoWindow /F graph_v0
        SetAxis bottom 0, 1200
        SetAxis left -20,100
End     !FirRat

Macro EPSPs()

        PauseUpdate; Silent 1
SetDataFolder root:DataAcq
        tm1=10          // Default : stim out 1
        tm2=0
        amp=0
        per=50; sweeplength= 2048; cyclePeriod=3;
                //default data acq parameters
        StimReset()
        stim3:= twoexp(cf1, x)+twoexp(cf2,x)
        LoadStim("load")
        DoWindow/F graph_v0
        SetAxis bottom 0,100
        SetAxis left, -10,20
End !Reset fep
```

DATA ANALYSIS PROGRAMS

```
// Does all EPSP analysis:
//1)fixing up raw waves (saving and removing base lines).
//2)Ploting groups of EPSPs (PLtEP)
//3) analysis of set averages.  Find Area ratios (bth/sum)using
//        a) whole EPSP area, b) first 15ms after S2 rises, c)first 20ms
//        ALso measure Px&Ds peak (Pk_b) & ratio of EPSP size just before
// start of S2. (to check for consistancy in size)
// Removed sub program that just measure ar_pk(ar_15) If there's a problem
// just do whole analysis over

// This version assumes use of Data folder. EPSPs_Ig2anal is for Exps analysized
// orginally without folders

Menu "Macros"
        SubMenu "EPSPs"
                "Fixset"
                "PltepSer"
                "AnalSet"
        end
end

Macro WaveTimes(Stime, n1,n2)
        Variable/D Stime
        Variable n1,n2

String vw="v"
Variable nc=n1

Silent 1; PauseUPdate
String FldrSav=Getdatafolder(1)
setdatafolder root:raw
do
        vw="v"+num2str(nc)
        Note $vw, "TIME:"+num2str((modDate($vw)-Stime)/60)
        nc +=1
while(nc<=n2)
setdatafolder FldrSav
End     //WaveTImes


Macro Fixset(set, DT)
        String set
        Variable DT

// Needs two waves in root:raw folder: stlab, stnum
// numbers should already be put in stnum,
```

```
// Waves already baseline subtracted
PauseUpdate; silent 1
Sort stnum stnum,stlab
//If highest number in stnum  is NOT the stop number, then stop you messed up
If (cmpstr(stlab[5], "stp")!=0)
        ABORT "check wvs numbers in stnum, the highest wv num should be the stop"
        endif

Variable i1=0, i2=1, n1, n2
string nb="notebook0", vw, tm, tmwv
Notebook $nb fstyle=5, text="SET "+set+", DT="+num2str(DT)+"\r"
Notebook $nb fstyle=0
do
        n1=stnum[i1]
        If (n1!=0)
                n2=stnum[i2]-1
                Notebook $nb text=num2str(n1)+"\t"+num2str(n2)+"\t"+NSD(mean(root:bv, n1,
n2), 1)+"\t"+stlab[i1]
                If (cmpstr(stlab[i1], "Sum")==0)
                        vw="v"+num2str(n1)
                        tmwv=note($vw)
                        sprintf tm, "%.1f" ,str2num(tmwv[5,20])
                        Notebook $nb text="\t"+tm
                  endif
                Notebook $nb text="\r"
                endif
        i1+=1
        i2+=1
while (i2<6)
END

Macro FixSsF(nstr, nend, What1, what2)// 3/7/97 currents not deleted anymore
        Variable nstr, nend
        String What1, what2

String fldrSav=Getdatafolder(1)  //Added 9/26/96  while analyszing 960725.1
SetDataFolder root:raw:                    // bv, bc stay in root folder
        Silent 1; PauseUpdate
        String vw="v"+num2str(nstr)
        String tmwv=note($vw), tm=""
        sprintf tm, "%.1f" ,str2num(tmwv[5,20])
        String savefile="\""+vw+"_"+num2str(nend)+what1+".awav\""
        SerBaseSub("c",nstr, nend, 0.1,9.5)
        // SeriesCmd(nstr, nend, "c", "killwaves/f")- Changed 3/7/97 so I for fakes not deleted

        Variable n=nstr, m=0
```

```
        String cmdlist=""

                m=0                         //Resets wave counter, and cmdlist.
                cmdlist = "Save/t  v"+num2str(n)
                n=n+1
                do
                        cmdlist += ", v"+num2str(n)
                        m +=1
                        n +=1
                while ((m < 61) %& (n<=nend))
        Execute cmdlist + " as " +savefile+"\n"
        If ((nend-nend+1)>61)
        do
                m=0
                cmdlist= "save/t/a v"+num2str(n)
                n=n+1
                do
                        cmdlist +=", v"+num2str(n)
                        m+=1
                        n+=1
                while((m<61) %& (n<=nend))
                Execute cmdlist + " as " +savefile +"\n"
        while (n<=nend)
        endif

        SerBaseSub("v",nstr, nend, 0.1,9.5)
        String nb="Notebook0"
        Notebook $nb text=num2str(nstr)+"\t"+num2str(nend)+"\t"+NSD( mean(::bv,nstr,nend),
1)+"\t"
                        // Changed HP output to shorter format with NSD 3/25/97
        Notebook $nb text=tm+"\t"+what1+"\t"+what2+"\r"
END

Macro PltepSer()

// Needs two waves in root:raw folder: stnum, stlab
// numbers should already be put in stnum,
PauseUpdate; silent 1

String fldrSav=Getdatafolder(1)
Setdatafolder root:raw

Variable i=0, j,n1,n2
string vw

do
```

```
        j=pltorder[i]
        n1=stnum[j]
        If (n1!=0)
                n2=stnum[j+1]-1
                Pltep(n1,n2)
          endif
        i+=1
while (i<=5)
setdatafolder fldrsav
END


// AnalSet - Analyzes selected stim s1+s2 and all sum waves in targeted graph.
// given start, stop and finds area
//Values put into wave anal_setn and notebook1. ALso puts ratio of sum/stim values in
Notebook1
//Make sure target graph is the one with the waves you want to analyze on it
// AND cursor is in Notebook1 where you want it. (If Notebook1 is not the right notebook need
to alter end)


Macro AnalSet(setn,str,stop,wv):GraphMarquee
        Variable str,stop
        String wv, setn
        Prompt wv, "Select stim s1+s2 wave", popup, WaveList("Av*",";","WIN:")

Silent 1; PauseUpdate
Variable pkm            // for finding peak of waves
String fldrSav=GetDataFolder(1)

WaveStats/q/r=(str,stop) $wv
pkm=V_max/2
String WvsGraph, curwv=wv, indv="st_"+setn+"_md", ratio="st_"+setn+"_rt"
Variable n=0,runSm=0, nSmwv=0
String info
        Wvsgraph=WaveList("S*",";","WIN:")  //Puts all sum waves in a list
        do
                curwv=GetStrFromList(WvsGraph,n,";")
                if (cmpstr(curwv,"")==0)
                        Break   lbreak out of loop when no waves left in list
                  endif
                n+=1
        while(1)
        nSmwv=n
        Make/o/N=9 $indv        // for storing abs for AR, pkar, pr, pk_bth
        Make/o/N=4 $ratio       // for storing ratio data (sum/stim)
```

```
String Arsm="Area", ar15sm="AR15", Prsm="pre", AR20sm="AR20"

//find area of all waves-ARsm
        n=0
        do
                curwv=GetStrFromList(WvsGraph,n,";")
                runSm+=area($curwv, str, stop)
                Arsm +="\t"+num2str(area($curwv,str,stop))
                n+=1
        while(n<nSmwv)
        $indv[0]=area($wv, str,stop)     // stim value
        $indv[1]=runSm/nSmwv                    //avg Sm value
        $ratio[0]=$indv[0]/$indv[1]             // ratio of stim/sum


// Changed to peak area on 8/6/96. Peak of bth stims is in indv[9]
// 8/6/96: Set area to be str+3 to str+18. Basically the first 15ms of the EPSP after real start of
2nd stim
// 1/12/98 changed area to be str , str+15. Makes more sense this way
        FindPeak/q/b=41/R=((str),(stop))/M=(pkm) $wv
        If (V_flag==1)
                DoAlert 1, "No Peak was found, do wish to go on?"
                If (V_flag==2)
                        Abort
                endif    // V_flag relating to alert message
          else
                Variable pk= V_PeakLoc
                $indv[8]=mean($wv, pk-0.5,pk+0.5)               // peak of bth wave
          endif // V_flag==1

//find Ar15 of all waves, area ratio using first 15ms after str (1 ms after beginning of 2nd EPSPs
                n=0; runSm=0
                Variable dif=0          // Added 1/10/98 to automatically find fractional
differnce between two sums
                do
                        curwv=GetStrFromList(WvsGraph,n,";")
                        If (n==1)
                                dif=runsm-area($curwv, str,str+15)
                                endif
                        runSm+=area($curwv, str,str+15)
                        ar15sm +="\t"+num2str(area($curwv,str,str+15))
                        n+=1
                while(n<nSmwv)
                $indv[2]=area($wv, str, str+15)
                $indv[3]=runSm/nSmwv                            //avg Sm value
                dif/=$indv[3]           //Fraction diference of two sum waves.
```

```
		$ratio[1]=$indv[2]/$indv[3]			// ratio of stim/sum

//10/2/96: find Ar20 of all waves, area ratio using first 20ms after start of S2
		n=0; runSm=0
		do
			curwv=GetStrFromList(WvsGraph,n,";")
			runSm+=area($curwv, str,str+20)
			ar20sm +="\t"+num2str(area($curwv,str,str+20))
			n+=1
		while(n<nSmwv)
		$indv[6]=area($wv, str, str+20)
		$indv[7]=runSm/nSmwv				//avg Sm value
		$ratio[3]=$indv[6]/$indv[7]			// ratio of stim/sum

//find mean value just before S2 start for all waves
	n=0; runSm=0
	do
		curwv=GetStrFromList(WvsGraph,n,";")
		runSm+=mean($curwv, str-3,str-1)
		prsm +="\t"+num2str(mean($curwv,str-3,str-1))
		n+=1
	while(n<nSmwv)
		$indv[4]=mean($wv, str-3,str-1)// stim value
		$indv[5]=runSm/nSmwv				//avg Sm value
		$ratio[2]=$indv[4]/$indv[5]			// ratio of stim/sum



String nb = "Notebook1"
//*** Finally put the data in the notbook!
Notebook $nb ruler=Normal, text="\rAnalyze  "+wv+": "+WvsGraph+"\r"
Notebook $nb text=Arsm+"\r"+AR15sm+"\t"+NSD(dif,3)+"\r"+ar20sm+"\r"+prsm+"\r"+"\r"
Notebook $nb text="\t\t"+wv+"\tSum\t"+"\tRatio\r"
Arsm=NSD($indv[0],1)+"\t\t"+NSD($indv[1],1)+"\t\t"+NSD($ratio[0],2)
ar15sm=NSD($indv[2],1)+"\t\t"+NSD($indv[3],1)+"\t\t"+NSD($ratio[1],2)
ar20sm=NSD($indv[6],1)+"\t\t"+NSD($indv[7],1)+"\t\t"+NSD($ratio[3],2)
prsm=NSD($indv[4],2)+"\t\t"+NSD($indv[5],2)+"\t\t"+NSD($ratio[2],2)
Notebook $nb text="A("+num2str(str)+","+num2str(stop)+")\t"+Arsm+"\r"
Notebook $nb text="P("+num2str(str)+","+NSD((str+15),1)+")\t"+ar15sm+"\r"
Notebook $nb text="P("+num2str(str)+","+NSD((str+20),1)+")\t"+ar20sm+"\r"
Notebook $nb text="preS2("+num2str(str-3)+")\t"+prsm+"\r"
Notebook $nb text="Peak of Ds+Px\t\t"+NSD($indv[8],2)		// Added 8/6/96 along with pk->
pkAR
//*** Add info to graph
Textbox/C/N=anal_tx "\\JC\\f01SET "+setn+"@ ? min"
AppendText/N=anal_tx "\\f00AR="+NSD($ratio[0],2)
```

```
AppendText/N=anal_tx "ar15="+NSD($ratio[1],2)+"\tar20="+NSD($ratio[3],2)
AppendText/N=anal_tx "pk="+NSD($indv[8],2)+"mV\tHP=?mV"
End     //AnalSet


Window st_fixplt() : Table
        PauseUpdate; Silent 1           | building window...
        String fldrSav= GetDataFolder(1)
        SetDataFolder root:raw:
        Edit/W=(12,166,311,331) stlab,stnum,pltorder
        ModifyTable width(Point)=18
        SetDataFolder fldrSav
EndMacro

#include <Strings as Lists>

//Procedures: Math On Waves plus dealing with baselines
//Series of operations performed on 2  or more waves, results stored in new waves
//AvgWaves: averages a series of waves into avN_N
//DelFromAvg: del a wave from an averaged wave, Creates wave note of deletion
//BaseSub: Subtracts baseline
//SerBaseSub: Repeats above on set of waves
//SubtractWvs: Subtracts two waves on targeted graph
//SumWvs: Adds two waves on targeted graph
//Marquee Procedures: Acts on all v* wave in marquee
//              AvgWvsMarquee: Avgerages waves together into avN
//              BVOffset, RmOffset: Offsets waves by baseline amount, set offset back to 0
// Programing Notes: 7/10/96: Marquee variables are acessed from root directory only. Need to
be
// in root directory to get current marquee numbers.

Menu "Jilda's"
        Submenu "Wave Math"
                "AvgWvs"
                "SE_serwvs"
                "SE_lstwv"
                "SerBaseSub"
                "SerARea"
                "SubtractWvs"
                "SumWaves"
        end
end

//AvgWvs
//Assumes existance of waves with tag basen, continuous numbers strn to endn
//Creates new wave with tag "A"+basen
```

```
Proc AvgWvs(basen, strn, endn)
        String basen
        Variable strn, endn

        Silent 1; PauseUpdate
        String destw, swn, wnote, tag="root:raw:"

        swn=tag+basen+num2str(strn)   //first source wave
        destw="A"+basen+num2str(strn)+"_"+num2str(endn)
        Duplicate/o $swn, $destw
        $destw=0
        wnote = "Average of "+swn+" to "
        Variable n=strn             //keeps track of waves in loop
        do
                swn=tag+basen+num2str(n)
                $destw += $swn
                n += 1
        while (n <= endn)
        Note $destw, wnote+swn
        $destw /= (n-strn)
        AppendtoGraph $destw
        ModifyGraph rgb($destw)=(2,39321,1)
end

//Standard Error of waves, finds SE of a group of voltage waves
//Assumes existance of waves with tag basen, continuous numbers strn to endn
//Creates new wave with tag "sdv"+basen
Proc SE_serwvs(strn, endn,avWv)
        String avWv
        Variable strn, endn

        Silent 1; PauseUpdate
        String destw, swn, wnote,fldrsav="",basen="root:raw:v"

         fldrsav=GetDataFolder(1)
         avwv=fldrsav+avwv
         destw=fldrsav+"sdv"+num2str(strn)+"_"+num2str(endn)
         Duplicate/o $avwv, $destw
        $destw=0
        Note/K $destw

        wnote = "Standard dev of "+swn+" to "
        Variable n=strn             //keeps track of waves in loop
        do
                swn=basen+num2str(n)
```

```
                $destw +=($swn-$avwv)^2       //Running total of diff between raw and avg
squared
                n += 1
        while (n <= endn)
        Note $destw, wnote+swn
        Duplicate/o $destw temp
        Print n-strn
        $destw =sqrt((temp)/(n-strn-1))/sqrt(n-strn)                    //gives standard ERROR
        Killwaves/f temp
        AppendtoGraph/c=(1,16019,65535) $destw
end


Proc SE_lstwv(avwv)
        String avwv

PauseUpdate; Silent 1
String sdwv, lstwv, curwv,fldrsav="",basen="root:raw:"
Variable n=1, numwvs=0

         fldrsav=GetDataFolder(1)
         sdwv=fldrsav+"sdv_"+avwv[3,4]
          avwv=fldrsav+avwv
         Print sdwv,avwv
         Duplicate/o $avwv, $sdwv
        $sdwv=0
        Note/K $sdwv
        lstwv=note($avwv)

        do      //for each wave in list
                curwv=GetStrfromList (lstwv, n,",")
                if (cmpstr(curwv[0],"v")!=0)     //you've reached the end
                        numwvs=n-1
                        Break
                        endif
                curwv=basen+curwv
                $sdwv +=($curwv-$avwv)^2 //running total of diff between raw and avg squared
                n+=1
        while(1)
        Note $sdwv,"stdev of waves in "+ avwv
        Duplicate/o $sdwv temp
        $sdwv = sqrt( (temp)/(numwvs-1) )/sqrt(numwvs)          //Gives SE of each wv
        Appendtograph/c=(1,16019,65535) $sdwv
End

//Self-Cointained,
```

```
//Changes value of avw
Function DelFromAvg(avw, delw, nws)
	Wave avw, delw
	Variable nws

	avw= (avw*nws - delw)/(nws-1)
	Note avw, "Deleted wave "+ NameOfWave(delw)+" from average. "
	end

//BaseSub: selfcontained
//Subtract baseline from wv, places result in bw[num]
//Need to keep track of baseline and subrtract it from wave.
Function BaseSub(wv, bw, num, strx, endx)
	Wave wv, bw
	Variable  num, strx, endx

	bw[num]= mean(wv, strx, endx)
	wv -= bw[num]
END //F_BaseSub

//Do BaseSub for a bunch of waves
//Need bc, bv waves before running!
Proc SerBaseSub(tag, nstr, nend, tm1, delay)
	String tag
	Variable nstr, nend, tm1, delay

	Silent 1; PauseUpdate
	Variable n=nstr
	String bwname="root:b"+tag, wname=tag+num2str(n)
		//Added 'root:' 9/26/96 while analyzing 960725.1

		// Bv, and bc now stay in root folder
	do
		BaseSub($wname, $bwname, n, tm1, delay)
		n +=1
		wname=tag+num2str(n)
	while (n<=nend)
END

//Finds the area in a given series of waves and puts it in a new wave
Proc SerARea(newv,avw, tm1)
	string newv,avw
	Variable tm1

	Silent 1; PauseUpdate
	Variable n1=0, n2, nD, npts,n=0
```

```
        String curwv, lstwv, rawhome="root:raw:"
        nD=finddash(avw)
        If (numtype(nD)==2)
                ABORT "ERROR input wave has no dash"
                endif
        Make/o/N=50 $newv
        AppendToTable $newv
        If (nd==2)
                //get wvs from note wv in form of av_N
                        lstwv=note($avw)
                        do      //for each wave in list
                                curwv=GetStrfromList (lstwv, n1+1,",")
                                if (cmpstr(curwv[0],"v")!=0)    //you've reached the end
                                        npts=n1
                                        Break
                                endif
                          curwv=rawhome+curwv
                          $newv[n1]=area($curwv, tm1, tm1+15)
                          n1+=1
                        while(1)

                else    // waves is in form of avN1_N2
                        n1=str2num(avw[2,nd-1])
                        n2=str2num(avw[nd+1, nd+4])
                        npts=n2-n1+1
                                do
                                        curwv=rawhome+"v"+num2str(n1)
                                        $newv[n]=area($curwv, tm1, tm1+15)
                                        n1+=1
                                        n+=1
                                while(n1<=n2)
                ENDIF
                //print npts
        DeletePoints (npts), 50, $newv  //Gets rid of excess points in wave
END

//Position cursor in notebook before start
//Added 12/1/97 to help with analysis. Does some stats on two waves and compares them
Macro Cmpw1w2(w1,w2)
        string w1, w2

        silent 1;Pauseupdate
        //string nb="Notebook0"
        variable av1, Sd1, SE1, av2, sd2, se2
        Wavestats/Q $w1
                av1=V_avg
```

```
                Sd1=V_sdev
                SE1=sd1/sqrt(V_npnts)
        Wavestats/Q $w2
                av2=V_avg
                Sd2=V_sdev
                SE2=sd2/sqrt(V_npnts)
        Variable av= (av1+av2)/2        //average of two averages
        Variable dav= (av1-av2)         //difference between two averages
        variable fdav=abs(dav)/av       // fractional diff between two averages
        Variable cvs=SE1/av1 + SE2/av2          // sum of the coefficient of variation of two
groups
        Variable sig=imag(StatTtest(1, $w1, $w2))               // Statistical difference based on
TTest
        Notebook $nb ruler=Normal, text="\t"+NSD(av1,1)
+"\t"+NSD(Sd1,1)+"\t"+NSD(SE1,1)
        Notebook $nb text="\t"+NSD(av2,1) +"\t"+NSD(Sd2,1)+"\t"+NSD(SE2,1)
        Notebook $nb text="\t"+NSD(av, 1)+"\t"+ NSD(dav, 1)+"\t"+ NSD(fdav, 2)+"\t"+
NSD(cvs, 2)
        If (Sig>0.05)
                Notebook $nb text="\tN.S."
        else
        If (Sig <0.001)
                Notebook $nb text="\tP<0.001"
        else
                NOtebook $nb text="\tP="+NSD(sig, 3)
        endif
        endif
        Notebook $nb text="\r"
END

//Meant to compare bth area and summed wave's area
Macro CmpBthSum(bth,S1,S2)
        string bth
        Variable S1, S2 //Algebraic sum area

        silent 1;Pauseupdate
        //string nb="Notebook0"
        variable av1, Sd1, SE1,cv
        Wavestats/Q $bth
                av1=V_avg
                Sd1=V_sdev
                SE1=sd1/sqrt(V_npnts)
                cv=SE1/av1

        Variable av= (S1+S2)/2 //average of two averages
        Variable dav= (S1-S2)   //difference between two averages
```

```
        variable fdav=abs(dav)/av        // fractional diff between two averages

        Notebook $nb ruler=Normal, text="bth\t"+NSD(av1,1)
+"\t"+NSD(Sd1,1)+"\t"+NSD(SE1,1)
        Notebook $nb text="\tcv="+NSD(cv,2) +"\tSUMs\t"
        Notebook $nb text=NSD(av, 1)+"\t"+ NSD(dav, 1)+"\t"+ NSD(fdav, 2)
        Notebook $nb text="\r"
END

//Subtracts two waves starting with "Av"
Proc SubtractWvs(bwv, gwv)
        String bwv, gwv
        Prompt bwv, "Select a wave", popup, WaveList("Av*",";","WIN:")
        Prompt gwv, "Select wave to be subratacted from first", popup,
WaveList("Av*",";","WIN:")

        Silent 1; PauseUpdate
        String s1=bwv[2,4]
        String s2=gwv[2,4]

        If ((char2num(s1[2]))==char2num("_"))
                s1=bwv[2,3]
                endif
        If((char2num(s2[2]))==char2num("_"))
                s2=gwv[2,3]
                endif
        String dwv="M"+s1+"_"+s2
        Print dwv
        Duplicate/o $Bwv $dwv

        $dwv =$bwv-$gwv      //Mainly what this program supposed to do

        //Fix up graph
        APpendtoGraph $dwv
        ModifyGraph rgb($dwv)=(2,39321,1)   //green
        ModifyGraph rgb($gwv)=(0,0,65535)   //blue for G
        ModifyGraph rgb($bwv)=(65535,0,0)   //red for both
        ModifyGraph lstyle($dwv)= 2
        ModifyGraph lstyle($gwv)=1
        ModifyGraph lstyle($bwv)=3
End

//Allows user to select two waves from top graph and sums them
//Gives new wave a name based on selected waves, with tag of "Sm"
Proc SumWaves(bwv, gwv)
        String bwv, gwv
```

```
	Prompt bwv, "Select a wave", popup, WaveList("A*",";","WIN:")
	Prompt gwv, "Select another wave", popup, WaveList("A*",";","WIN:")

	Silent 1; PauseUpdate
	String s1=bwv[2,4]
	String s2=gwv[2,4]

	If ((char2num(s1[2]))==char2num("_"))
		s1=bwv[2,3]
		endif
	If((char2num(s2[2]))==char2num("_"))
		s2=gwv[2,3]
		endif
	String swv="S"+s1+"_"+s2
	Print swv
	Duplicate/o $bwv $swv

	$swv =($bwv)+($gwv)  //Mainly what this program supposed to do

	//Fix up graph
	APpendtoGraph $swv
	ModifyGraph rgb($swv)=(2,39321,1)    //green
	ModifyGraph lstyle($swv)= 2
End


// @@@@@@********* GRAPH MARQUEE FUNCTIONS **********@@@@@@@
Function AvgWvMarquee() : GraphMarquee

	String WvsGraph, curwv, fldrSav, sumwv,notewv, rawhome="root:"
	Variable n=0, numwvs=0,pnt, endpnt

	fldrSav= GetDataFolder(1)
	sumwv=UniqueName("av_",1,1)
	Print fldrSav+sumwv
	notewv=sumwv
SetDataFolder root:
	GetMarquee left, bottom; DoUpdate
	if (V_Flag == 0)
		Print "There is no marquee"
	endif
	Print v_left, v_right, V_top, V_bottom
SetDataFolder RawHOme
	Wvsgraph=TraceNameList("",";",1)
	curwv=GetStrFromList(WvsGraph,n,";")
	Wave cw=TraceNameToWaveRef("",curwv)
```

```
	Duplicate/o cw $sumwv
	Wave sw=$sumwv

	sw=0
	do	//for each wave in list
		if (cmpstr(curwv,"")==0)
			Break
			endif
		if ((cmpstr(curwv,"v0")!=0)%& (cmpstr(curwv[0],"v")==0))	//only do if
wave is not v0
			pnt=x2pnt($curwv, V_left)
			endpnt=x2pnt($curwv, V_right)
			do
				If((cw[pnt]<= V_top) %&(cw[pnt]>=V_bottom))
					notewv=notewv+","+curwv
					numwvs+=1
					sw+= cw
					BREAK			//stop searching!!
				 else
					pnt+=1
				endif
			while(pnt<=endpnt)
		  endif  // End condition if not v0
		n+=1
		curwv=GetStrFromList(WvsGraph,n,";")
	Wave cw=TraceNameToWaveRef("",curwv)
	while(1)
Note sw,"avg of "+ notewv+","+num2str(numwvs)
sw /= numwvs
Appendtograph/c=(3,52428,1) sw

	MoveWave sw, $fldrSav
SetDataFolder fldrSav

End



Function CAvgWv() : GraphMarquee

	String WvsGraph, curwv, fldrSav, sumwv
	Variable n=0, numwvs=0,pnt, endpnt

	fldrSav= GetDataFolder(1)
	sumwv=UniqueName("aC_",1,1)
	Print fldrSav, sumwv
```

```
SetDataFolder root:
	GetMarquee left, bottom; DoUpdate
	if (V_Flag == 0)
		Print "There is no marquee"
	endif
	Print v_left, v_right, V_top, V_bottom
SetDataFolder root:raw
	Wvsgraph=TraceNameList("",";",1)
	curwv=GetStrFromList(WvsGraph,n,";")
	Wave cw=TraceNameToWaveRef("",curwv)
	Duplicate/o cw $sumwv
	Wave sw=$sumwv

	sw=0
	do	//for each wave in list
		if (cmpstr(curwv,"")==0)
			Break
			endif
		if ((cmpstr(curwv,"c0")!=0)%& (cmpstr(curwv[0],"c")==0))	//only do if
wave is not v0
			pnt=x2pnt($curwv, V_left)
			endpnt=x2pnt($curwv, V_right)
			do
				If((cw[pnt]<= V_top) %&(cw[pnt]>=V_bottom))
					sumwv=sumwv+","+curwv
					numwvs+=1
					sw+= cw
					BREAK			//stop searching!!
				 else
					pnt+=1
				endif
			while(pnt<=endpnt)
		  endif  // End condition if not c0
		n+=1
		curwv=GetStrFromList(WvsGraph,n,";")
	Wave cw=TraceNameToWaveRef("",curwv)
	while(1)
Note sw,"avg of "+ sumwv+","+num2str(numwvs)
sw /= numwvs
Appendtograph/c=(3,52428,1) sw

	MoveWave sw, $fldrSav
SetDataFolder fldrSav

End
```

```
// Finds peak of waves inside Marquee. Peak area must fall inside of marquee to be found.
Proc FindPkMarquee() : GraphMarquee

String fldrSav= GetDataFolder(1)
string nb="Notebook1"
SetDataFolder root:
        GetMarquee left, bottom
        if (V_Flag == 0)
                Print "There is no marquee"
        endif
        Variable left=V_left, right=V_right, bottom=V_bottom, top=V_top
Silent 1
        String WvsGraph, curwv, tgn
        Variable n=0, numwvs=0,pnt, endpnt, V_pk, runAvg=0, navg=0
SetDataFolder fldrSav
        Wvsgraph=WaveList("*",";","WIN:")
        curwv=GetStrFromList(WvsGraph,n,";")
        Notebook $nb ruler=Normal
        do      //for each wave in list
                if (cmpstr(curwv,"")==0)
                        Break
                  endif
                pnt=x2pnt($curwv, left)
                endpnt=x2pnt($curwv, right)
                If((Mean($curwv,left,right)<= top) %&(Mean($curwv,left,right)>=bottom))
                        do
                          pnt +=1
                          If ($curwv[pnt]> top)
                            BREAK     // cuts out if curwv goes above top of marquee
                          endif
                        while (pnt <= endpnt)
                If (pnt >= endpnt)        // if search made it to the end
                        FindPeak/q/b=29/M=(bottom)/R=(left, right) $curwv
                        If (V_Flag==1)
                                Print " Try again, no peak was found! for "+curwv
                         else
                                V_pk=mean($curwv, V_peakLoc-0.5, V_peakLoc+0.5)
                                runAvg += V_pk; navg+=1
                                V_pk=Round(V_pk*10)/10
                                Notebook $nb
text="Pk"+curwv+"="+NSD(V_pk,1)+"mV@"+NSD(V_peakLoc,1)+"\t"
                        endif // V_flag==1
                 endif // pnt => endpnt
                 endif
                n+=1
```

```
                curwv=GetStrFromList(WvsGraph,n,";")
        while(1)
        tgn=root:type+"_avg"
        Notebook $nb text="\r"+tgn+"= " +NSD(runAvg/navg,3)+ "\r"
        TextBox/N=$tgn/A=MC root:type+"_pk="+NSD(runAvg/navg,1)
End

Proc FastPkfind() : GraphMarquee
//Doesn't search wave and doesn't give textbox at end

Silent 1 ;PauseUpdate
String fldrSav= GetDataFolder(1), nb="Notebook0"
SetDataFolder root:
        GetMarquee left, bottom
        if (V_Flag == 0)
                Print "There is no marquee"
        endif
        Variable left=V_left, right=V_right, bottom=V_bottom, top=V_top
        String WvsGraph, curwv, tgn
        Variable n=0, numwvs=0,pnt, endpnt, V_pk, runAvg=0, navg=0
SetDataFolder fldrSav
        Wvsgraph=WaveList("*",";","WIN:")
        curwv=GetStrFromList(WvsGraph,n,";")
        Notebook $nb ruler=Normal
        do      //for each wave in list
                if (cmpstr(curwv,"")==0)
                        Break
                  endif
                pnt=x2pnt($curwv, left)
                endpnt=x2pnt($curwv, right)
                If((Mean($curwv,left,right)<= top) %&(Mean($curwv,left,right)>=bottom))
                        FindPeak/q/b=29/M=(bottom)/R=(left, right) $curwv
                        If (V_Flag==1)
                                Print " Try again, no peak was found! for "+curwv
                         else
                                V_pk=mean($curwv, V_peakLoc-0.5, V_peakLoc+0.5)
                                runAvg += V_pk; navg+=1
                                Notebook $nb
text="Pk"+curwv+"="+NSD(V_pk,1)+"mV@"+NSD(V_peakLoc,1)+"\t"
                                        endif // V_flag==1
                         endif
                n+=1
                curwv=GetStrFromList(WvsGraph,n,";")
        while(1)
        tgn=root:type+"_avg"
        Notebook $nb text="\r"+tgn+"= " +NSD(runAvg/navg,3)+ "\r"
```

```
End

Proc FindPkAPs() : GraphMarquee

        String fldrSav= GetDataFolder(1)
        SetDataFolder root:

        GetMarquee left, bottom
        if (V_Flag == 0)
                Print "There is no marquee"
        else
                Variable top=V_top, bottom= V_bottom, left=V_left, right=V_right
        endif
Silent 1
        String WvsGraph, curwv, tgn
        Variable n=0, numwvs=0, V_pk, runAvg=0, navg=0

SetDataFolder root:raw
        Wvsgraph=WaveList("v*",";","WIN:")
        curwv=GetStrFromList(WvsGraph,n,";")
        do      //for each wave in list
                if (cmpstr(curwv,"")==0)
                        Break
                  endif
                If((Mean($curwv,left,right)<= top) %&(Mean($curwv,left,right)>=bottom))
                        WaveStats/q/R=(left, right) $curwv
                                V_pk=V_max
                                runAvg += V_pk; navg+=1
                         endif
                n+=1
                curwv=GetStrFromList(WvsGraph,n,";")
        while(1)
        tgn="tx_Avg"
        TextBox/N=$tgn/A=MC "Peak avg  = "+num2str(round(runAvg/navg*10)/10)
SetDataFolder fldrsav
End


//UTILITY PROCEDURES
#include <Strings as Lists>
#include <SaveGraph>

//Utility Functions, Generally usefull
//SeriesCmd : creates list of waves for specified cmd, Avoides having to type long list of wave
names
//SeqCmd: Sequential execute cmd on list of waves
```

```
// Tempgr: displays temp a general wave
// ChangeNAN20: changes all NAN values to 0 for input wave
Menu "Jilda's"
        SubMenu "List o' Cmds"
                "SeriesCmd"
                "SeqCmd"
                "DupSeq"
        end
end

//SeriesCmd: Creates a list of waves(specified by tag, nstr, nend): TagNstr, ..., TagNend
//Then executes cmd on that list.  List is printed into history area
Proc SeriesCmd(nstr, nend, tag, cmd)
        Variable nstr, nend
        String tag, cmd

        Silent 1; PauseUpdate
        Variable n=nstr, m=0
        String cmdlist=""

        do
                m=0                     //Resets wave counter, and cmdlist.
                cmdlist = cmd+ " " +tag+num2str(n)
                n=n+1
                do
                        cmdlist += ","+tag+num2str(n)
                        m +=1
                        n +=1
                while ((m < 61) %& (n<=nend))
                                //Stops when 61 waves in list, prevents overburdened cmd area

                Execute cmdlist
                //Print m, cmdlist      //cmd and number of waves in list printed to area.
                                                //Note: this happens even if
there is error in Execute cmd.
        while(n <= nend)                //Keeps going until all waves have received cmd.
END //Function CmdSeries

//Similar to above except generates cmd many times on each wave in series
Proc SeqCmd(nstr, nend, tag, st1, st2)
        Variable nstr, nend
        String tag, st1, st2

silent 1; PauseUPdate
Variable n=nstr
String cmd
```

```
do
        cmd=st1+tag+num2str(n)+st2
        Execute cmd
        //Print cmd
        n +=1
while (n<=nend)
END    //SeqCmd


//duplicates a series of waves from root:raw to current folder with new tag , tg2
Proc DupSeq(nstr, nend, tag, tg2)
        Variable nstr, nend
        String tag, tg2

silent 1; PauseUPdate
Variable n=nstr
String cmd
string fldrname=GetDatafolder(1)
Setdatafolder root:raw
do
        cmd = "Duplicate "+tag+num2str(n)+" "+fldrname+tg2+num2str(n)
        Execute cmd
        //Print cmd
        n +=1
while (n<=nend)
setdatafolder fldrname
END    //SeqCmd

// Like seq cmd only performs operation on all waves in current folder
Proc DotoallwvsinGraph(tag,st1,st2)
        String tag, st1, st2

silent 1; PauseUPdate
String cmd,lstwv,curwv
Variable n=0

lstwv=WaveList(tag+"*", ",", "")

do      //for each wave in list
        curwv=GetStrfromList (lstwv, n,",")
        if (cmpstr(curwv[0],"")==0)      //you've reached the end
                Break
                endif
        if (wavetype($curwv)!=0)         //If not a textwave than do following
                cmd=st1+curwv+st2
```

```
                Execute cmd
                Print cmd
            endif
        n +=1
while (1)
END    //SeqCmd

Function FindDash(nmwv)
        string nmwv

        Variable n1=0,n2=strlen(nmwv)
        do
                If (cmpstr(nmwv[n1],"_")==0)
                        Return n1
                        else
                        n1+=1
                        endif
        while (n1<n2)
        DoAlert 0, "No \"_\" was found in "+nmwv
        Return NAN
end

//*****************************
 // Quick way to "format" a number to specified number of decimal points
 // NSD is short for NumberStringDecimal, ND is NumberDecimal

Function/S NSD(value, decp) // Returns a STRING of value rounded to decp decimal points.
        Variable value, decp

Return num2str(round(value*10^decp)/(10^decp))

end

Function ND(value, decp) //Returns a number instead of a string
        Variable value, decp

Return round(value*10^decp)/(10^decp)

end
```

VITA

Jilda S. Nettleton

University of Washington

1998

Education

- Ph.D. Candidate in Physiology and Biophysics, University of Washington
- Molecular Neurobiology Laboratory Course, Friday Harbor Laboratories
- Graduate Student, Department of Physics, University of Washington (9/90-12/91)
- Bachelor of Science in Physics, University of Rochester (Awarded May 1987)
  graduated *cum laude* and with departmental distinction. GPA 3.5/4.0

Research Projects

Thesis project: Summation of EPSPs in rat neocortical neurons
Supervisor: Dr. William Spain, M.D, U. of Washington

- Designed computer programs using data analysis package (Igor Pro)
  created interface between computer and digitizing board
  generated electrical commands to and read in signals from neurons
  analyzed and organized data
- Improved existing histological procedures to visualize cells
- Designed protocols and procedures unique to this study
- Prepared and obtained grants to fund projects
- Awarded: NIH training fellowship in Neurobiology, Epilepsy Foundation Health Sciences Student Fellowship
- Prepared reports and presentations of research progress and results to colleagues

Skills involved in this and other research projects:

- Intracellular electrical recordings using microelectrodes and whole-cell patch clamping
- In vitro slice and dissociated cell preparation
- Confocal microscopy
- Florescent imaging
- Database management and statistical analysis
- Computer assisted data acquisition, analysis, organization, and storage on both Macintosh and PC operating systems

Additional Research Projects:

- Insulin effects on rat neocortical neurons
- Effects of GTP on light response of outer rod cells from Geckos.
- Persistent sodium current in dissociated rat cortical cells.
- Measured flexural rigidity of actin filaments in free solution
- Theoretical calculation of quark-gluon plasma size.(Physics Department)

Employment

Research Technician: Brigham and Women's Hospital, Harvard Medical School, Boston, MA Supervisor Dr. Ging Kuo Wang, Ph.D.(2/88-8/90)

- Investigated effects of local anesthetics on single BTX-activated sodium channels incorporated into lipid bilayers.

Teaching Experience

Teaching Assistant : ***Human Physiology Course*** *for graduate nursing, dental and bioengineering students covering introduction to Neurophysiology, Cardiac Physiology, and Respiratory Physiology*

- Conducted weekly conference sections and exam review sessions for 20-40 students
- Prepared weekly handouts and study sessions
- Provided students with individual tutoring on specific concepts

Teaching Assistant: ***Introductory Physics course*** *for undergraduates*

- Prepared and Instructed weekly laboratory and recitation sections for 15-25 students.
- Evaluated students' laboratory reports
- Tutored students with extra physics problems

Professional Organizations and Activities

- Career Day Symposium Committee member
- University Toastmasters chapter of International Toastmasters
- Society for Neuroscience
- Puget Sound Biotechnology Society
- American Women in Science, Local Seattle Chapter

Publications

Nettleton, Jilda S and William J Spain. Post-synaptic Conductances Cause Non-linear Summation of AMPA-mediated EPSPs in Rat Neocortical Layer V Pyramidal Neurons. (*Manuscript submitted*)

Spain, William, JFM van Brederode, and **Jilda S Nettleton** (1999) Intracellular Recordings from Neurons in Brain Slice *in* Electrophysiological Methods for the Study of the Mammalian Nervous System. (Kocsis, JD ed) Appleton and Lange (*in press*)

Gittes, Frederick, Brian Mickey, **Jilda S Nettleton,** and Joe Howard (1993) Flexural Rigidity of Microtubules and Actin Filaments. *J. of Cell Biology* **120**(4):923-934

Nettleton, Jilda S, Neil A. Castle, and Ging Kuo Wang (1991) Block of Single Batrachotoxin-Activated Na^+ Channels by Clofilium. *Molecular Pharmacology* **39**: 352-358

Nettleton, Jilda S and Ging Kuo Wang (1990) pH-Dependent Binding of Local Anesthetics in Single Batrachotoxin-Activated Na^+ Channels. *Biophysical Journal* **58**: 95-106

Abstracts

Nettleton, Jilda S and William J Spain. (1996) Post-synaptic Conductances Cause Non-linear Summation of AMPA-mediated EPSPs in Rat Neocortical Layer V Pyramidal Neurons. *Soc Neurosci. Abstr.* Vol. **22**, Part 1, p.796

Nettleton, Jilda (1994) "Synaptic Integration: How do neurons process information from other neurons?" Chimera Graduate and Professional Student Research Forum, University of Washington, Seattle, WA

Nettleton, Jilda and Ging Kuo Wang. (1989) "Hydrogen ions affect the cocaine binding affinity in BTX-activated Na^+ Channels in planar bilayers" Biophysical Meeting. Cincinnati, OH

IMAGE EVALUATION
TEST TARGET (QA-3)

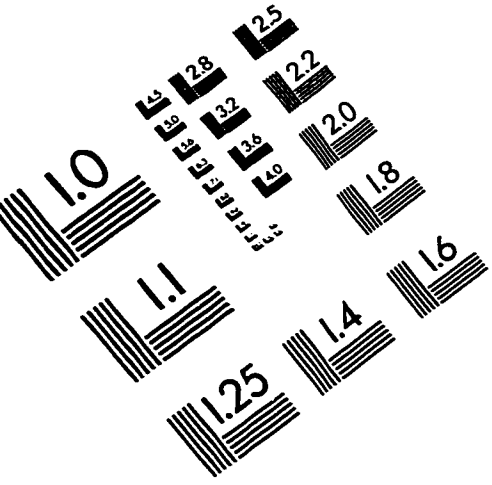

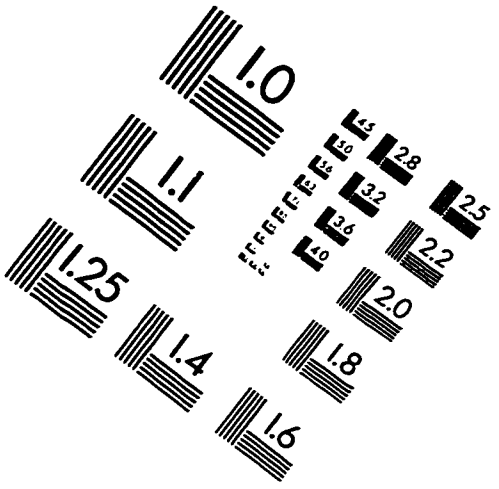

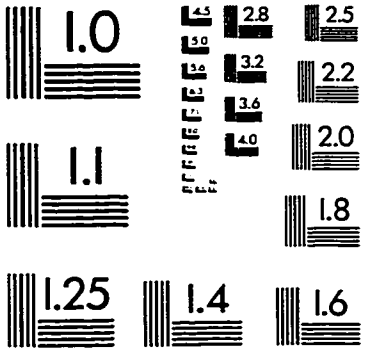

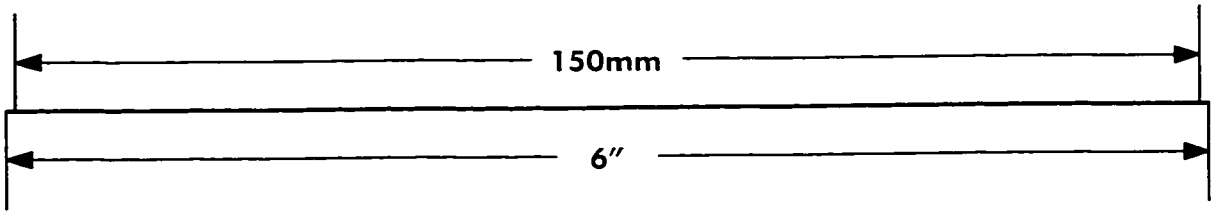

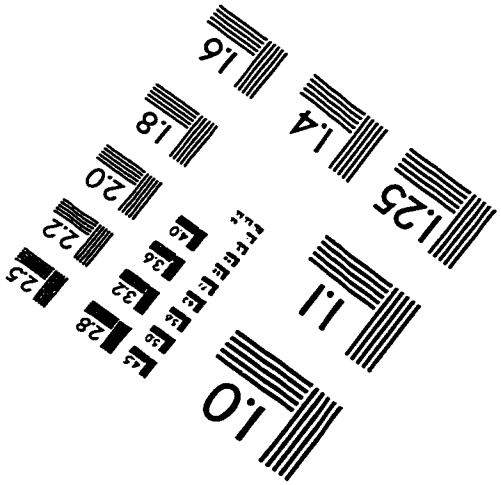

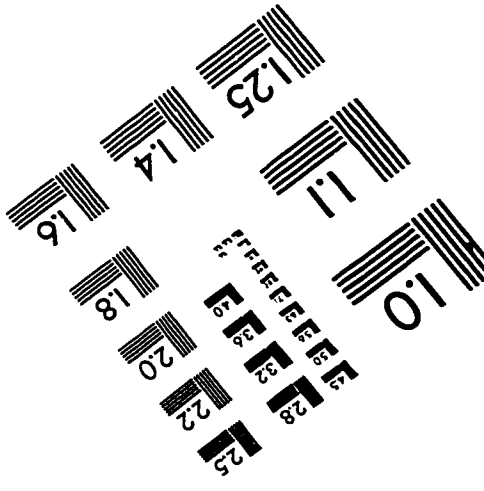

APPLIED IMAGE, Inc
1653 East Main Street
Rochester, NY 14609 USA
Phone: 716/482-0300
Fax: 716/288-5989